Nucleus-nucleus collision models and simulations for hadrontherapy.

Daniel Cussol

Nucleus-nucleus collision models and simulations for hadrontherapy.

Daniel CUSSOL

LPC Caen, ENSICAEN, Université de Caen Normandie, IN2P3/CNRS

March 3^{rd} 2023

Overview

1. Simulations for hadrontherapy
2. The role of nucleus-nucleus collisions
3. Nucleus-nucleus collision models
4. Benchmarking models to data
5. Nuclear Physics methods for hadrontherapy

1 Simulations for hadrontherapy

2 The role of nucleus-nucleus collisions

3 Nucleus-nucleus collision models

4 Benchmarking models to data

5 Nuclear Physics methods for hadrontherapy

Goal of numerical simulations

- Compute the dose deposited by a particle all along its path in living tissues
- The accuracy has to be better than **3%** in the tumour area
- The range has to be known within a 1 mm accuracy
- The computation time in clinical routine should not exceed 10-20 minutes
- This dose calculation module has to be included in a Treatment Planning System

the Treatment Planning System (TPS)

Treatment Planning System

A software to compute the parameters of the accelerator in order to deliver a given 3D dose map for:

- a given accelerator
- a given patient
- a given pathology

Existing TPS's

- **HIMAC** (Japan): Physical dose computed using RBE taken ~ 2.
- **TRiP** (HIT, heidelberg): Physical dose computed using , RBE computed using the Local Effect Model (LEM) (Krämer and Scholz, 2000; Krämer et al., 2000)

Mandatory elements of a TPS

- Computing the dose profile for each geometrical configuration
  - by using empirical formula
  - by use Monte-Carlo calculations
  - by transforming reference profiles computed in a given material
  - Apply on physical dose profiles the suited biological factors to take into account the biological damages induced by the projectile
- Define areas on which a given dose has to be delivered
- Define areas for which the dose deposition can not exceed a maximum value (Organs At Risk)
- A minimisation procedure which computes the weight of each profile in order to satisfy the dose deposits requirements

Different possible TPS Strategies

Analytical calculations

- Each beam LET and dose profiles are computed using analytical formula for water once for all
- For each geometrical configuration a simple transform of water profiles is applied
- the minimisation procedure is applied on transformed profiles

Hybrid calculations

- Each beam LET and dose profiles are computed using Monte-Carlo simulations for water once for all
- For each geometrical configuration a simple transform of water profiles is applied
- the minimisation procedure is applied on transformed profiles

"Monte-Carlo" calculations

- Each beam LET and dose profiles are computed using Monte-Carlo simulations for each geometrical configuration
- the minimisation procedure is applied on the resulting profiles

Example of an analytical dose profile computation

$$R(A, Z, E) = b_w \frac{A}{Z^2} E^{a_w}$$

protons at 191 MeV

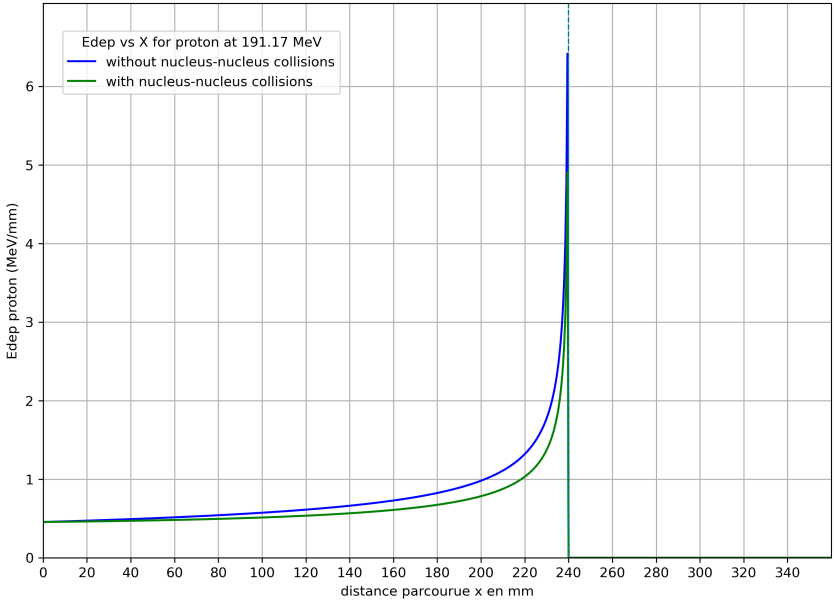

^{12}C at 358 MeV/u

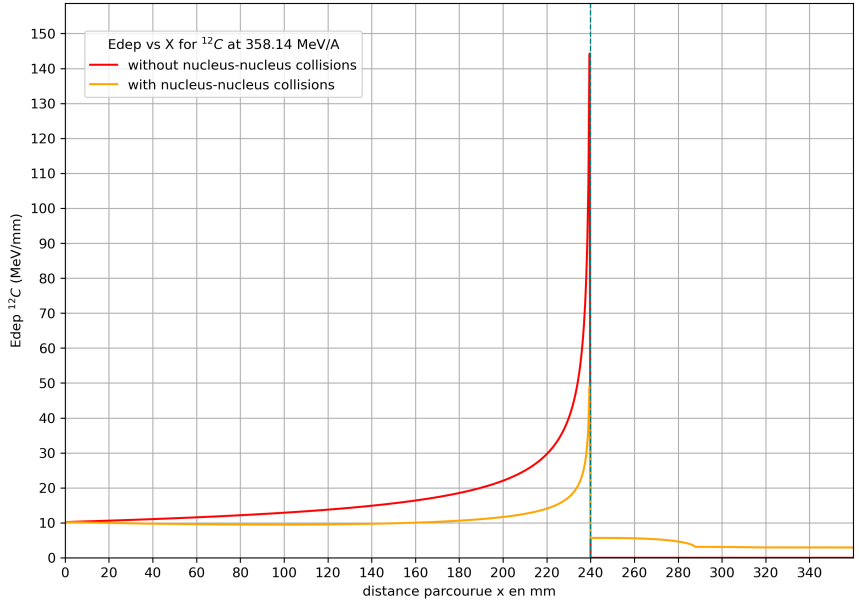

Analytical dose profile transformation

Characteristics

- Fast dose calculations
- Based on geometrical transforms of a reference Bragg curve in liquid water
- Empirical formulas
- Medium accuracy

An example: Water equivalent transform

- One parameter: the water equivalent factor $k_{we} = R_{Water}/R_{tissue}$
- $E_{tissue}(x) = k_{we} E_{Water}(k_{we} \times x)$

Water Equivalent Transform

protons at 135 MeV

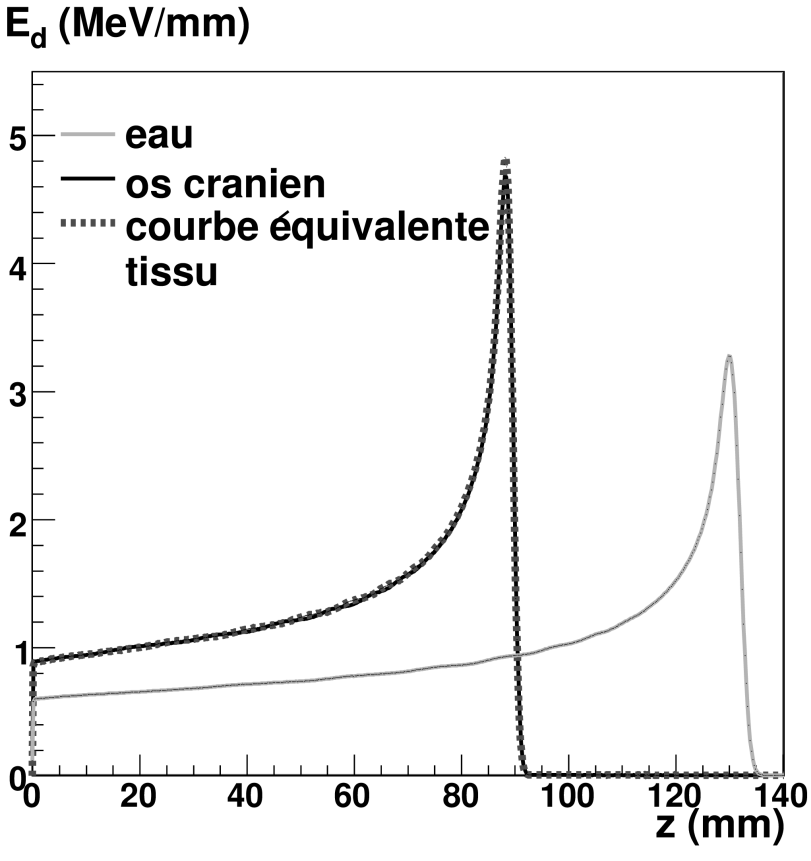

^{12}C at 290 MeV/u

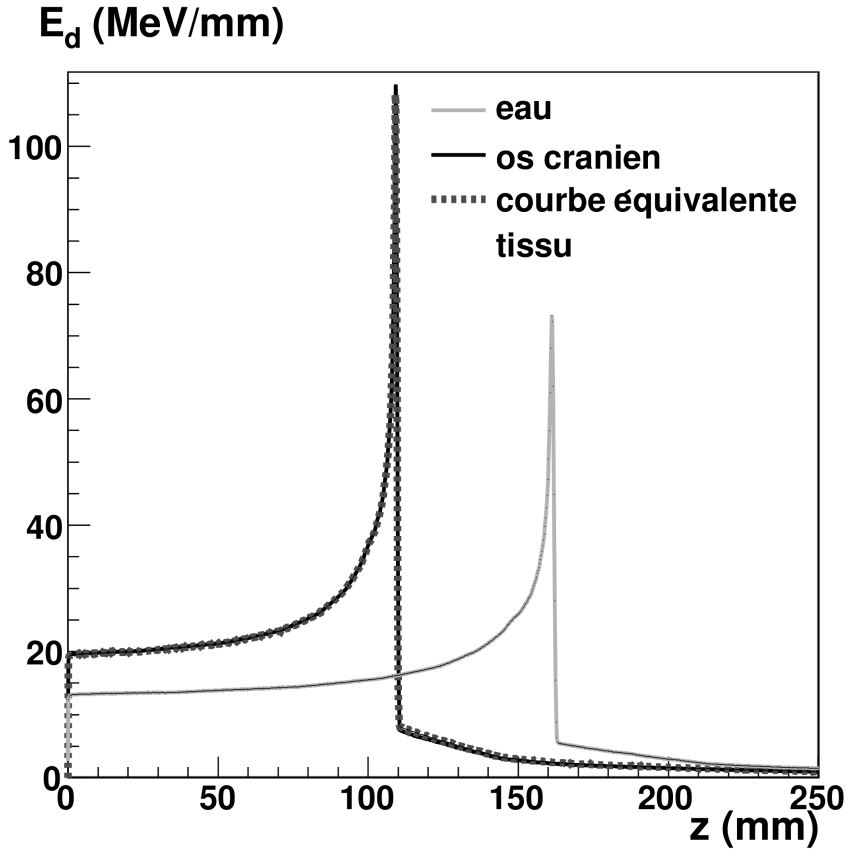

Computing the dose profiles weights: a simple example

The requirements

- One wants to irradiate a 1 cm large volume located 8 cm in water.
- Summation of the contributions of many individual beams.
- For an individual beam i with incident energy E_i the dose $D_i(x)$ has been deposited at depth x.
- For a set of beams with different energies, the dose at depth x is given by: $D(x) = \sum_i N_i D_i(x)$.
- The biological dose is $D(x) = \sum_i N_i D_i(x) BF(x)$. The biological factor $BF(x)$ is equal to RBE for aerobic cells or is equal to $\frac{RBE}{OER}$ for hypoxic cells.

The goal is to find the values of N_i to deposit a wanted biological dose $D_{wanted}(x)$ at depth x.

One solution

find the set of N_i values which minimizes the following quantity
$\chi^2 = \int (D_{wanted}(x) - \sum_i N_i D_i(x) BF(x))^2 dx$

Physical SOBP for ^{12}C

Resolution

Solve the system of n equations with n unknown N_i values:

$$\frac{\partial \chi^2}{\partial N_i} = 0 \Rightarrow \int D(x) D_i(x) dx = \sum_j N_j \int D_j(x) D_i(x) dx$$

Weigths distribution for ^{12}C

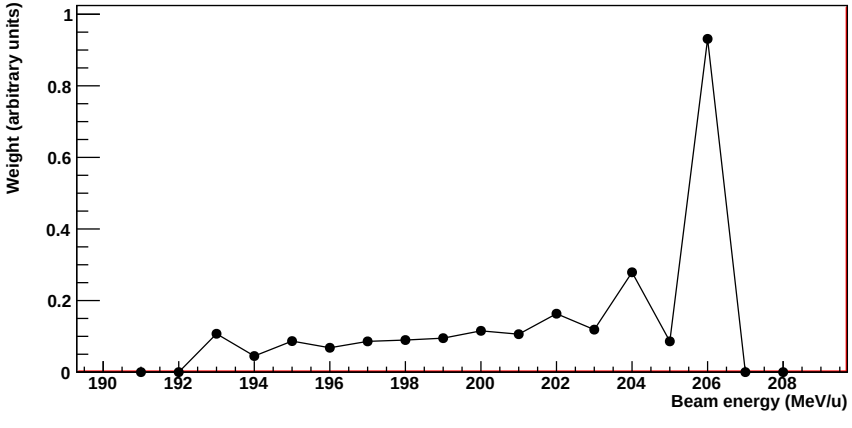

Spread Out Bragg Peak

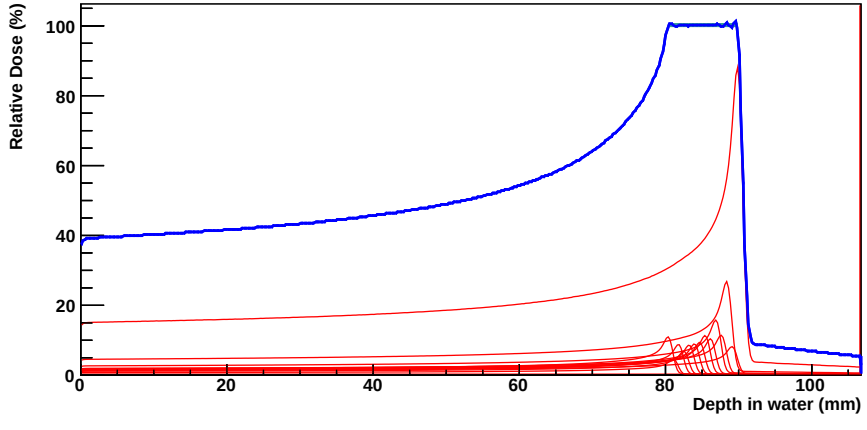

Simplified biological model

Relative Biological Efficiency

$$RBE = f(TEL) \approx f(\frac{dE}{dx})$$

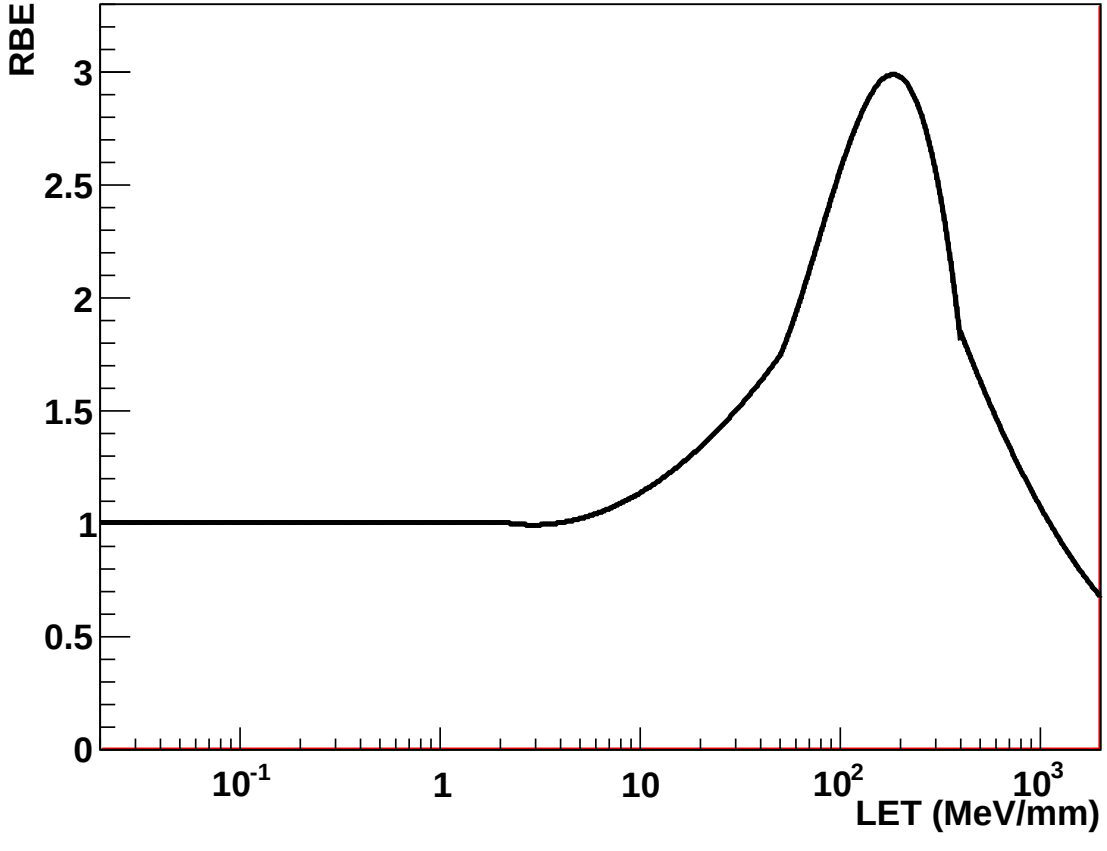

Simplified biological model

Relative Biological Efficiency

$$RBE = f(TEL) \approx f(\frac{dE}{dx})$$

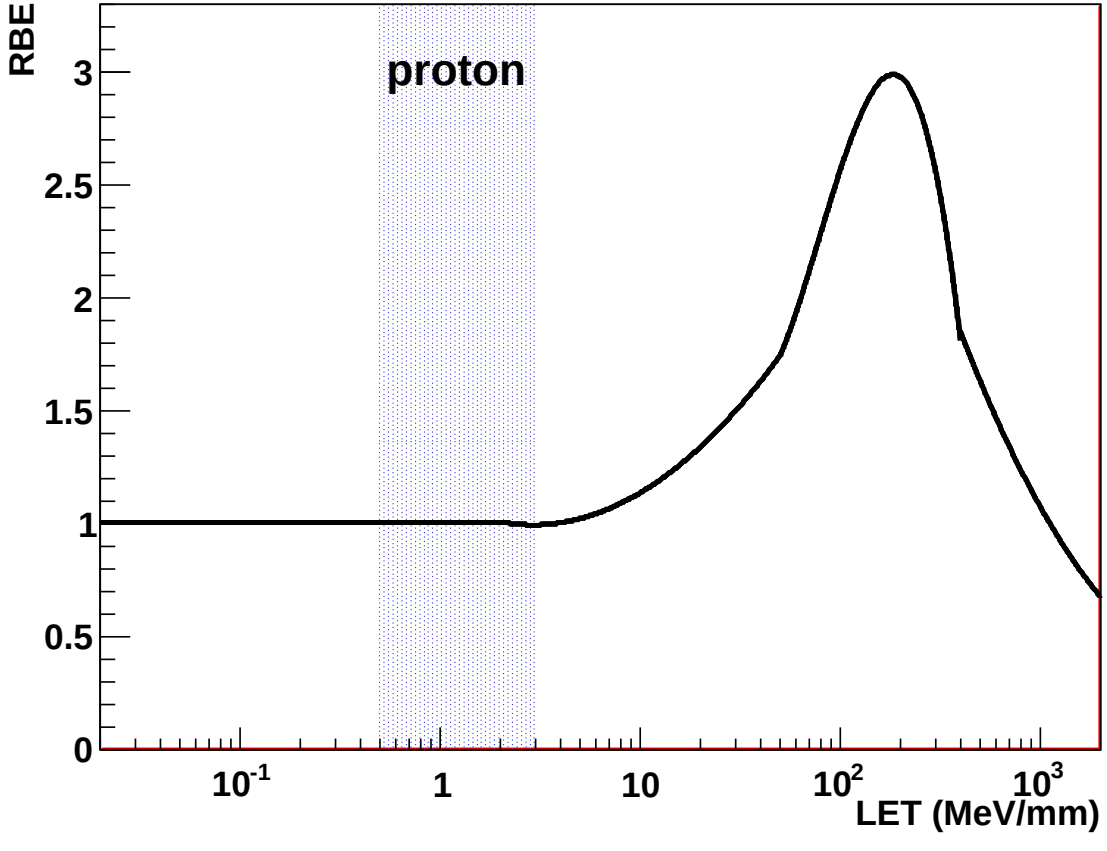

Simplified biological model

Relative Biological Efficiency

$$RBE = f(TEL) \approx f(\frac{dE}{dx})$$

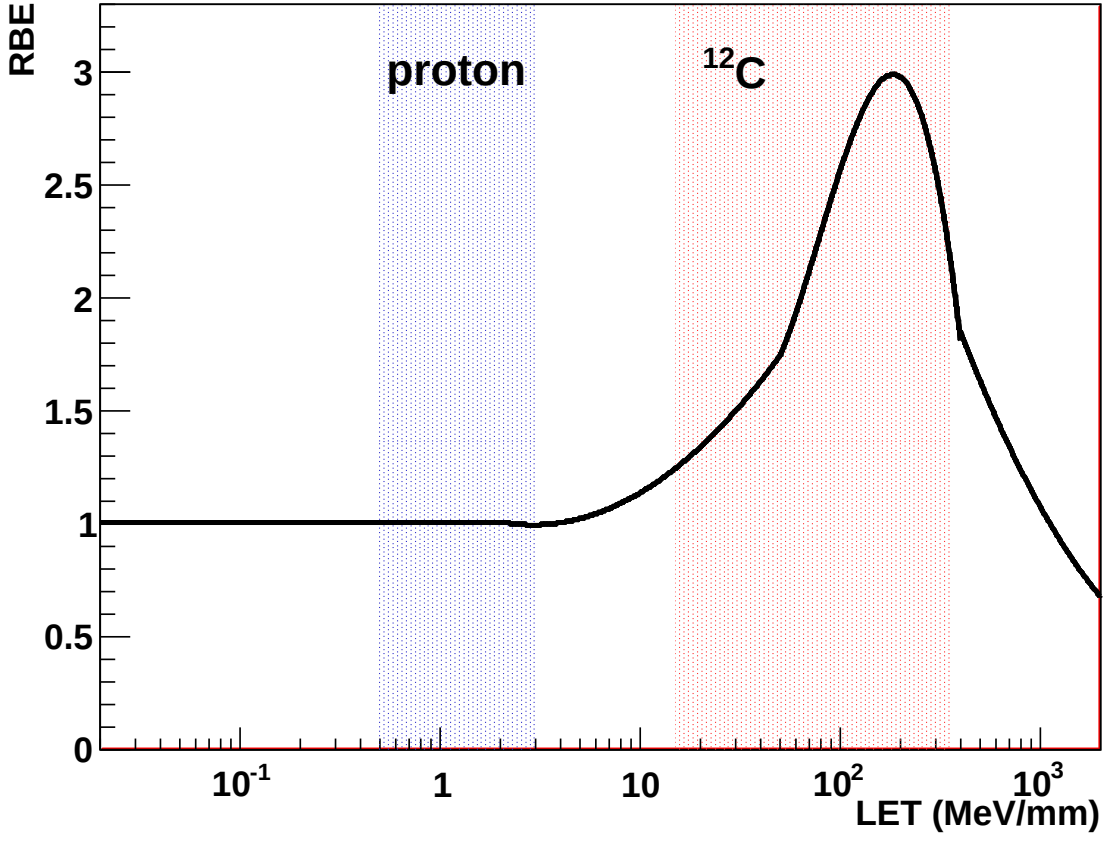

Biological SOBP for ^{12}C

Resolution

Solve the system of n equations with n unknown N_i values:

$$\int D(x)D_i(x)RBE_i(x)dx = \sum_j N_j \int D_j(x)RBE_j(x)D_i(x)RBE_i(x)dx$$

Weigths distribution for ^{12}C

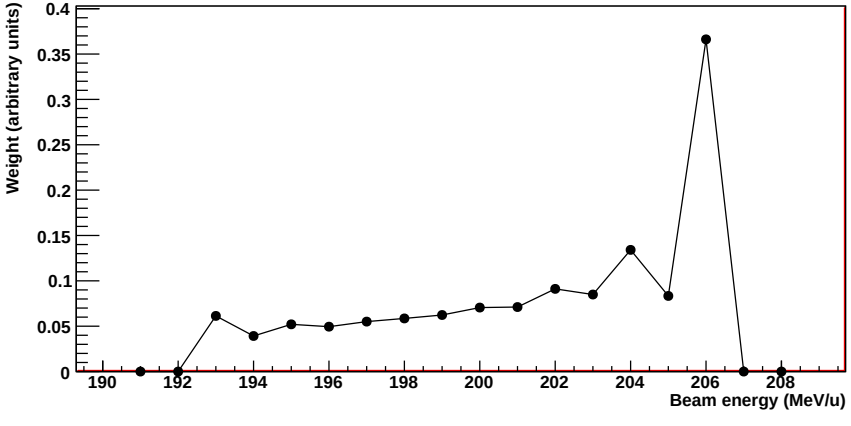

Spread Out Bragg Peak

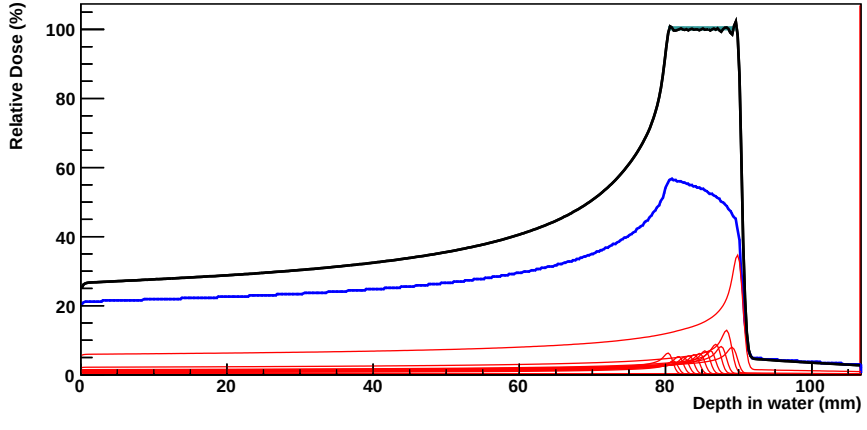

Numericals values

For protons

$\frac{dE}{dx} \approx 3\,MeV/mm$ at the Bragg Peak.

To deposit 1 Gy at the Bragg peak in liquid water ($\rho = 1\,mg/mm^3$):

$1\,Gy = \frac{N}{dS}\frac{3\,10^6 \times 1.6\,10^{-19}}{10^{-6}} \implies \frac{N}{dS} \approx 2\,10^6 protons/mm^2$

$\Rightarrow$ intrinsic error due to statistics : $1/\sqrt{2\,10^6} \approx 0,07\%$

For ^{12}C

$\frac{dE}{dx} \approx 80\,MeV/mm$ at the Bragg Peak.

To deposit 1 Gy at the Bragg peak in liquid water ($\rho = 1\,mg/mm^3$):

$1\,Gy = \frac{N}{dS}\frac{80\,10^6 \times 1.6\,10^{-19}}{10^{-6}} \implies \frac{N}{dS} \approx 8\,10^4\,{}^{12}C/mm^2$

$\Rightarrow$ intrinsic error due to statistics : $1/\sqrt{8\,10^4} \approx 0,35\%$

Using Water Equivalent Transform in TPS

1. apply the water equivalent transform for each water profile referenced in the TPS : $LET_i^{Water}(x) \longrightarrow LET_i^{WE}(x)$
2. compute the physical dose profile from the LET profile : $D_i^{WE}(x) = LET_i^{WE}(x)/\rho(x)$
3. determine the biological factor from the LET profile : $BF_i(x) = f\left(LET_i^{WE}(x)\right)$
4. determine the target (tumor) area
5. Indicate the dose to apply on the target area
6. Compute the weight N_i of each water equivalent profile using the minimisation of $\chi^2 = \int \left(D_{wanted}(x) - \sum_i N_i D_i^{WE}(x) BF(x)\right)^2 dx$

An example in 1D

Material properties

Material	k_{we}	ρ (g/cm^3)
Water	1.0	1.0
Air	0.001189	0.001189
Skin	1.088	1.090
Bone	1.474	1.61
Brain	1.042	1.040

Material stack

Material	width (mm)
Air	100.0
Skin	2.0
Bone	8.0
Brain	180.0
Bone	8.0
Skin	2.0
Air	100.0

An example in 1D for protons

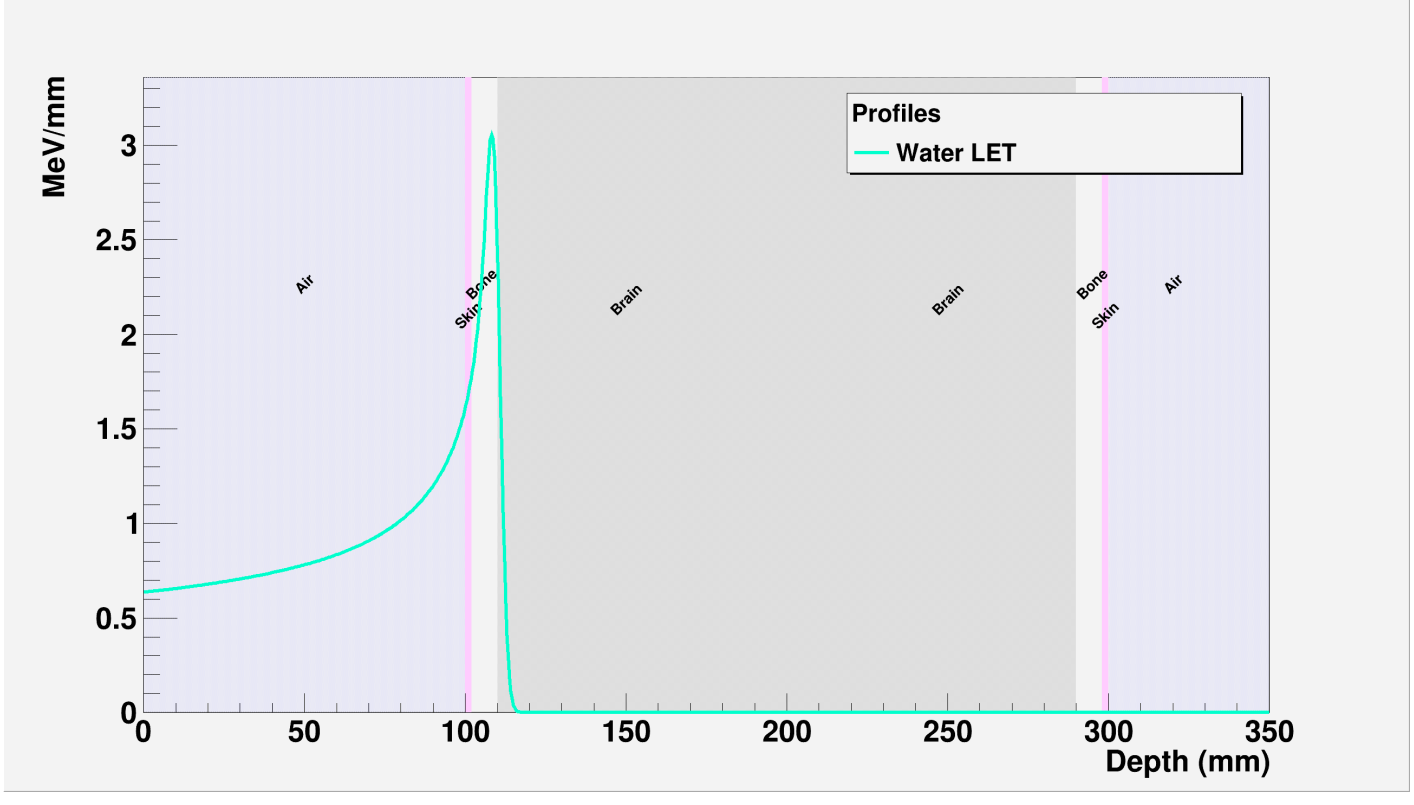

An example in 1D for protons

$$LET_i^{Water}(x) \longrightarrow LET_i^{WE}(x)$$

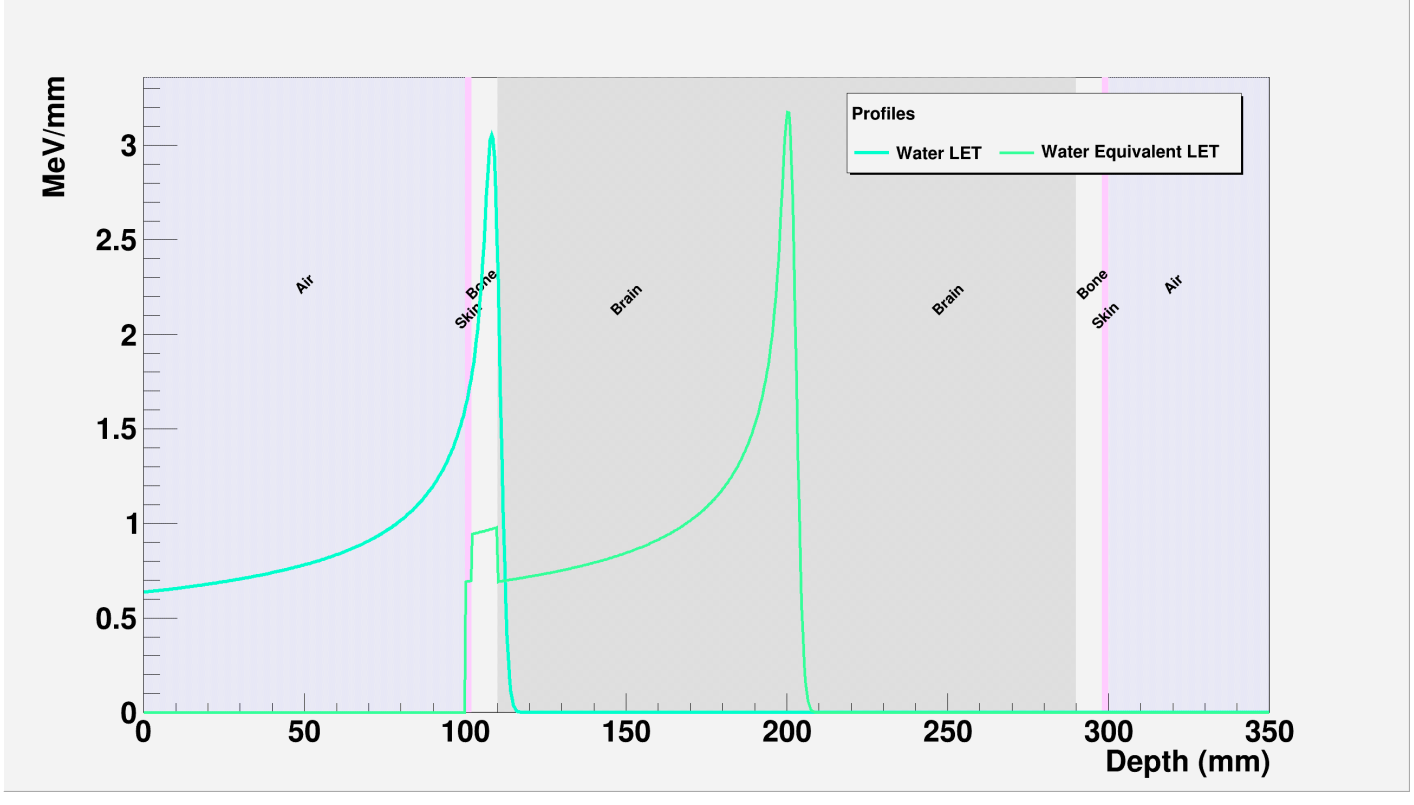

An example in 1D for protons

$$D_i^{WE}(x) = LET_i^{WE}(x)/\rho(x)$$

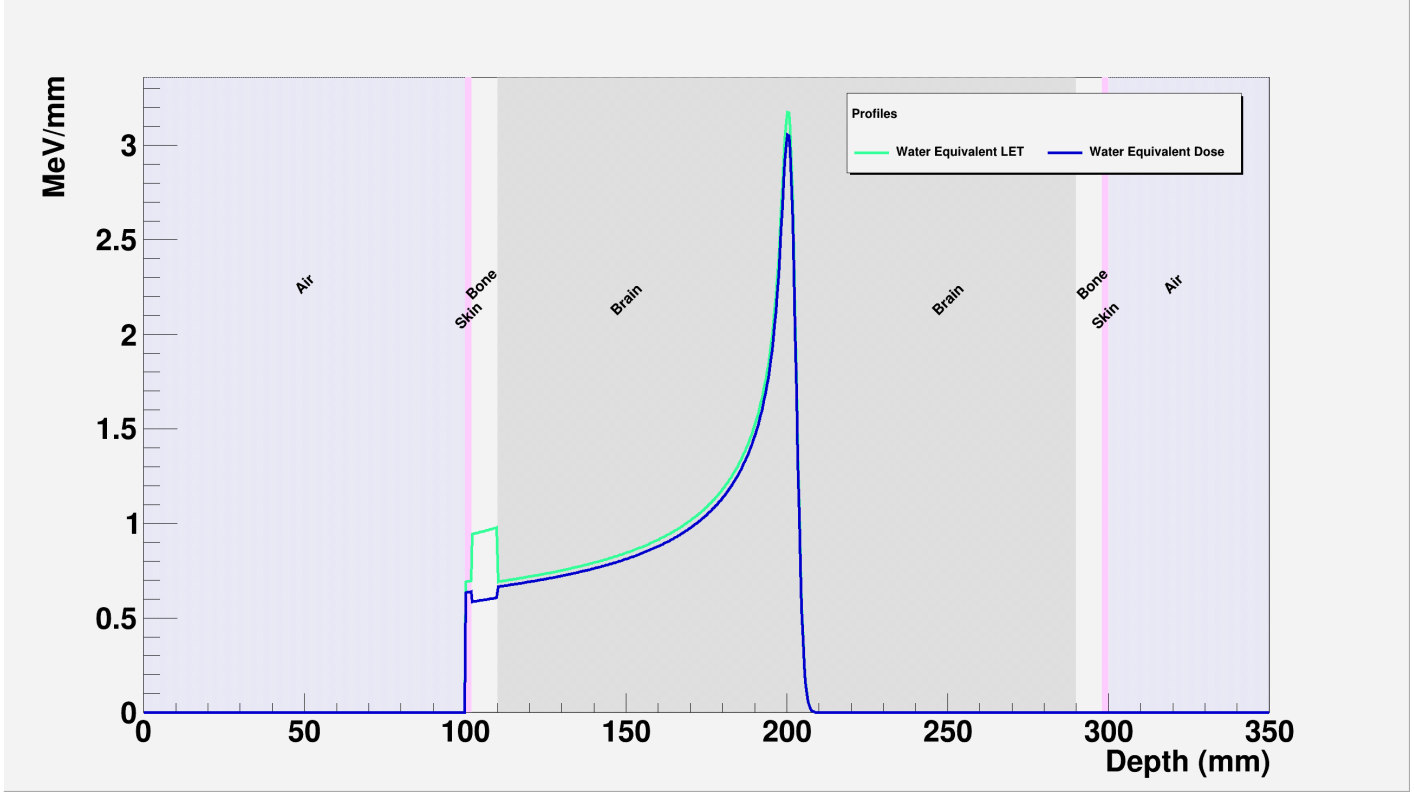

An example in 1D for protons

$$D_{bio,i}^{WE}(x) = D_i^{WE}(x) \times RBE(LET_i^{WE}(x))$$

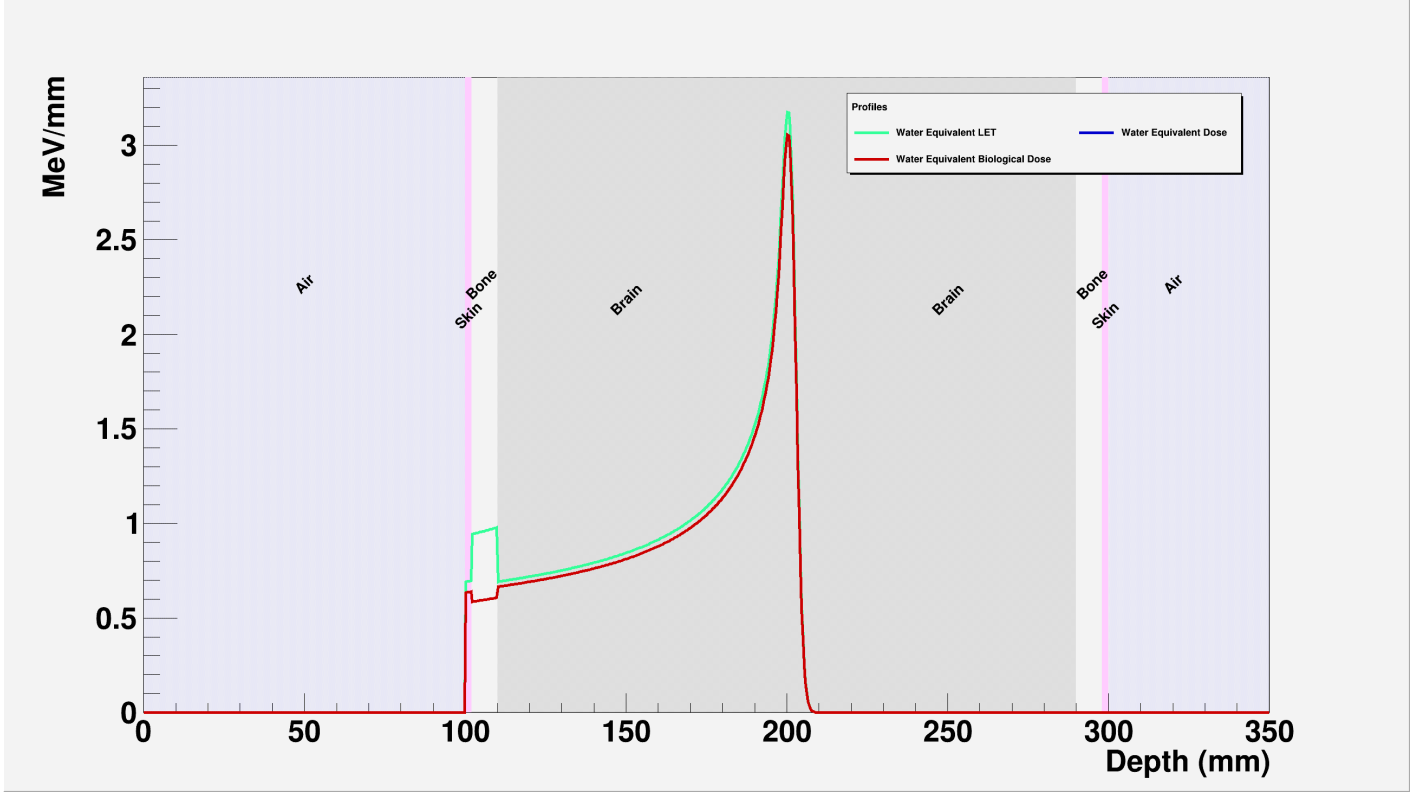

An example in 1D for ^{12}C

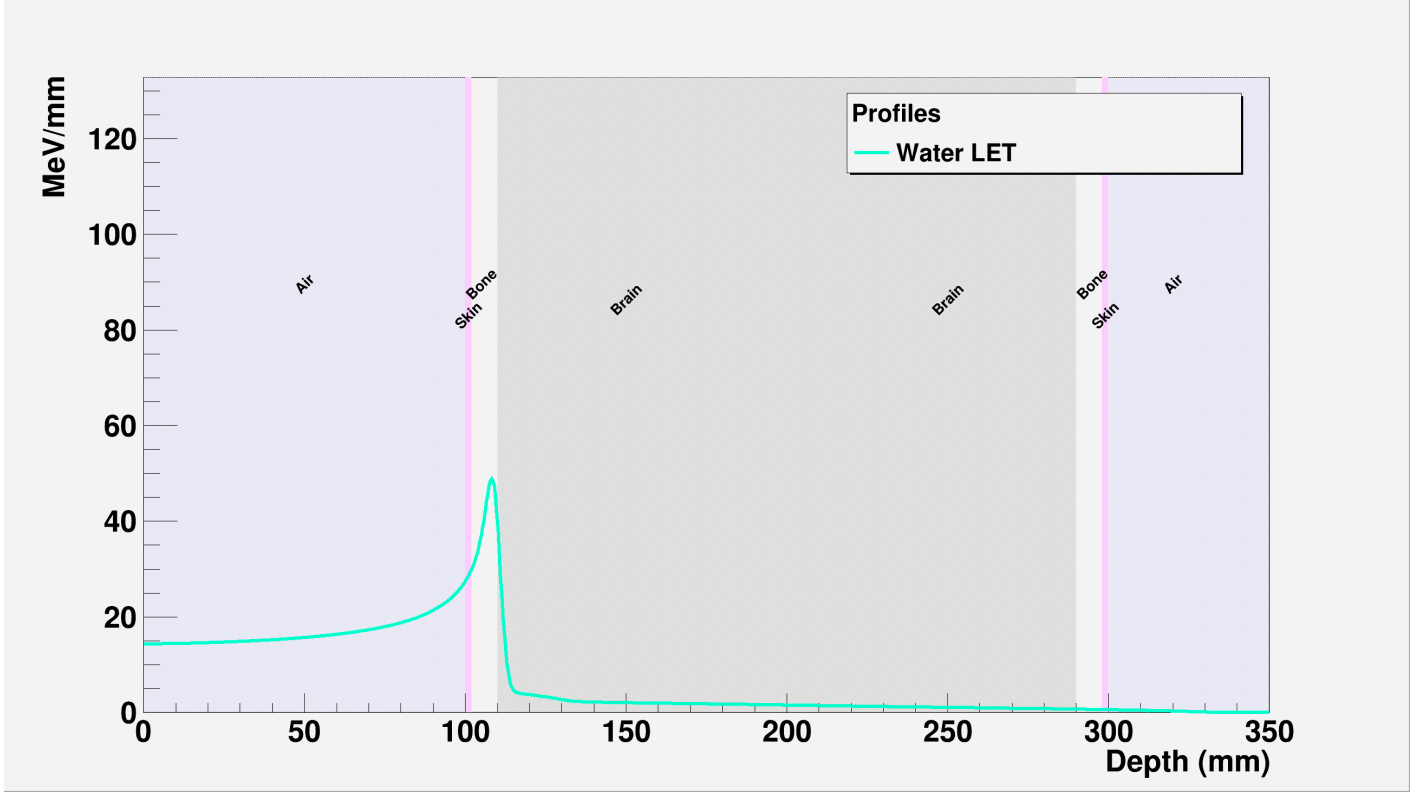

An example in 1D for ^{12}C

$$LET_i^{Water}(x) \longrightarrow LET_i^{WE}(x)$$

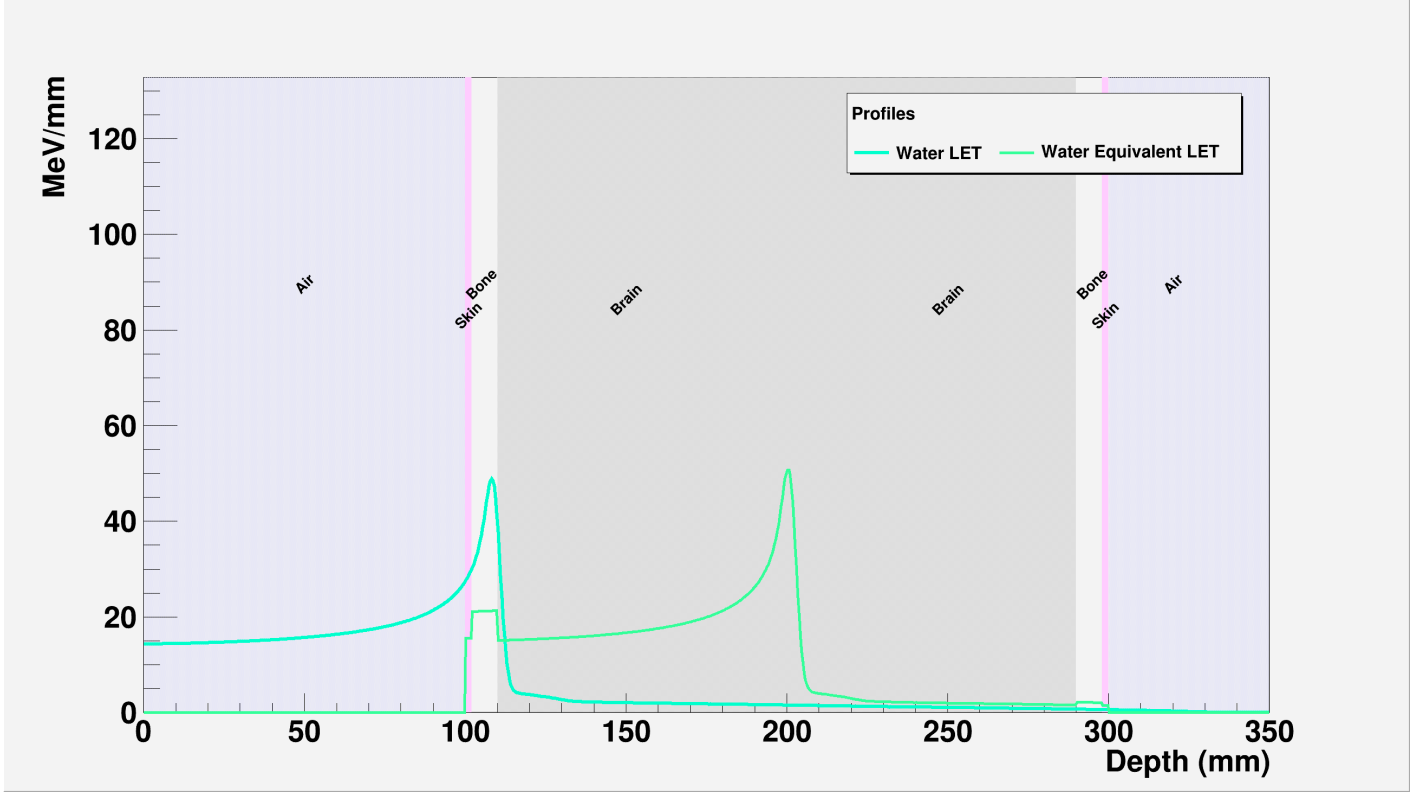

An example in 1D for ^{12}C

$$D_i^{WE}(x) = LET_i^{WE}(x)/\rho(x)$$

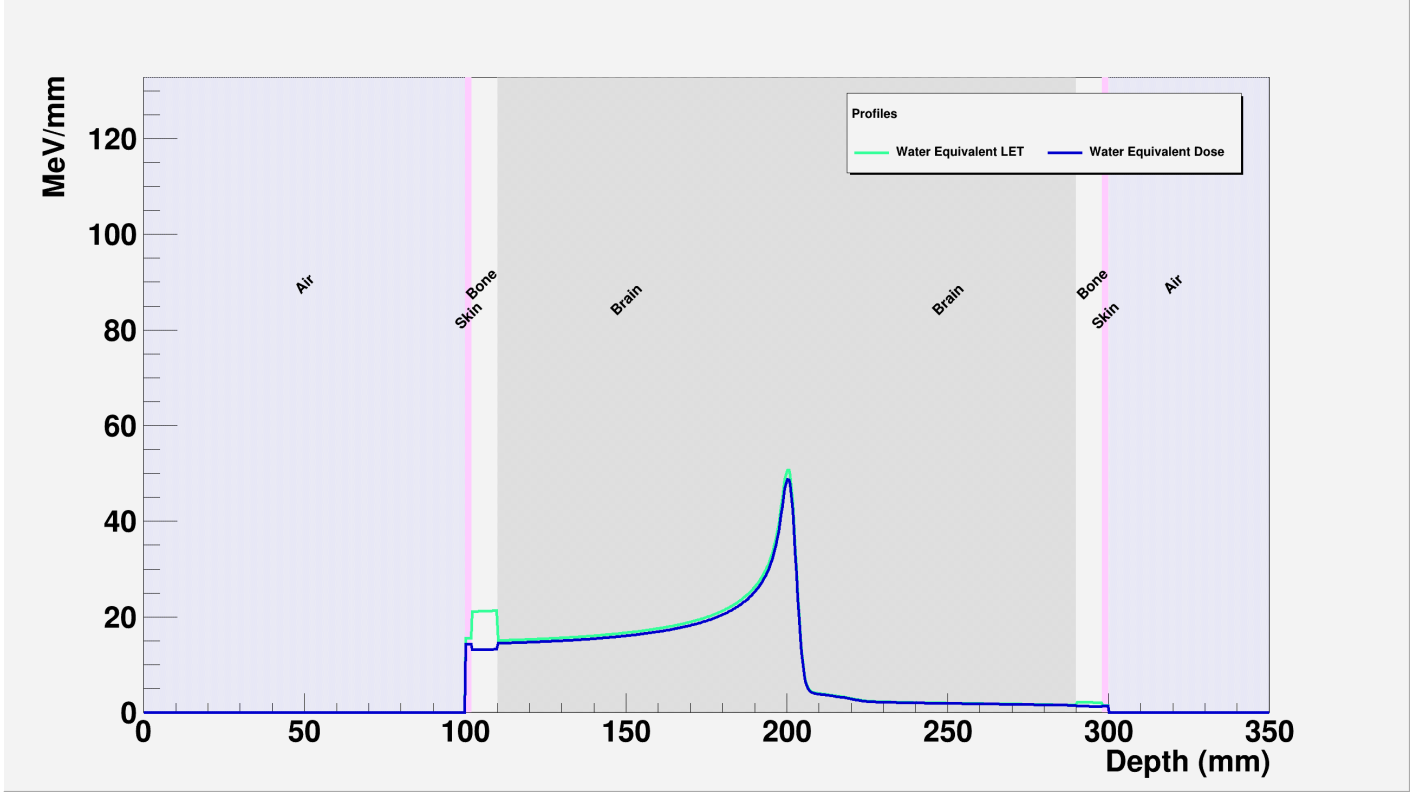

An example in 1D for ^{12}C

$$D_{bio,i}^{WE}(x) = D_i^{WE}(x) \times RBE(LET_i^{WE}(x))$$

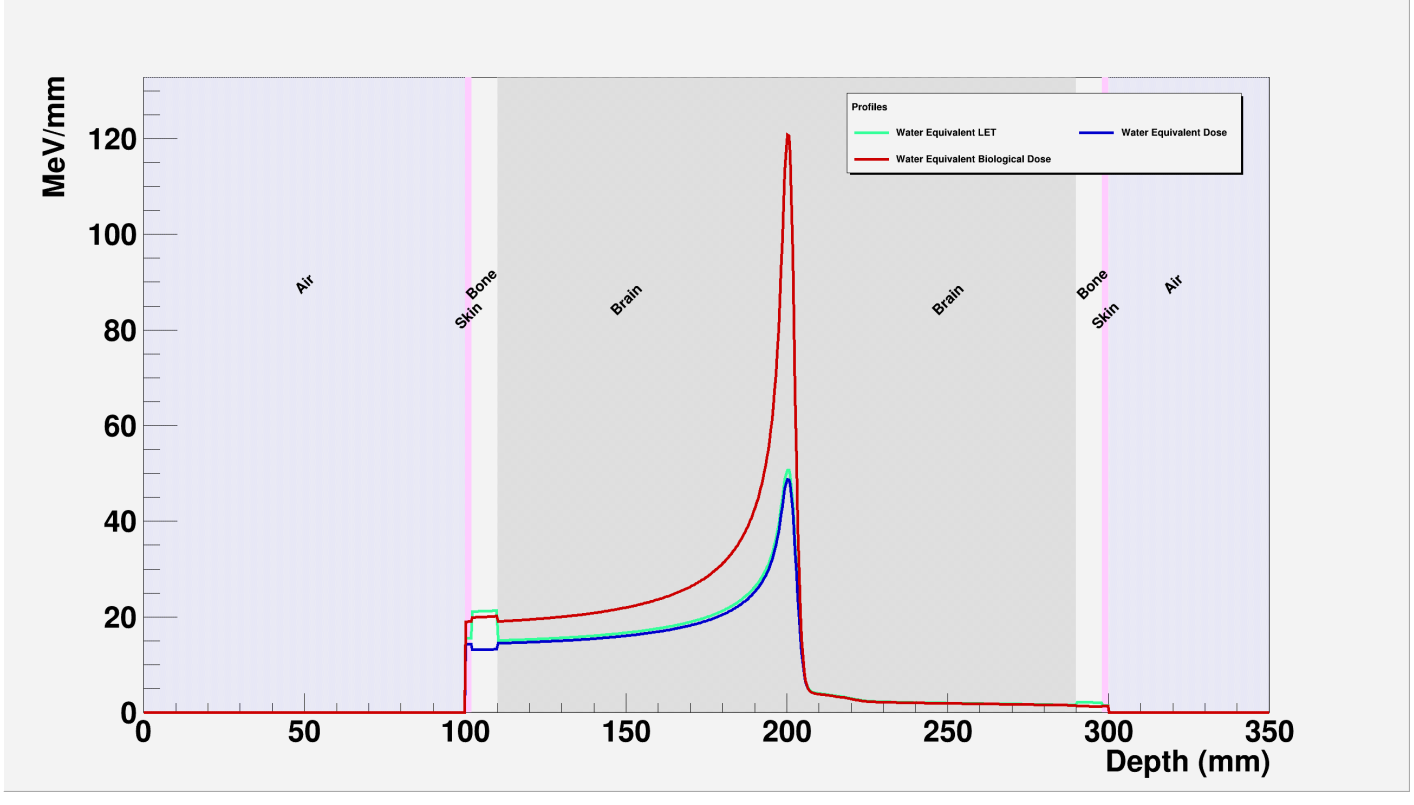

Computed 1D SOBP for ^{12}C

$$D_{wanted}(x) = 2.0\,Gy \quad \text{if } 198\,mm < x < 216\,mm$$

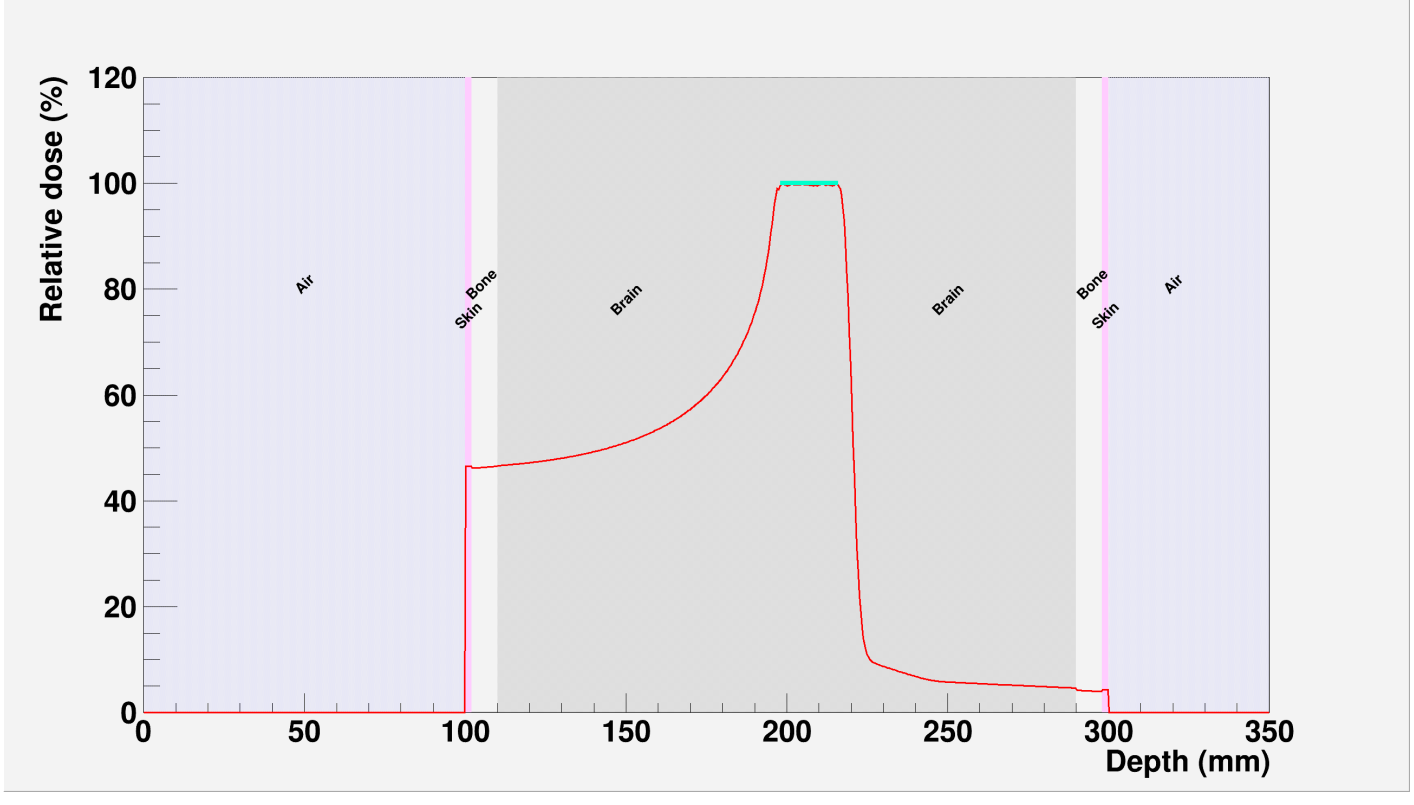

"Monte-Carlo" calculations

Goals

- Following the trajectories of all particles involved in the process
- Taking into account all physical processes that may occur all along the paths of particles
- Having a detailed description of the geometry of the problem
- Taking into account the chemical composition of all tissues and materials

Most used frameworks

- GEANT4 : GEometry ANd Tracking (CERN)
- FLUKA: Italy (CERN)
- PHITS: Japan
- MCNP/MCNPx : USA

Trajectories of nuclei in materials

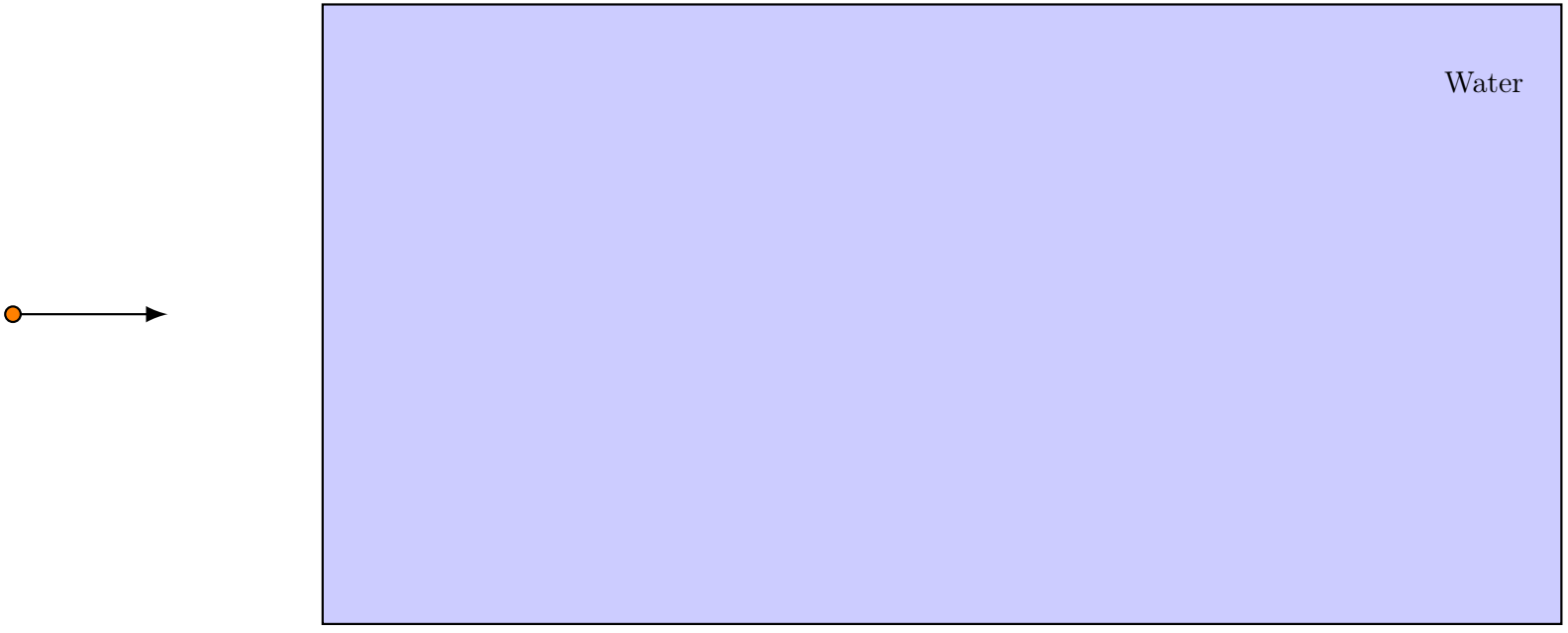

Trajectories of nuclei in materials

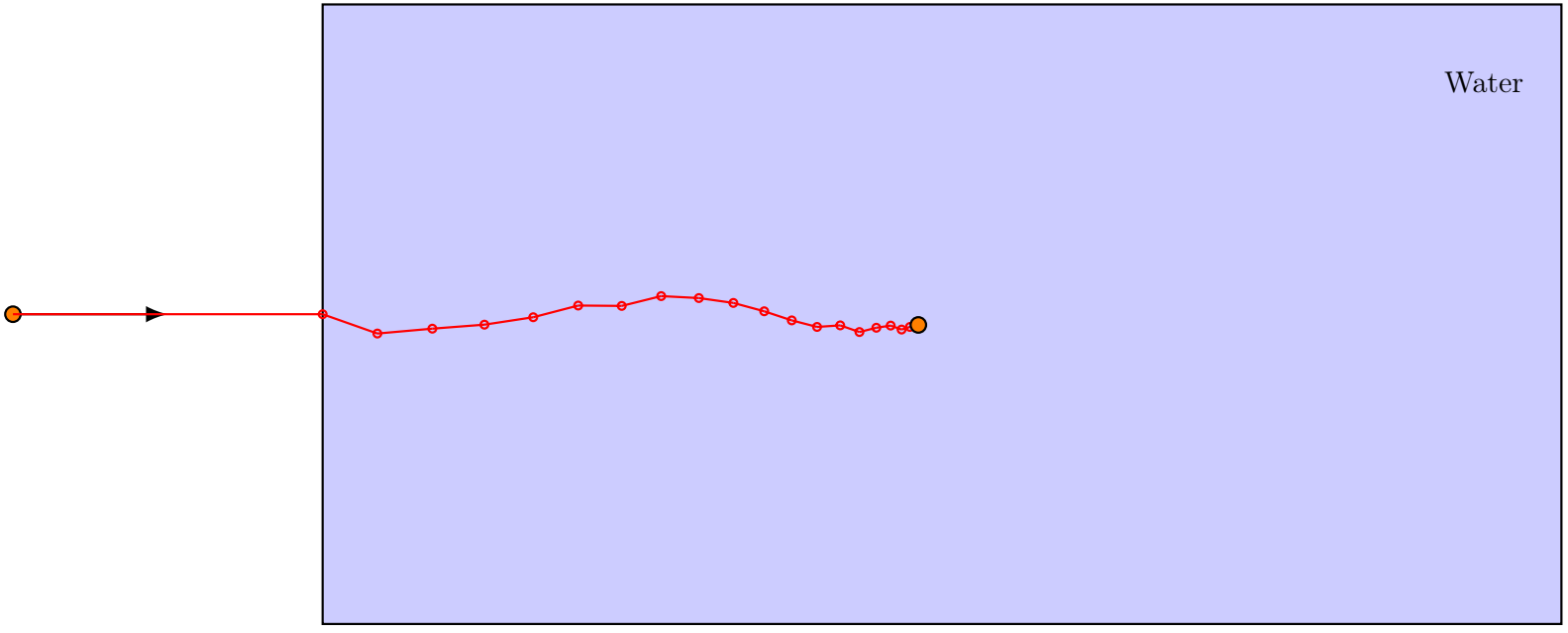

Trajectories of nuclei in materials

Reminder:

- range $\longrightarrow \frac{A}{Z^2}$, $< I >$, for the same velocity $R(^{12}C) = \frac{1}{3}R(proton)$
- LET $\longrightarrow Z^2$, $< I >$, for the same velocity $LET(^{12}C) = 36\, LET(proton)$

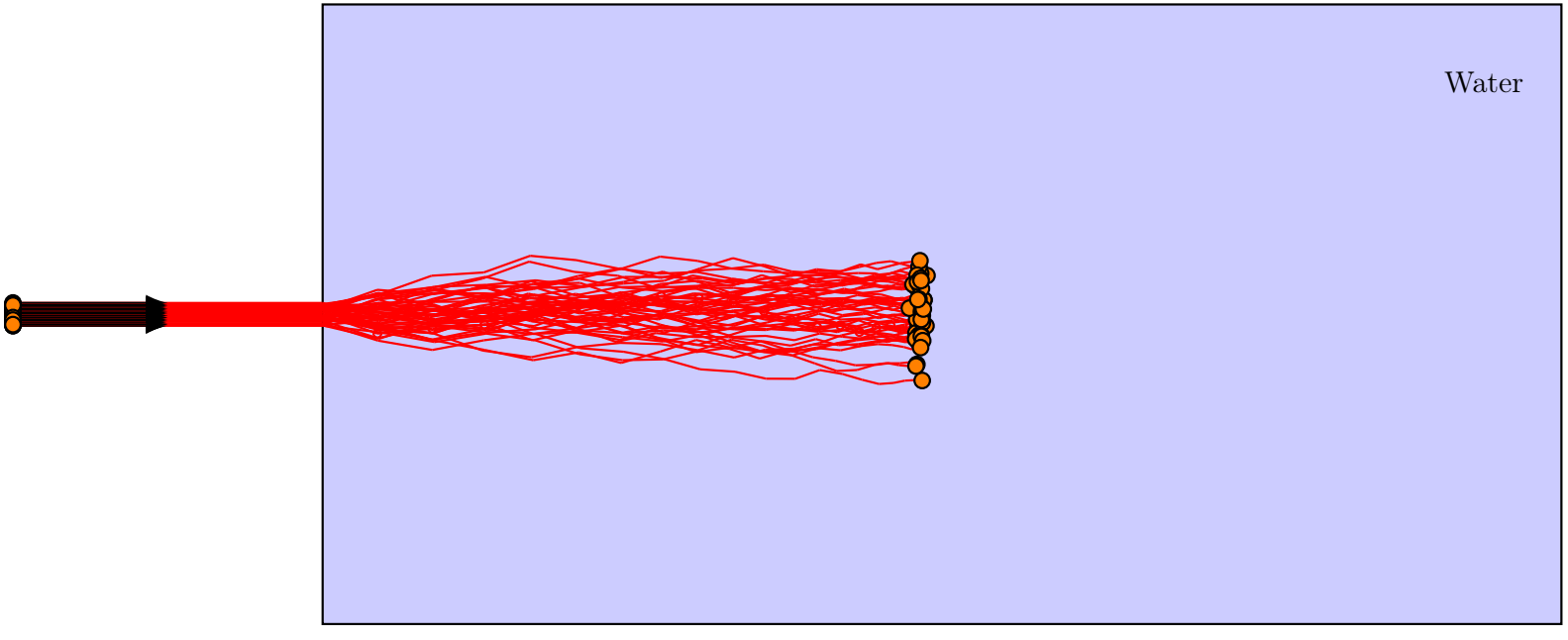

Trajectories of nuclei in materials

GEANT4 Simulation

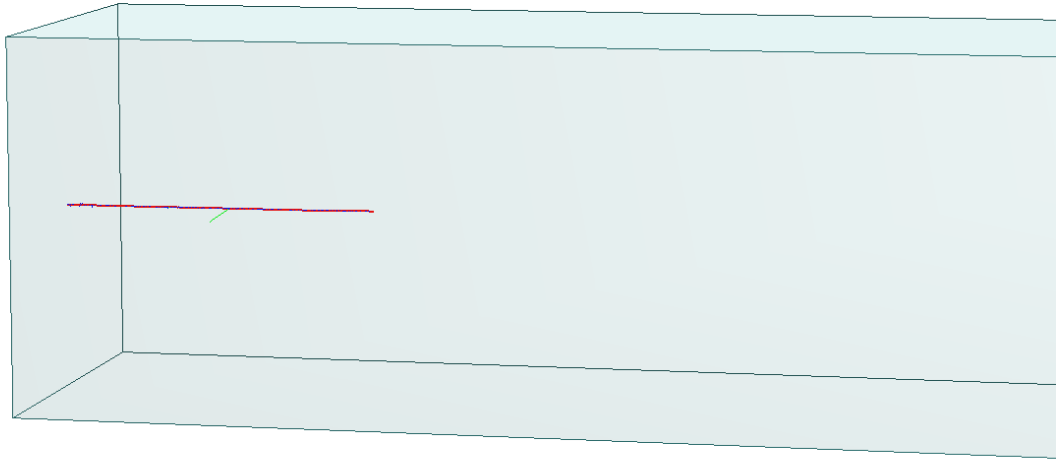

Trajectories of nuclei in materials

GEANT4 Simulation

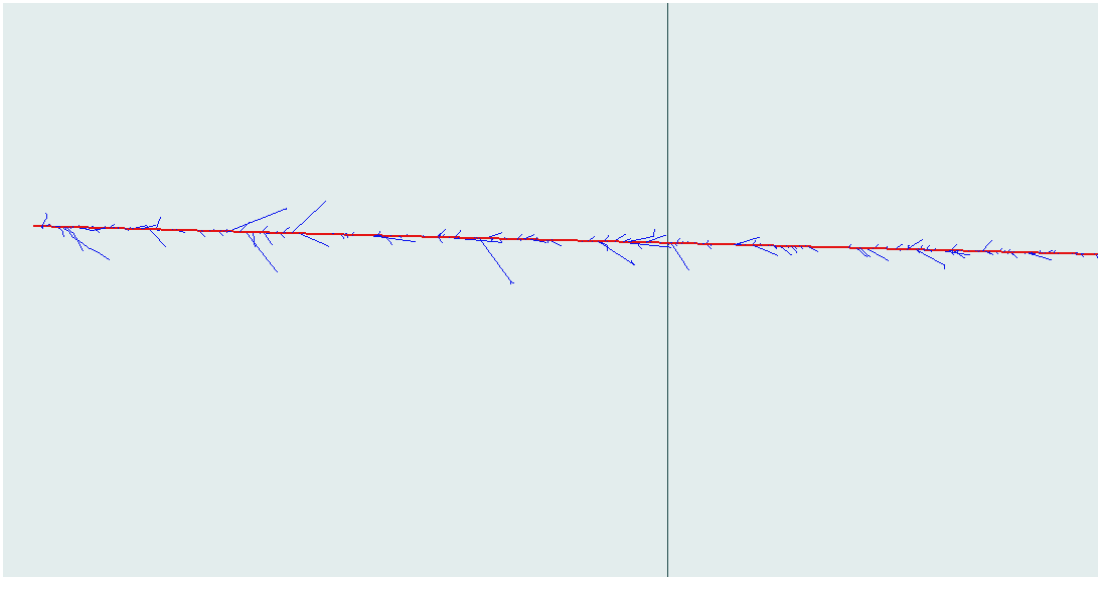

Summary on TPS Strategies

Analytical calculations

- short computation times for dose profiles and the transformed profile
- loss of accuracy both on dose profile computations and on profile transformations

Hybrid calculations

- long computation times for initial dose profiles and short computation times for the transformed profile
- loss of accuracy limited to the profile transformation

"Monte-Carlo" calculations

- The slowest since the number of Monte-Carlo calculations corresponds to the number of geometrical configurations taken into account
- The most accurate

1 Simulations for hadrontherapy

2 The role of nucleus-nucleus collisions

3 Nucleus-nucleus collision models

4 Benchmarking models to data

5 Nuclear Physics methods for hadrontherapy

Nucleus-Nucleus reactions

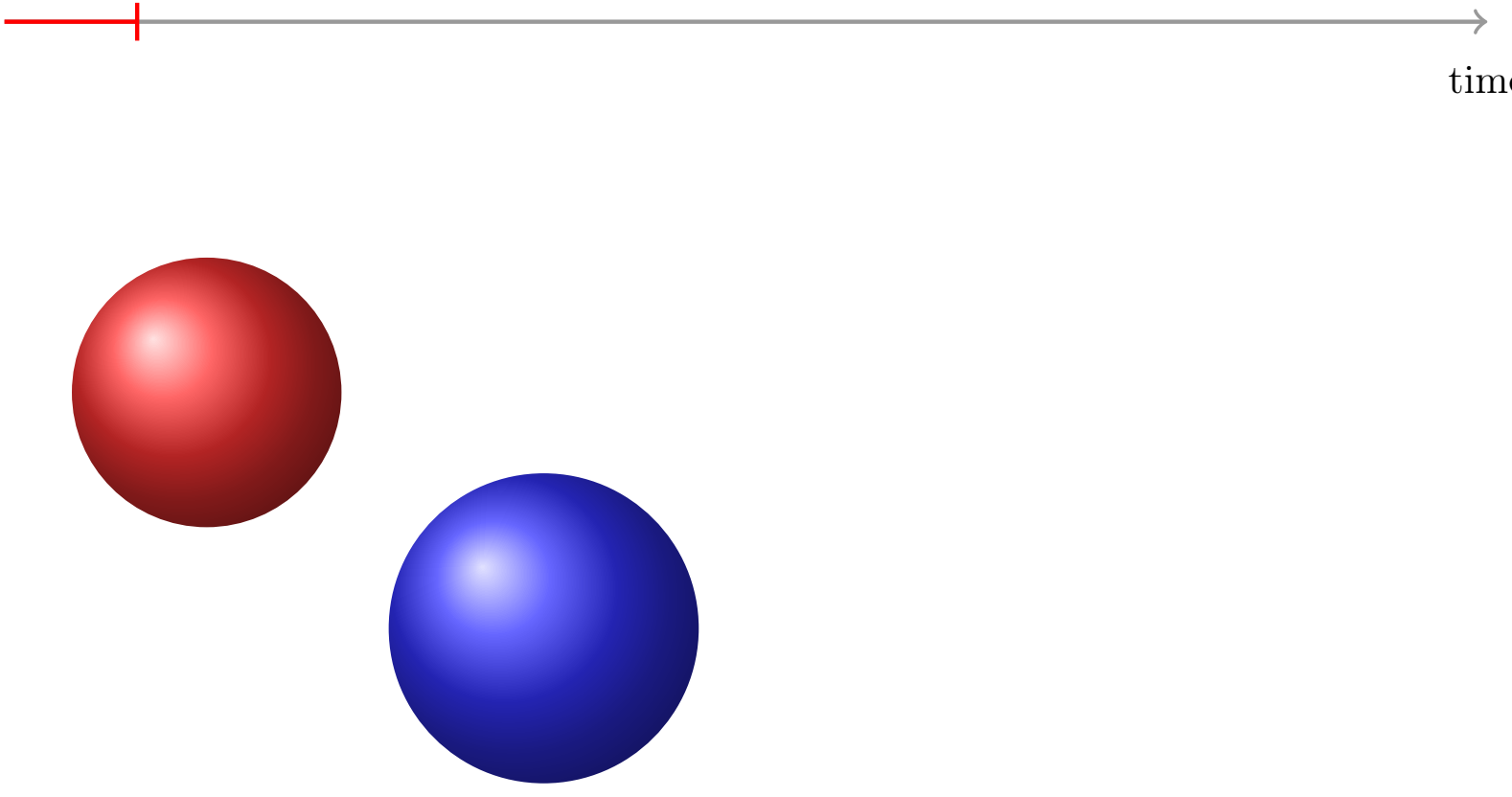

Nucleus-Nucleus reactions

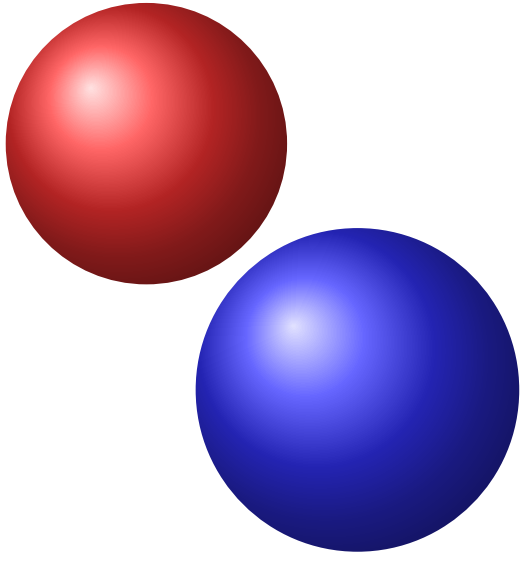

Nucleus-Nucleus reactions

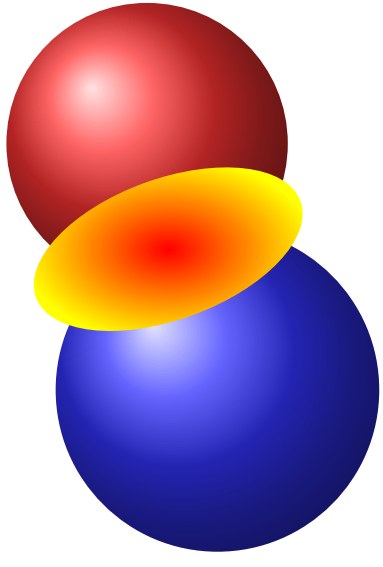

Nucleus-Nucleus reactions

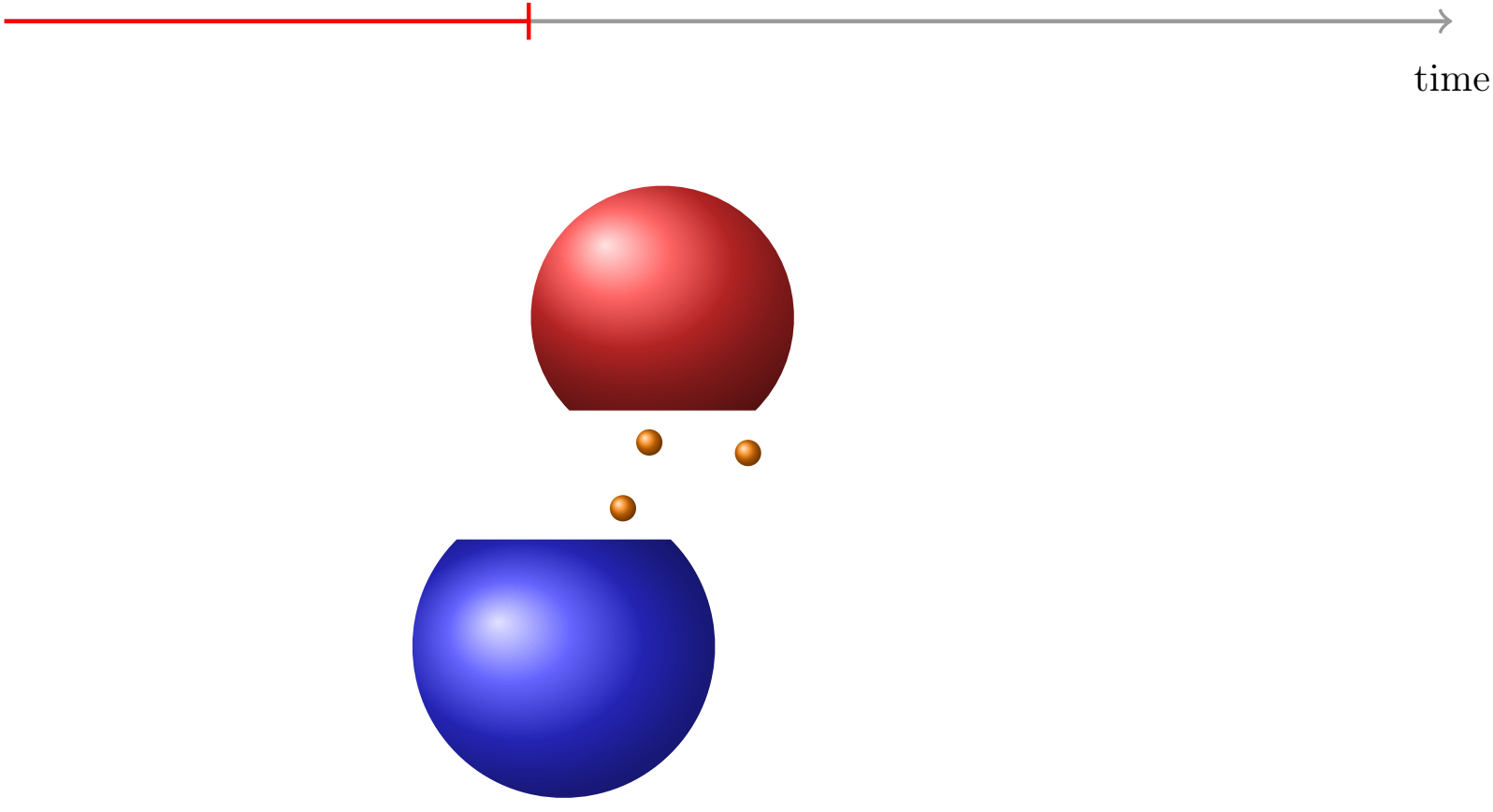

Nucleus-Nucleus reactions

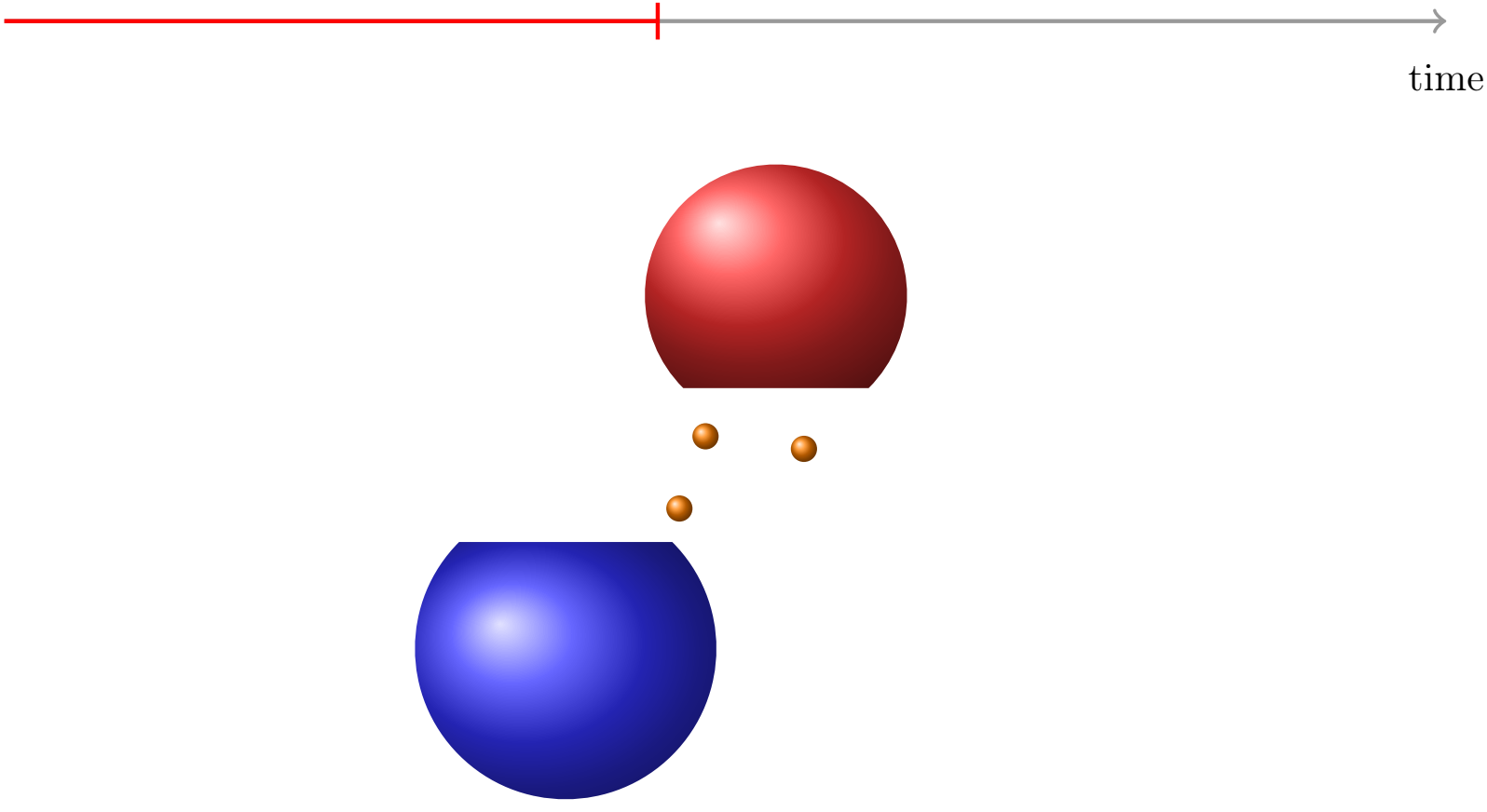

Nucleus-Nucleus reactions

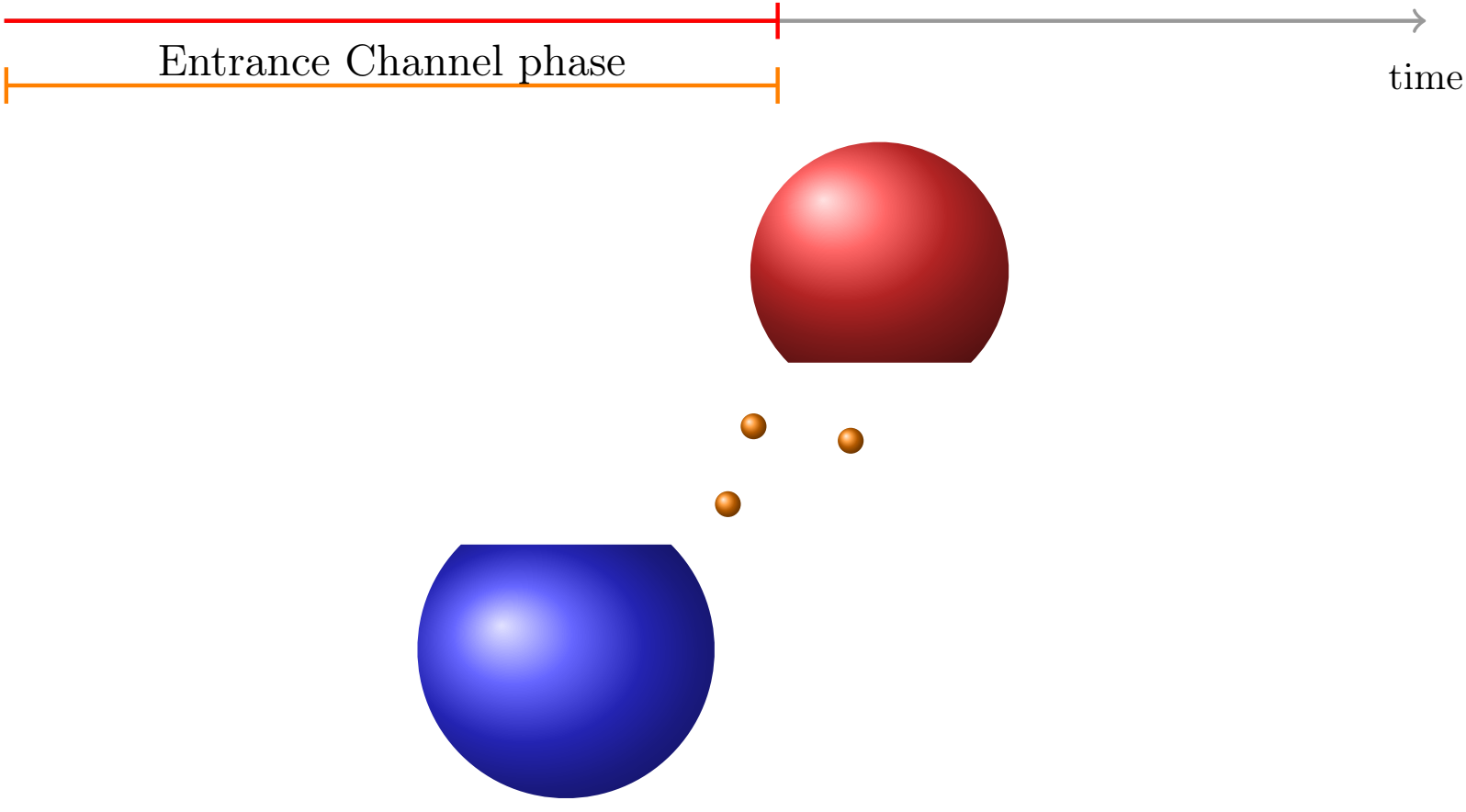

Nucleus-Nucleus reactions

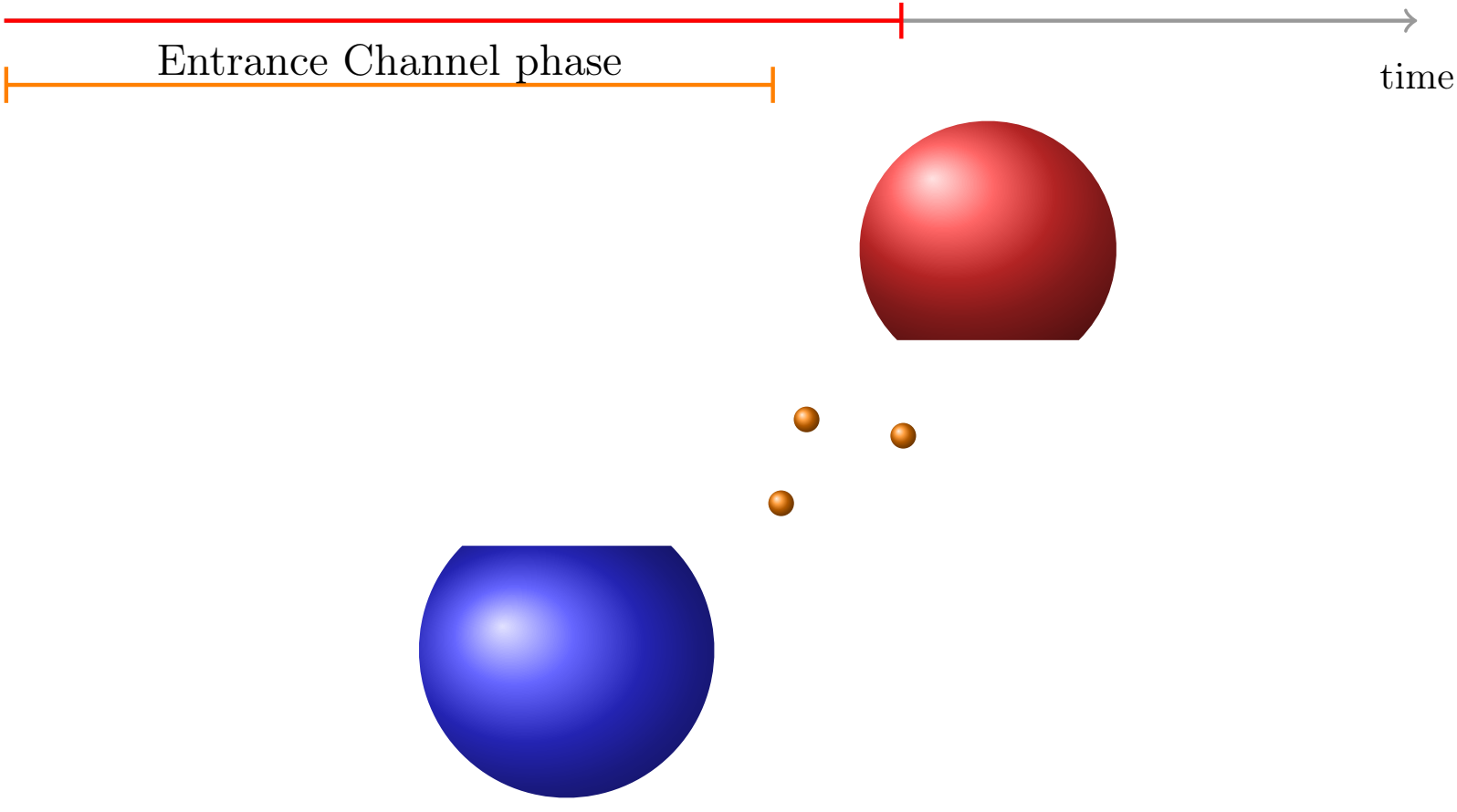

Nucleus-Nucleus reactions

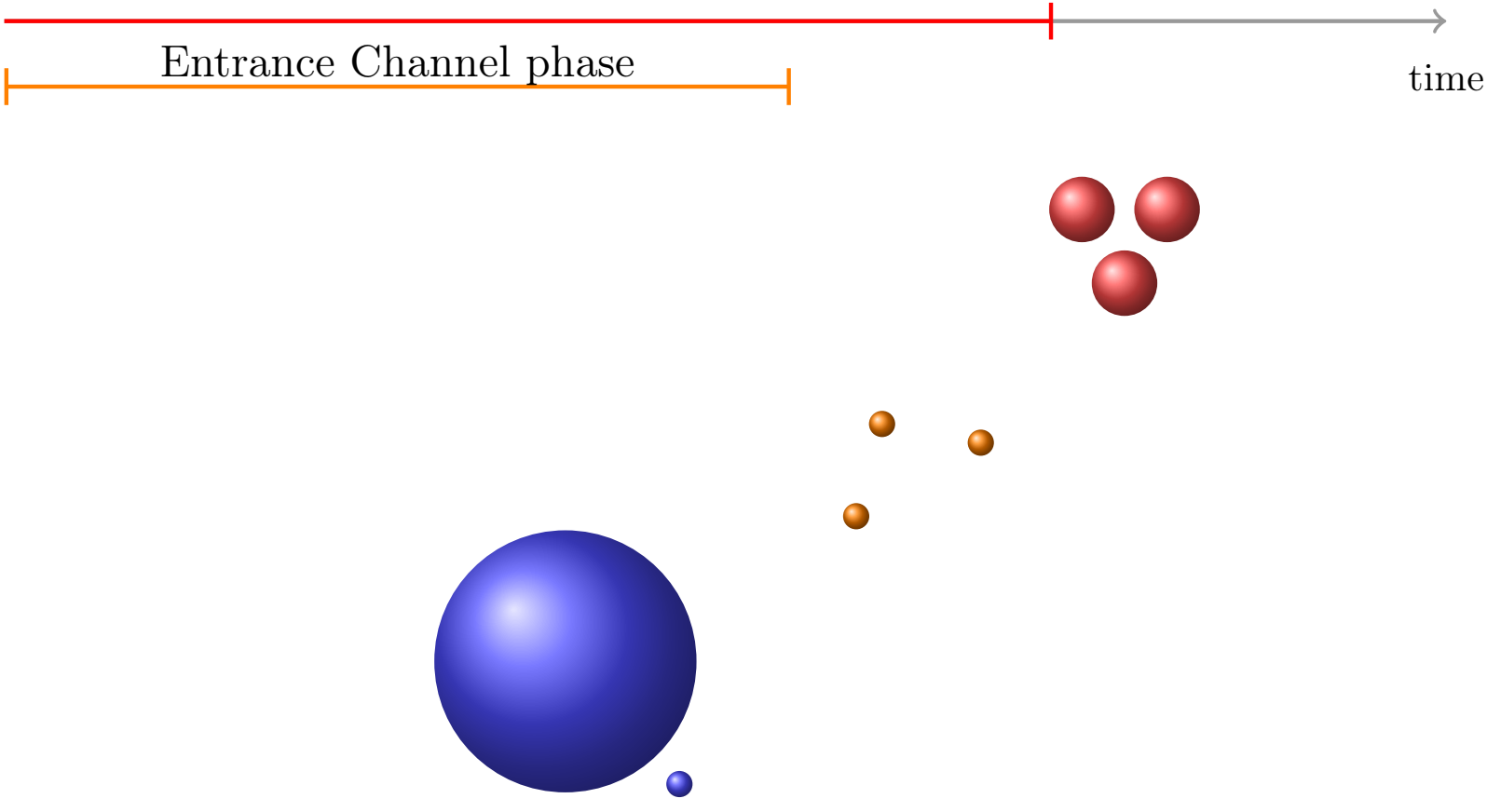

Nucleus-Nucleus reactions

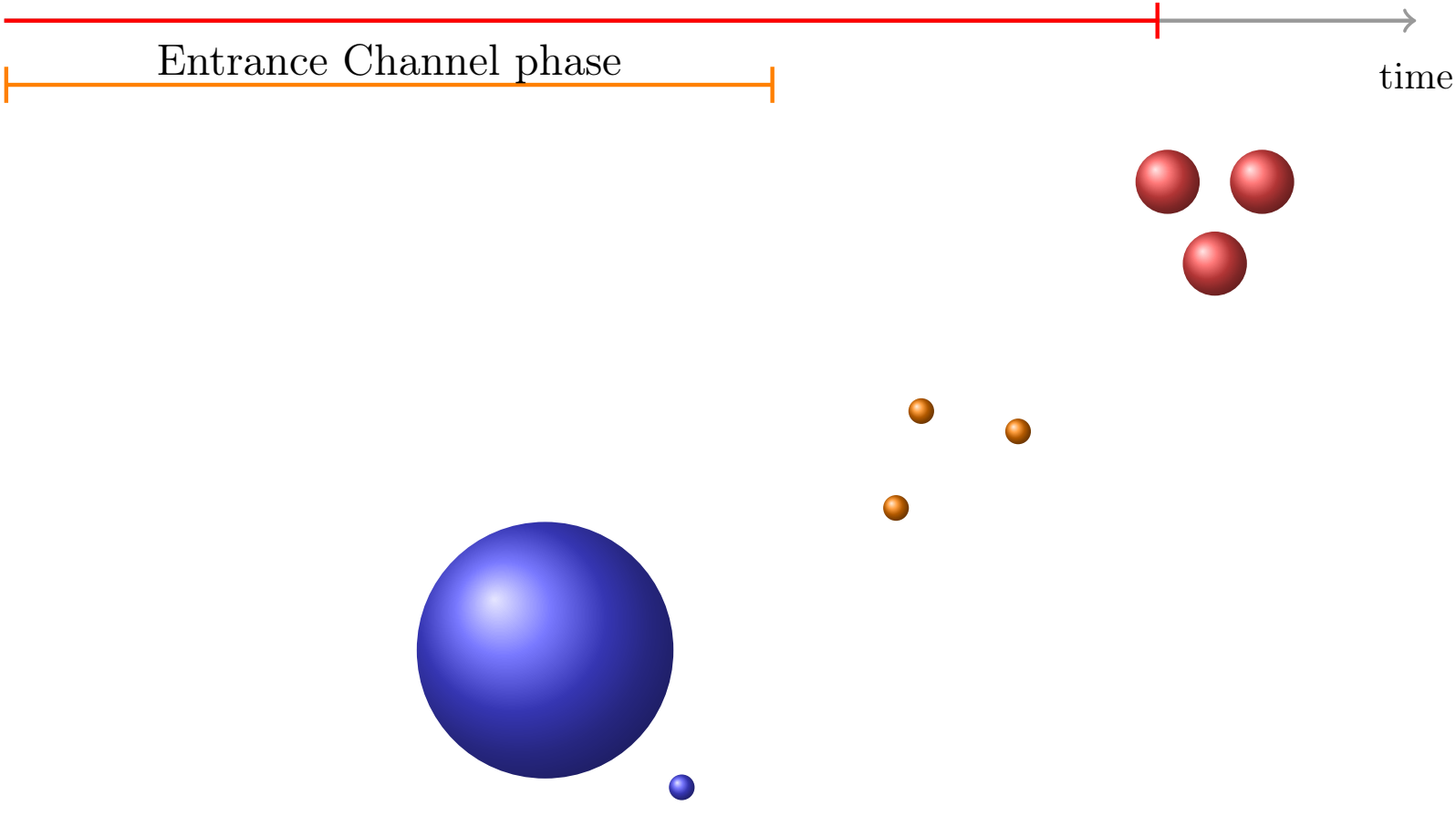

Nucleus-Nucleus reactions

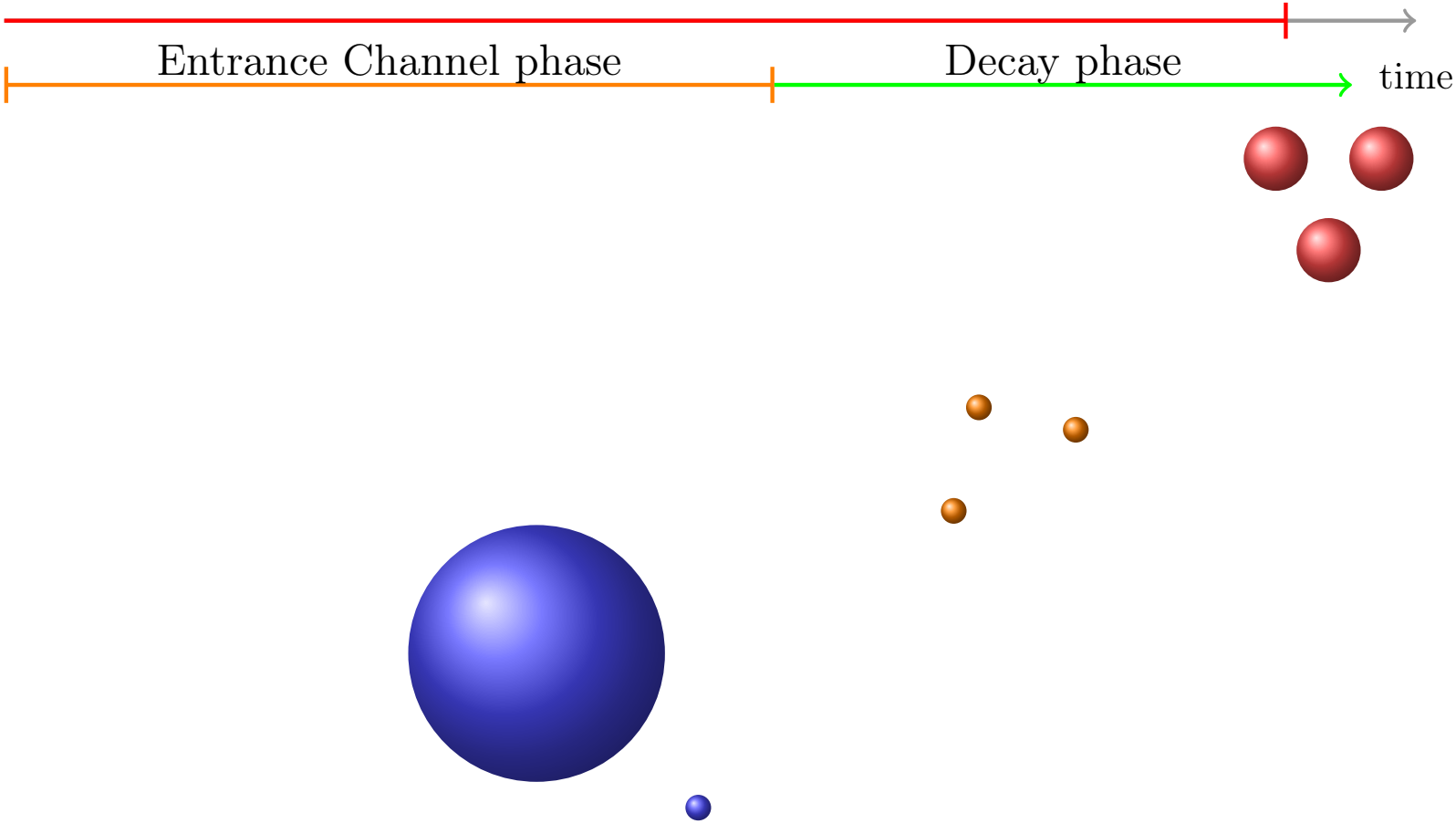

Nucleus-Nucleus reactions

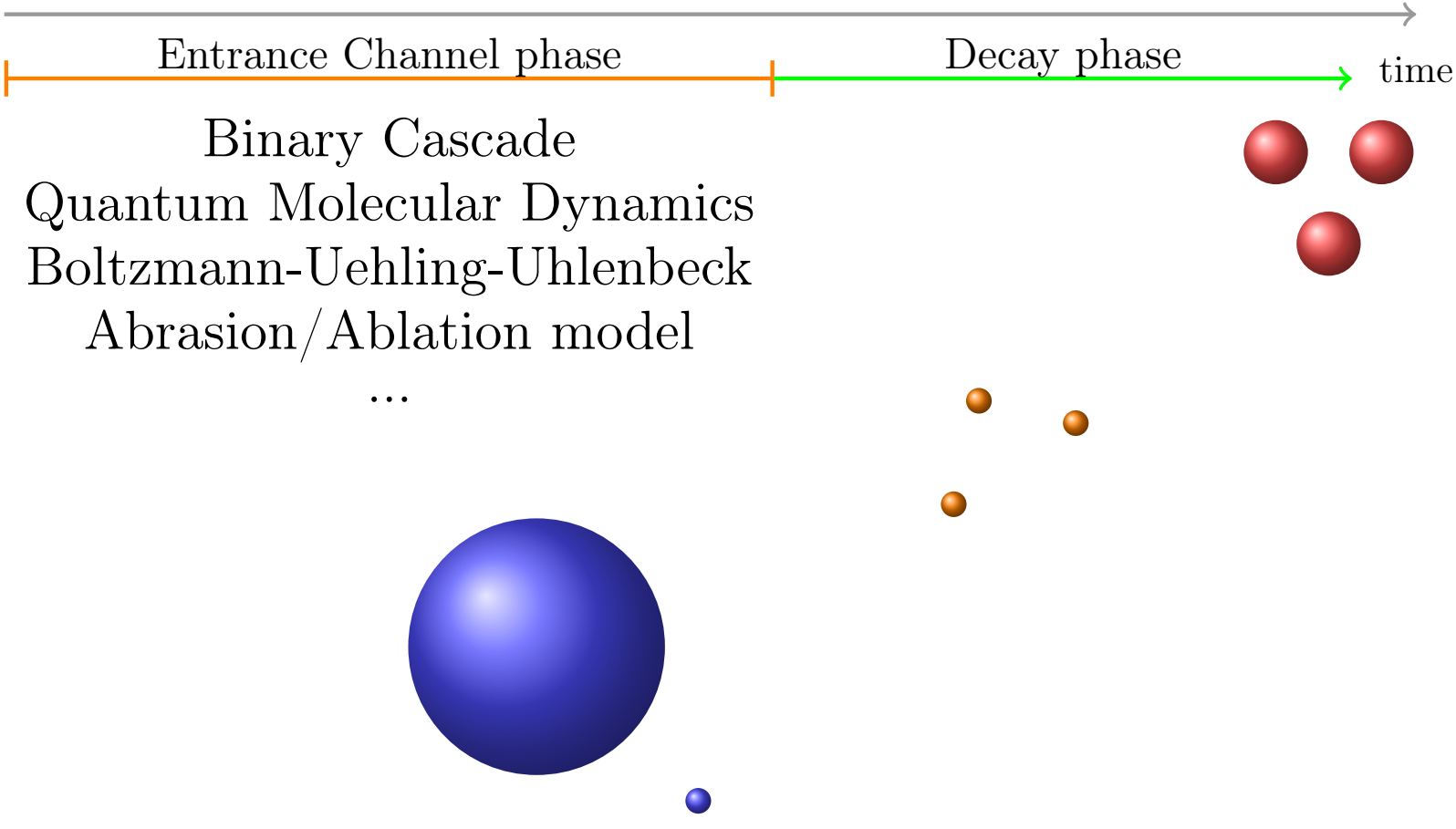

Nucleus-Nucleus reactions

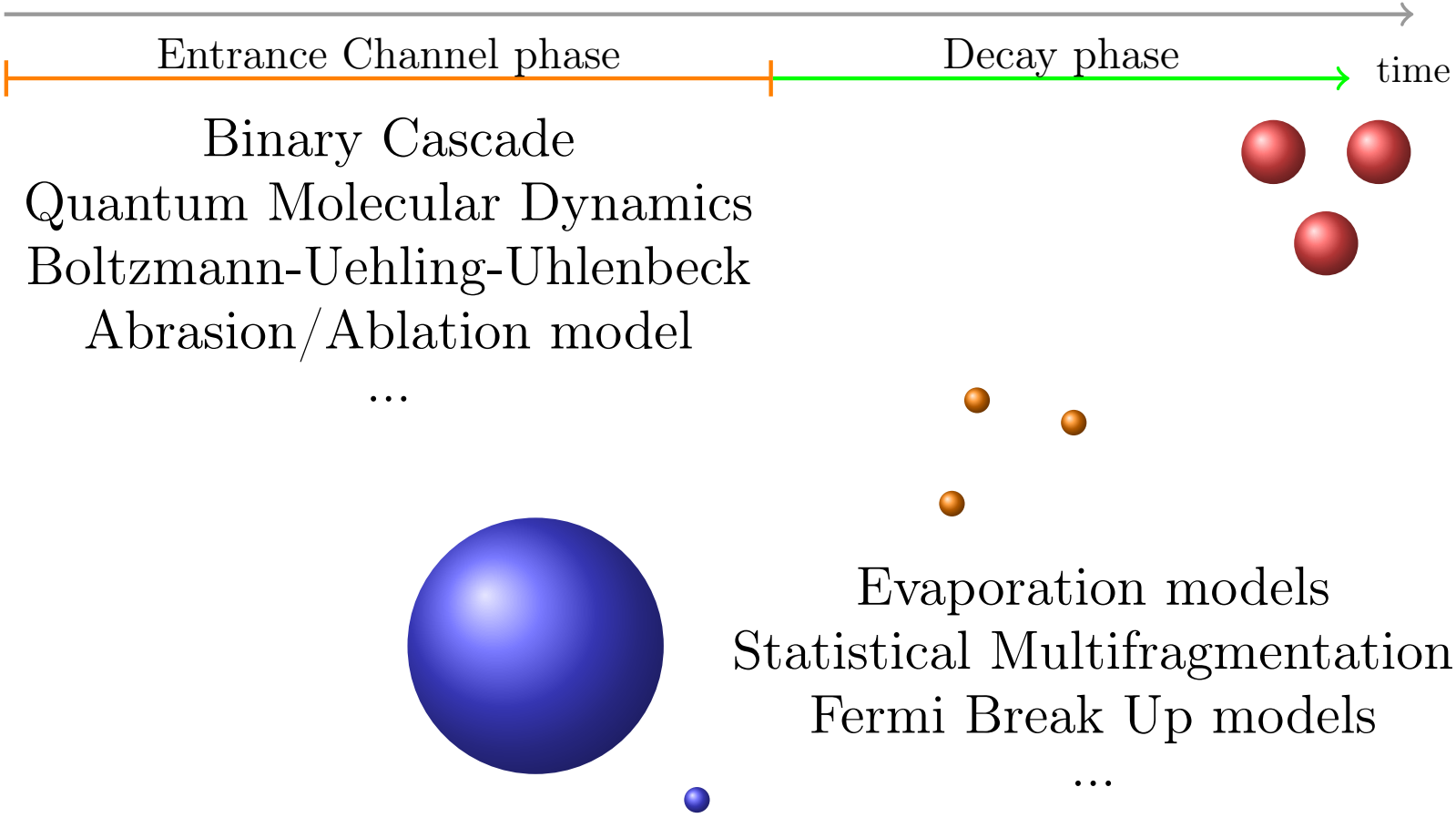

Trajectories of nuclei in materials (continued)

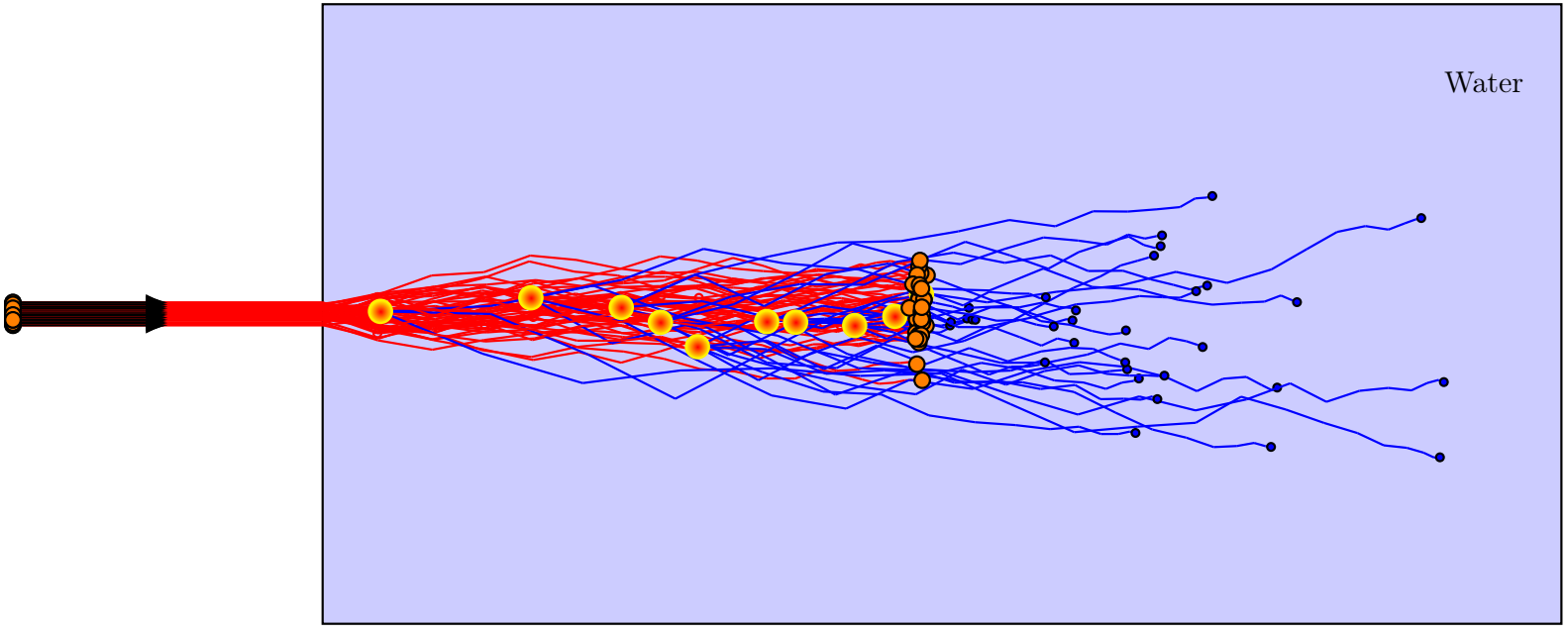

Trajectories of nuclei in materials (continued)

- less projectiles will reach the Bragg Peak.
- the fragments have roughly the same velocity than the fragmenting nucleus and will deposit their energy at a longer range $\longrightarrow$ *LET* distribution at a given depth.
- the fragmentation is an endothermic process.

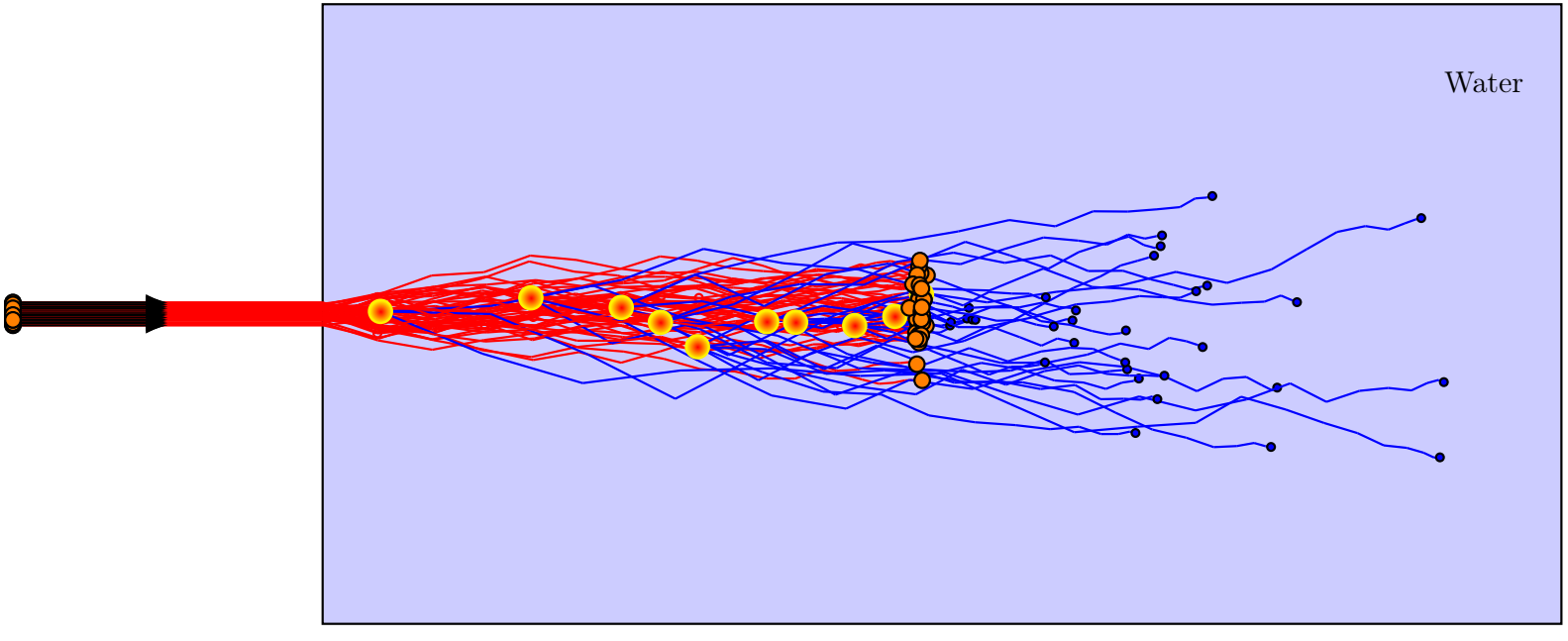

Trajectories of nuclei in materials

GEANT4 Simulation

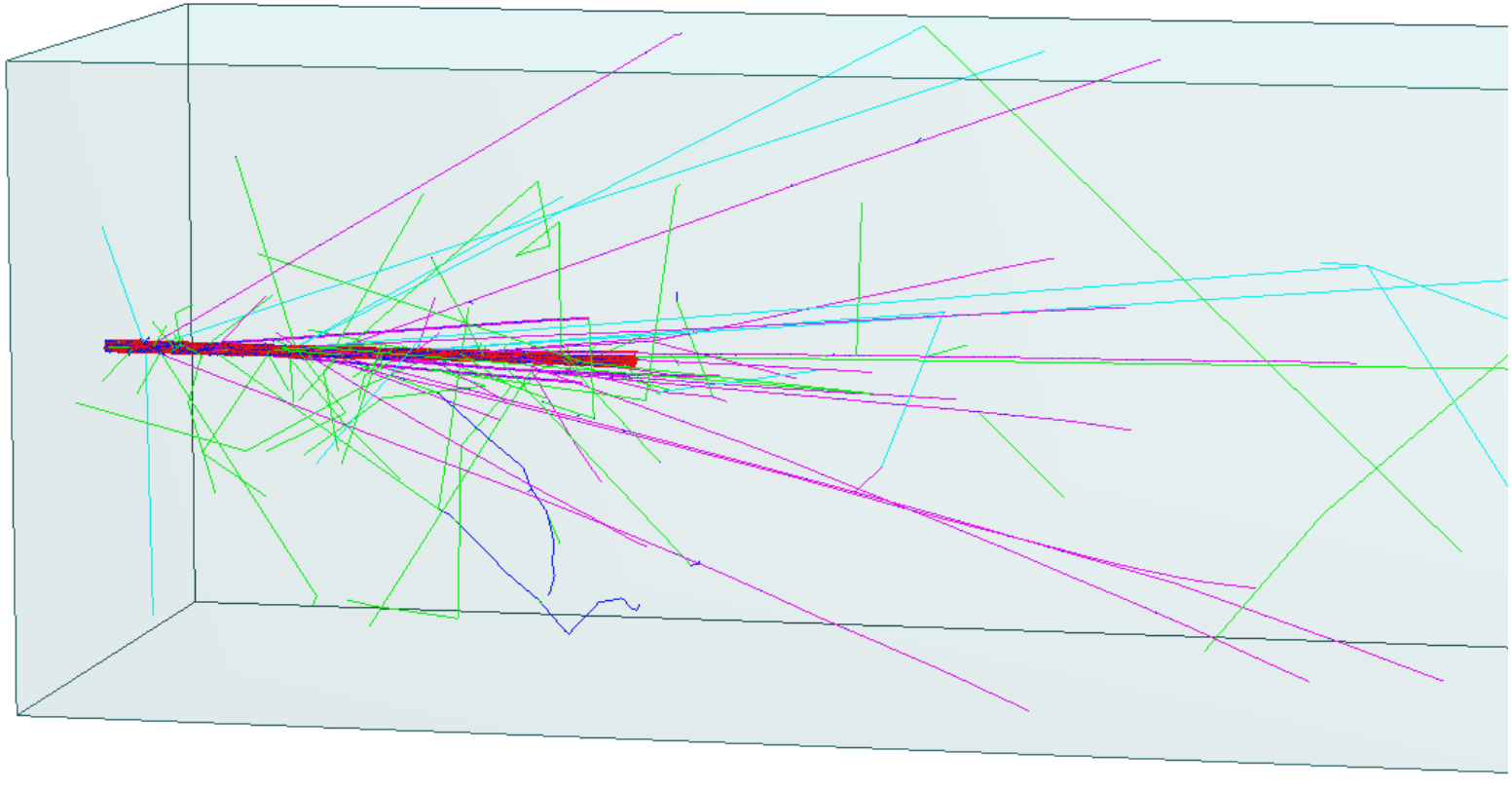

Contribution of secondary fragments

- the fragments emitted by the quasi-projectile have a velocity close to the projectile velocity and hence a longer range than the projectile range

Contribution of secondary fragments

- the fragments emitted by the quasi-projectile have a velocity close to the projectile velocity and hence a longer range than the projectile range
- the fragments emitted by the quasi-target have a small velocity and have a very small range (few μm at most)

Contribution of secondary fragments

- the fragments emitted by the quasi-projectile have a velocity close to the projectile velocity and hence a longer range than the projectile range
- the fragments emitted by the quasi-target have a small velocity and have a very small range (few μm at most)
- the mid-velocity fragments have also a slightly longer range than the projectile range

Contribution of secondary fragments

- the fragments emitted by the quasi-projectile have a velocity close to the projectile velocity and hence a longer range than the projectile range
- the fragments emitted by the quasi-target have a small velocity and have a very small range (few μm at most)
- the mid-velocity fragments have also a slightly longer range than the projectile range
- the most probable collisions are the peripheral collisions

Contribution of secondary fragments

- the fragments emitted by the quasi-projectile have a velocity close to the projectile velocity and hence a longer range than the projectile range
- the fragments emitted by the quasi-target have a small velocity and have a very small range (few μm at most)
- the mid-velocity fragments have also a slightly longer range than the projectile range
- the most probable collisions are the peripheral collisions
  - $v_{QP} \lesssim v_{proj}$, $A_{QP} \approx A_{proj}$, $Z_{QP} \approx Z_{proj}$, E^*_{QP} small
  - $v_{fragments} \approx v_{QP}$
  - only very few mid-rapidity fragments

Contribution of secondary fragments

- the fragments emitted by the quasi-projectile have a velocity close to the projectile velocity and hence a longer range than the projectile range
- the fragments emitted by the quasi-target have a small velocity and have a very small range (few μm at most)
- the mid-velocity fragments have also a slightly longer range than the projectile range
- the most probable collisions are the peripheral collisions
  - $v_{QP} \lesssim v_{proj}$, $A_{QP} \approx A_{proj}$, $Z_{QP} \approx Z_{proj}$, E^*_{QP} small
  - $v_{fragments} \approx v_{QP}$
  - only very few mid-rapidity fragments

As a consequence

The dose delocalisation is mainly due to the fragments emitted by the quasi-projectile.

Energy balance

Energy conservation law

$$\Delta m_{A_p,Z_p}c^2 + T_{A_p,Z_p} + \Delta m_{A_t,Z_t}c^2 = \sum_i \left[\Delta m_{A_i,Z_i}c^2 + T_i\right]$$

$$\sum_i T_i = T_{A_p,Z_p} + Q$$

$$Q = \Delta m_{A_p,Z_p}c^2 + \Delta m_{A_t,Z_t}c^2 - \sum_i \Delta m_{A_i,Z_i}c^2$$

for the small systems ($Z < 26$), Q is negative $\Longrightarrow \sum_i T_i < T_{A_p,Z_p}$

Example

$$^{12}C + ^{16}O \longrightarrow 3\,\alpha + ^{12}C + 2\,p + 2\,n$$

$$Q = \Delta m_{^{12}C}c^2 + \Delta m_{^{16}O}c^2 - 3\,\Delta m_{^4He}c^2 - \Delta m_{^{12}C}c^2 - 2\,\Delta m_{proton} - 2\,\Delta m_{neutron}$$

$$Q = 0.\,keV - 4737.05\,keV - 3 \times 2424.91\,keV - 0.\,keV - 2 \times 7289.03\,keV - 2 \times 8071.37\,keV = -42732.58\,keV$$

$\approx 42.7\,MeV$ are lost due to the nucleus-nucleus collision!

Effect on the Bragg curve for protons

GEANT4 simulations

$N(x) \approx N_0 e^{-x/\lambda}$

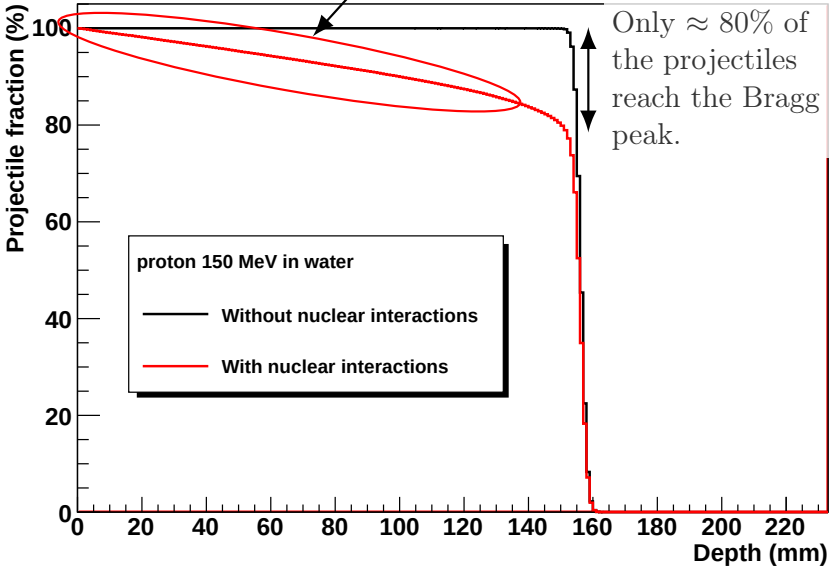

The Bragg Peak location is not modified

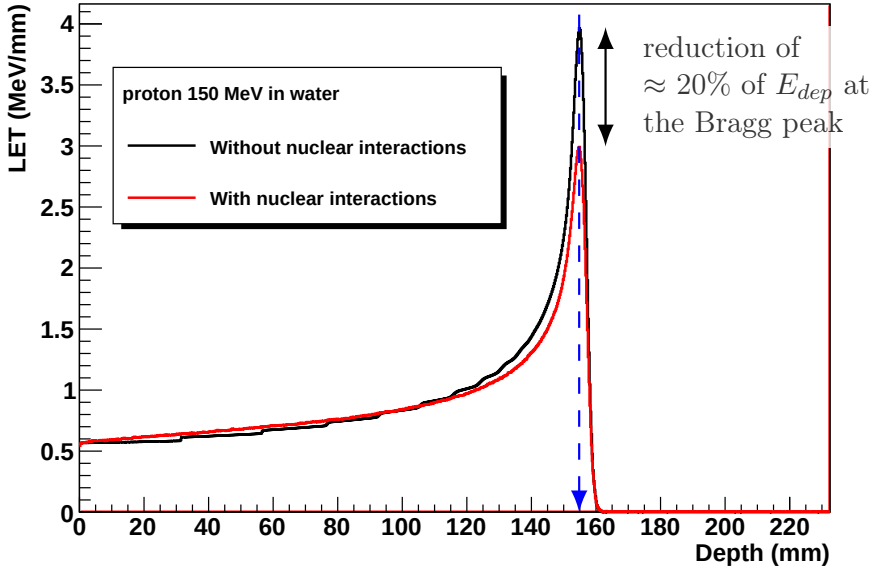

$\int LET(x)dx = E_{proj}$

$\int LET(x)dx = 0.97\ E_{proj}$

Effect on the Bragg curve for ^{12}C

GEANT4 simulations

$N(x) \approx N_0 e^{-x/\lambda}$

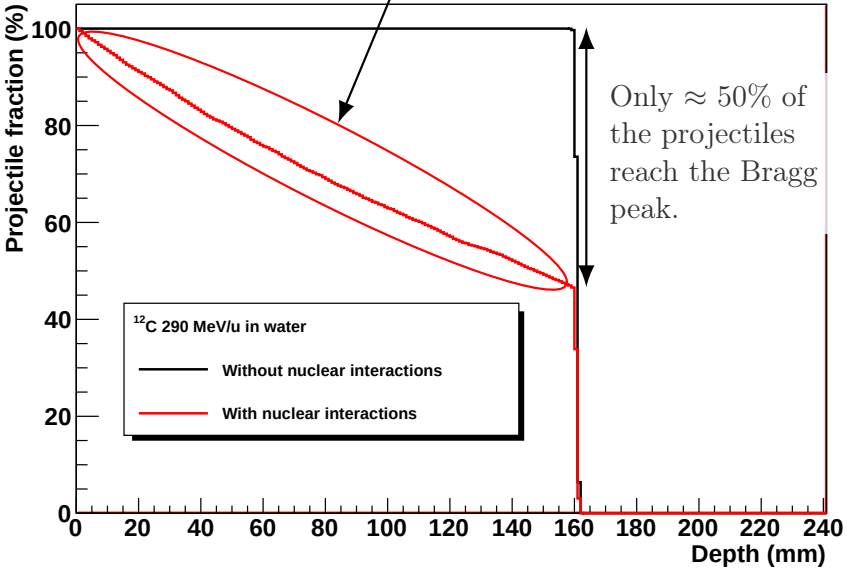

The Bragg Peak location is not modified

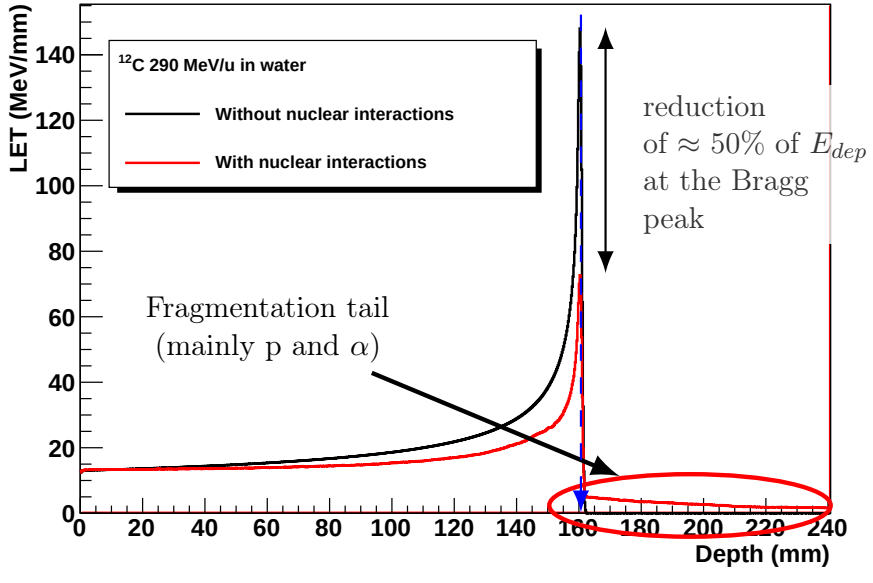

$\int LET(x)dx = E_{proj}$

$\int LET(x)dx = 0.93\ E_{proj}$

To summarize...

The nucleus-nucleus collisions:

- Do not change the location of the Bragg peak.
- Reduce the number of projectiles all along the path $N(x) \approx N_0 e^{-x/\lambda}$ with $\lambda = \frac{M_{mol}}{\mathcal{N}_a \, \rho \, \sigma}$.
- Reduce the energy deposition at the Bragg peak $LET_{Nuc}(x_{BP}) \approx LET_{EM}(x_{BP}) e^{-x_{BP}/\lambda}$.
- Lead to an energy deposition beyond the Bragg peak: contribution of secondary particles.
- Reduces the total energy deposited in the target.

To summarize...

The nucleus-nucleus collisions:

- Do not change the location of the Bragg peak.
- Reduce the number of projectiles all along the path $N(x) \approx N_0 e^{-x/\lambda}$ with $\lambda = \frac{M_{mol}}{\mathcal{N}_a \rho \sigma}$.
- Reduce the energy deposition at the Bragg peak $LET_{Nuc}(x_{BP}) \approx LET_{EM}(x_{BP}) e^{-x_{BP}/\lambda}$.
- Lead to an energy deposition beyond the Bragg peak: contribution of secondary particles.
- Reduces the total energy deposited in the target.

As a consequence

The dose map is significantly changed by the nucleus-nucleus collisions!

Influence of the nucleus-nucleus collision cross section

GEANT4 simulations

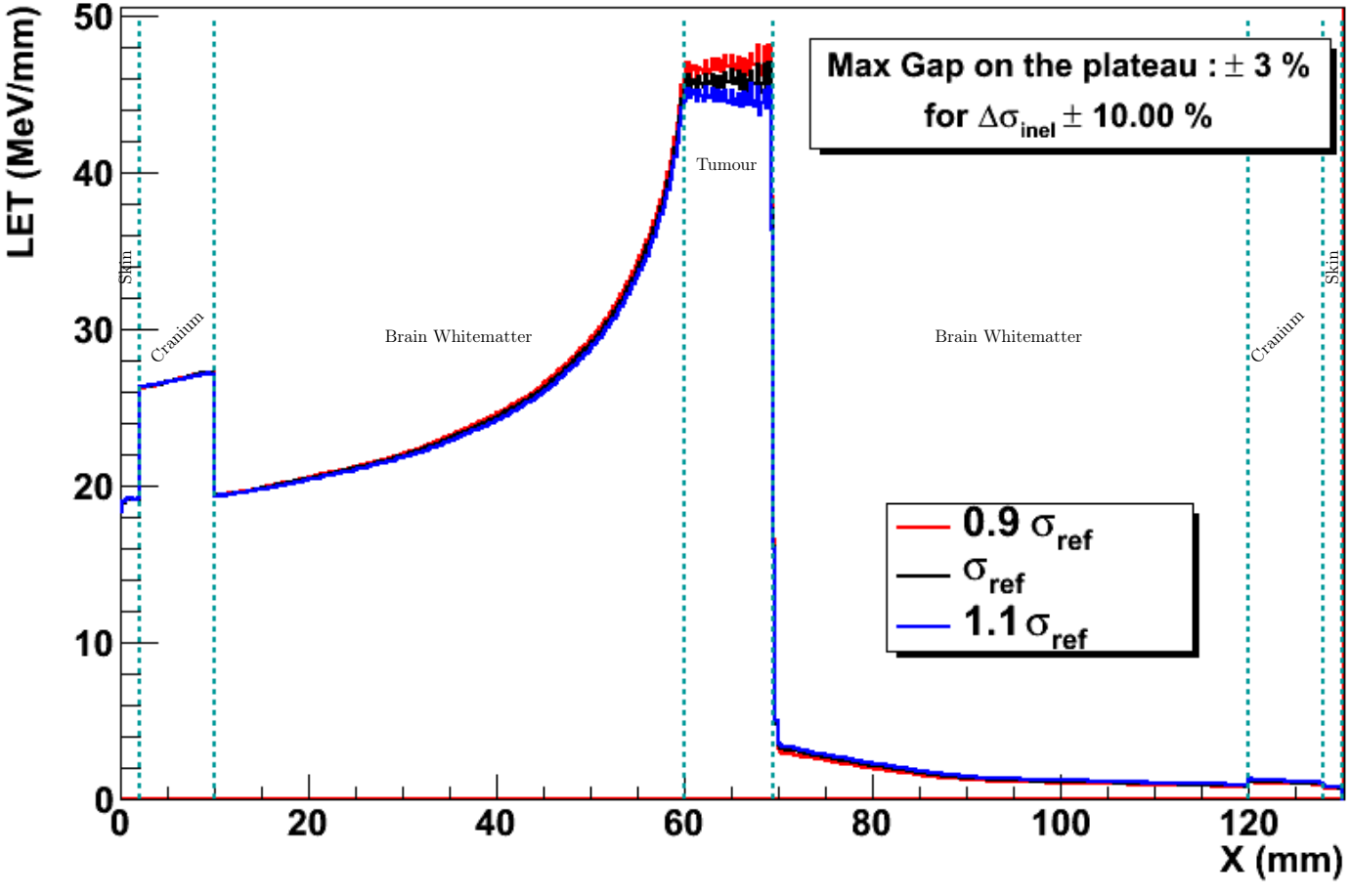

Secondary particles multiplicities

Experimental data (GSI)

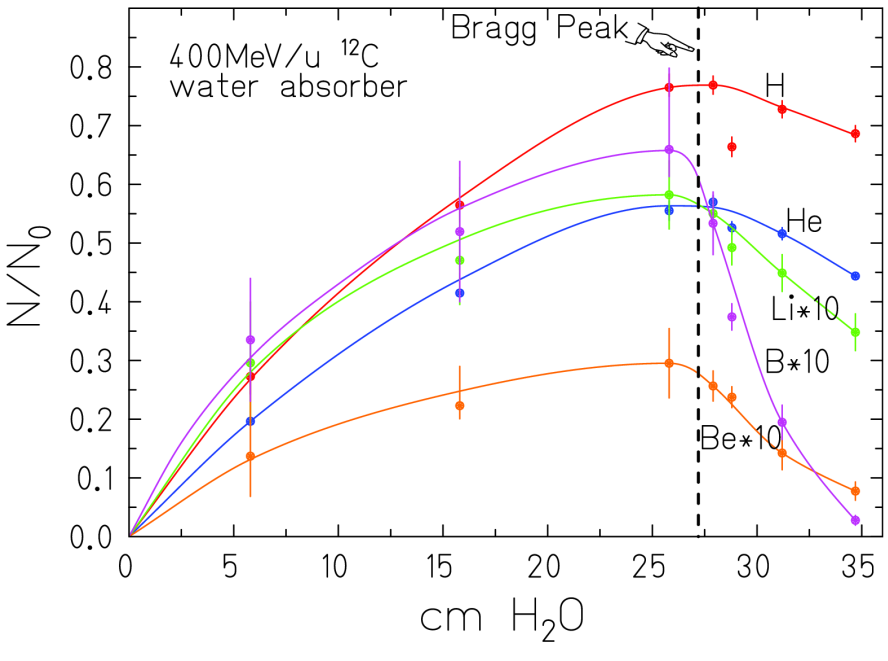

E.Haettner, H. Iwase, and D. Schardt,
Radiat. Prot. Dosim. 122 (2006) 485–487

GEANT4 simulation

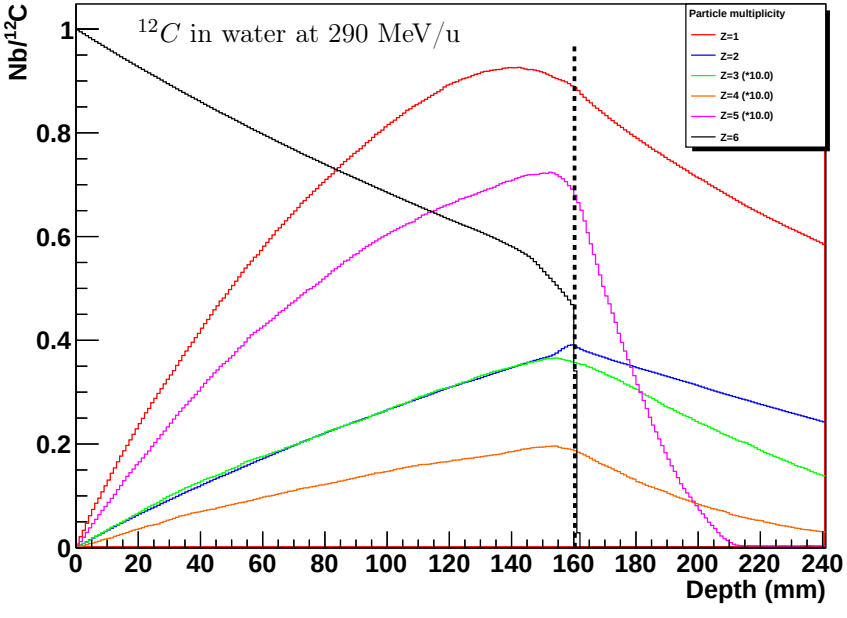

Secondary particles multiplicities

Experimental data (GSI)

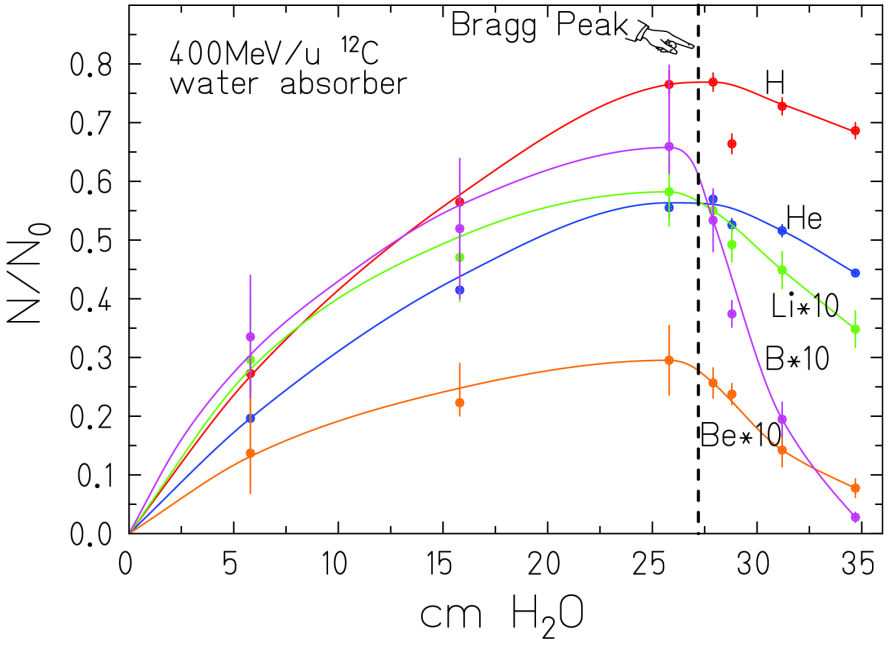

E.Haettner, H. Iwase, and D. Schardt,
Radiat. Prot. Dosim. 122 (2006) 485–487

Analytic calculation

^{12}C in water at 284 MeV/u

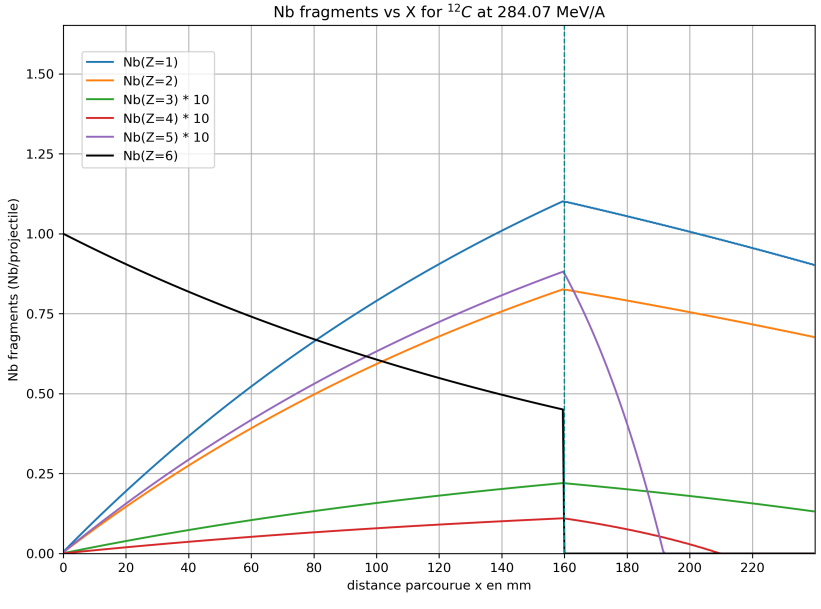

Secondary particles energy deposition

GEANT4 simulations

^{12}C in water at 290 MeV/u

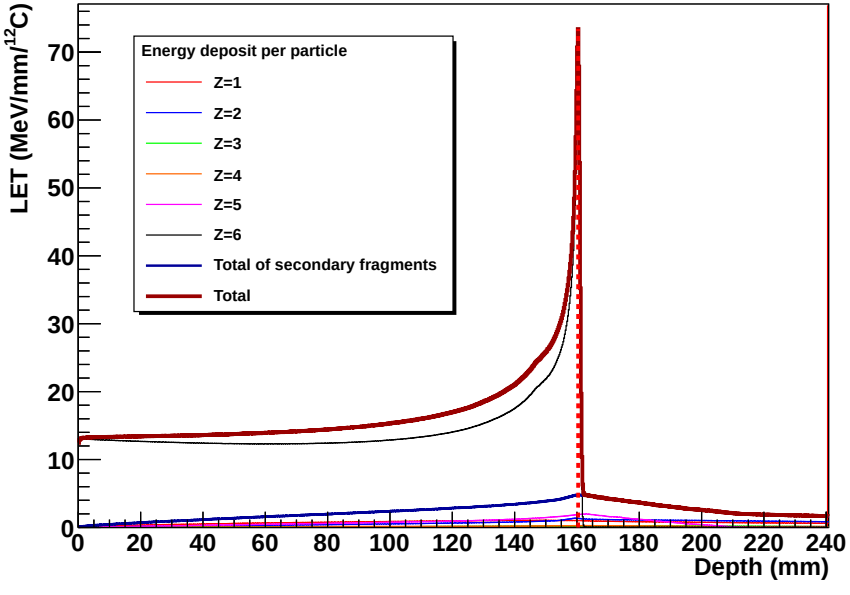

zoom on low LET values

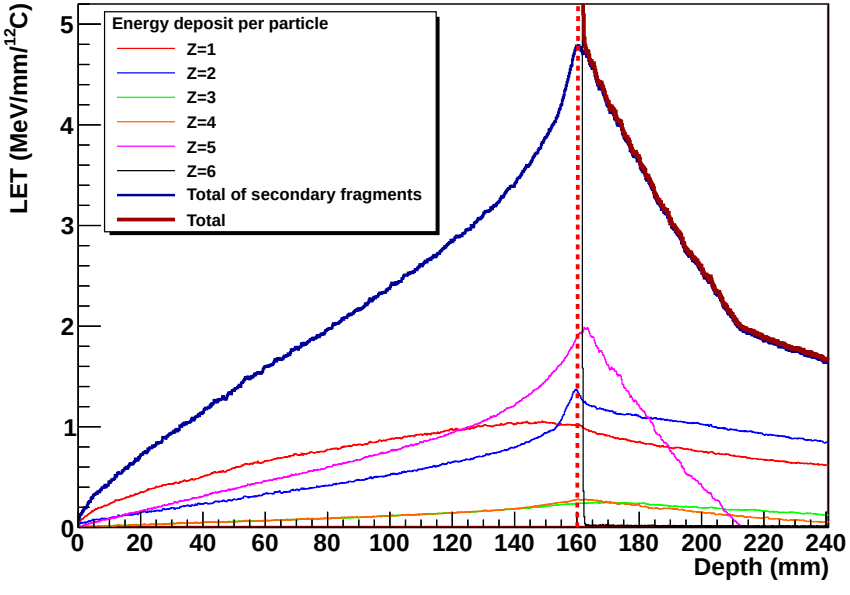

The contribution of secondary particles is ≈ 7 % at the Bragg Peak

Secondary particles energy deposition

Analytic calculation

^{12}C in water at 284 MeV/u

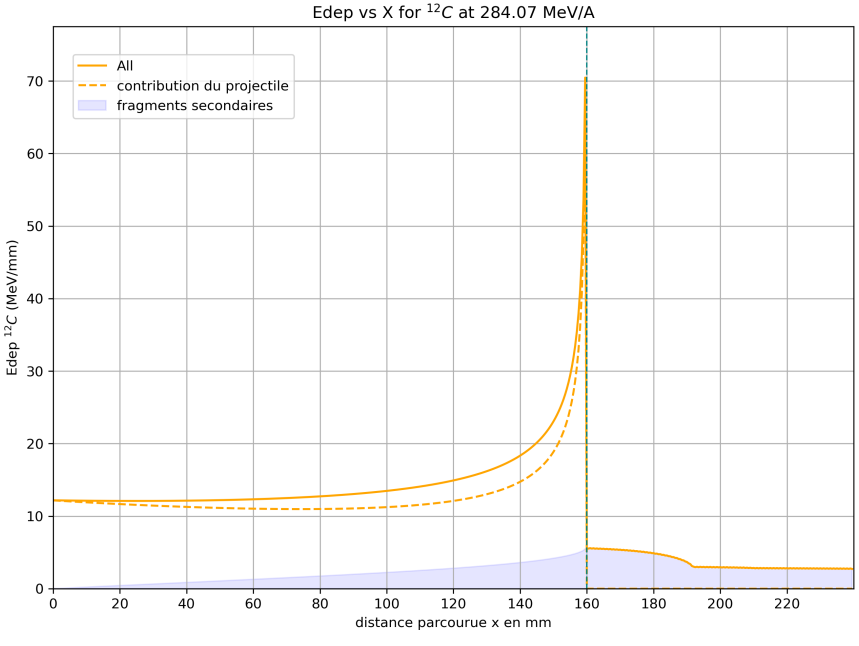

zoom on low LET values

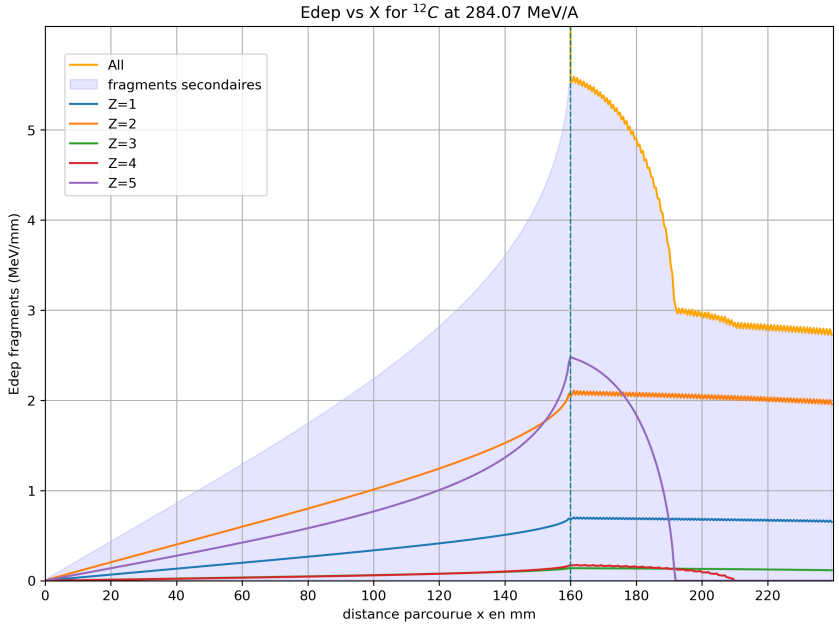

The contribution of secondary particles is ≈ 7 % at the Bragg Peak

1 Simulations for hadrontherapy

2 The role of nucleus-nucleus collisions

3 Nucleus-nucleus collision models

4 Benchmarking models to data

5 Nuclear Physics methods for hadrontherapy

Analytical collision model

Average fragment multiplicities

Fragment	$< N_{frag} >$
neutron	2.02
proton	2
α	1.5
^{6}Li	0.04
^{7}Be	0.02
^{10}B	0.16

$$\sum_{fragments} < N_{frag} > \times A_{frag} = A_{proj}$$

$$\sum_{fragments} < N_{frag} > \times Z_{frag} = Z_{proj}$$

The nucleus-nucleus collision models in GEANT4

The entrance channel models in GEANT4

- Binary Cascade (BIC)
- Quantum Molecular Dynamics (QMD)

The decay models in GEANT4

- Evaporation model (EVAP) or Generalized Evaporation Model (GEM) for all nuclei.
- Fermi Break Up (FBU) for $4 < A < 17$ and $Z < 9$.
- Statistical Multifragmentation Model (MF) for $A > 5$ and $E^*/A > 3\,MeV$.

The decay models can be used simultaneously in GEANT4 for the first decay of the excited nucleus. The secondary decays are always done through the evaporation model.

The BIC model in GEANT4

J.Cugnon, C. Volant and S. Vuillier, Nuc. Phys. A 620 (1997) 475-509

G. Folger, V.N. Ivanchenko, and J. P. Wellisch, Eur. Phys. Jour. A 21, 407-417 (2004)

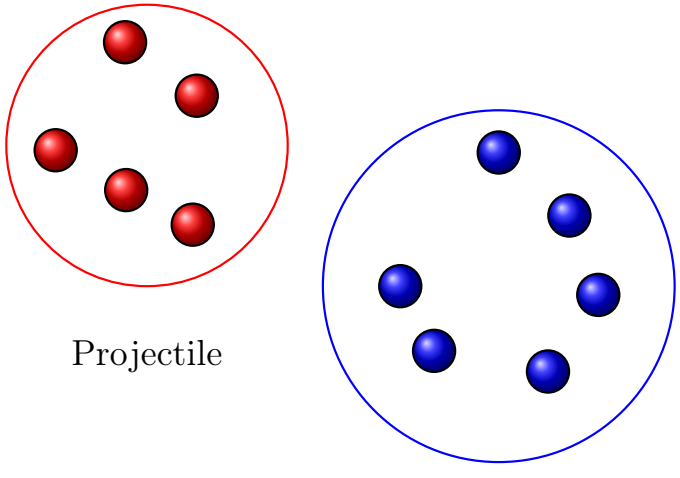

Projectile

Target

The BIC model in GEANT4

J.Cugnon, C. Volant and S. Vuillier, Nuc. Phys. A 620 (1997) 475-509

G. Folger, V.N. Ivanchenko, and J. P. Wellisch, Eur. Phys. Jour. A 21, 407-417 (2004)

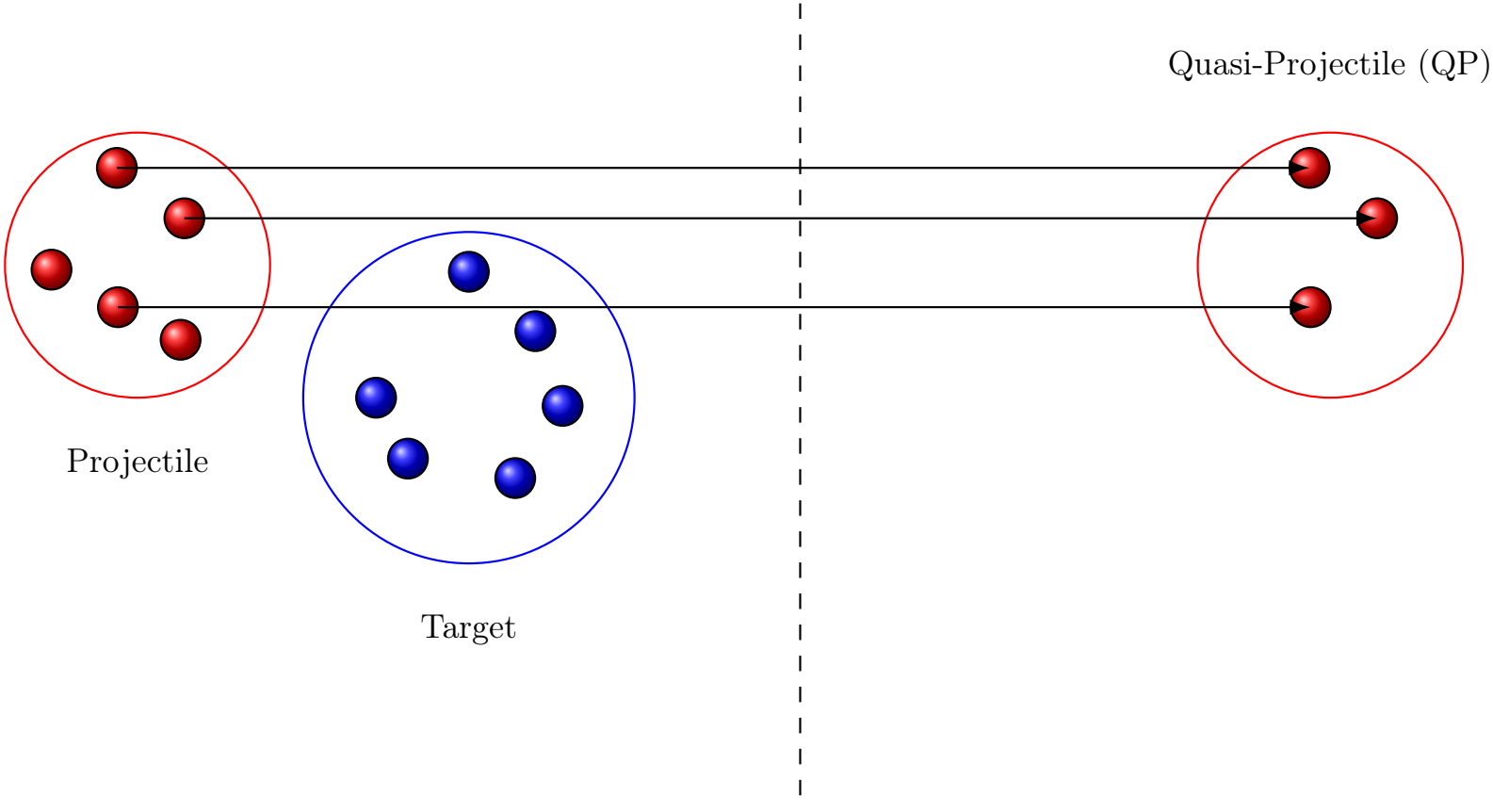

The BIC model in GEANT4

J.Cugnon, C. Volant and S. Vuillier, Nuc. Phys. A 620 (1997) 475-509

G. Folger, V.N. Ivanchenko, and J. P. Wellisch, Eur. Phys. Jour. A 21, 407-417 (2004)

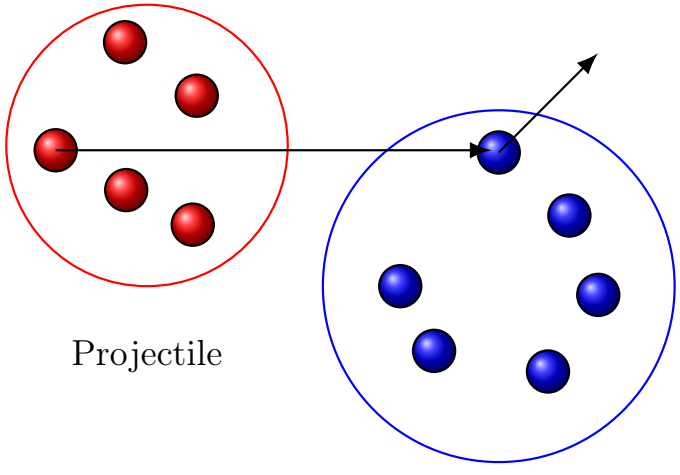

Quasi-Projectile (QP)

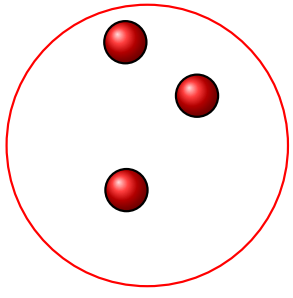

The BIC model in GEANT4

J.Cugnon, C. Volant and S. Vuillier, Nuc. Phys. A 620 (1997) 475-509

G. Folger, V.N. Ivanchenko, and J. P. Wellisch, Eur. Phys. Jour. A 21, 407-417 (2004)

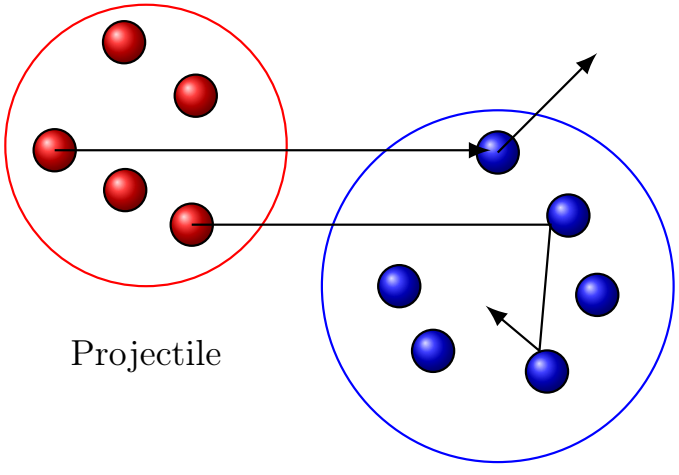

Projectile

Target

Quasi-Projectile (QP)

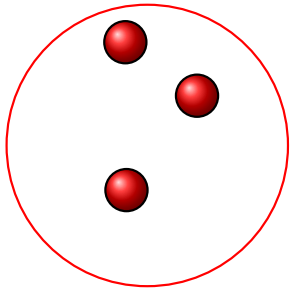

The BIC model in GEANT4

J.Cugnon, C. Volant and S. Vuillier, Nuc. Phys. A 620 (1997) 475-509

G. Folger, V.N. Ivanchenko, and J. P. Wellisch, Eur. Phys. Jour. A 21, 407-417 (2004)

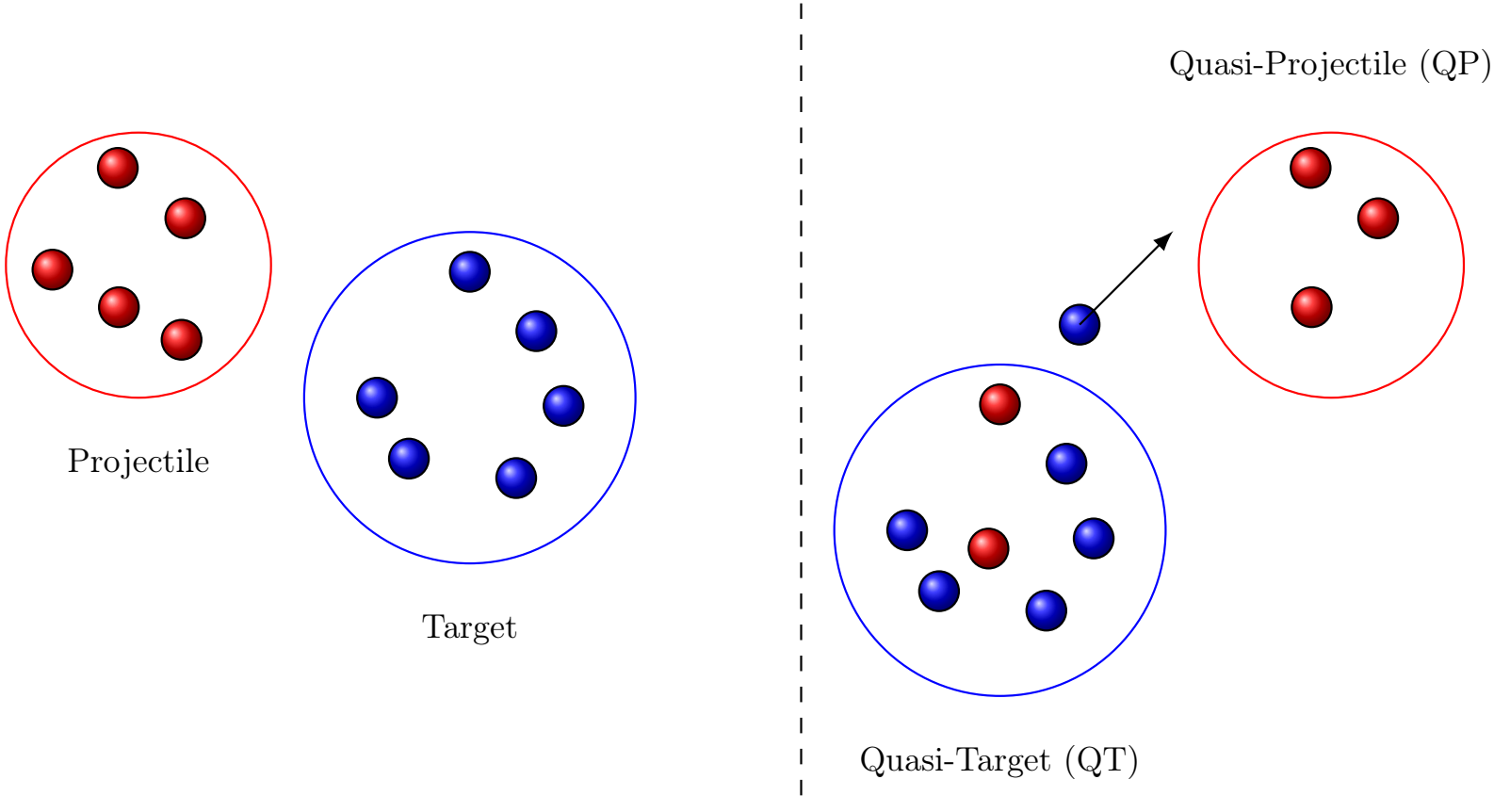

The QMD model in GEANT4

$$f(\overrightarrow{r},\overrightarrow{p},t)=\sum_i\left[\lambda_i e^{-\frac{(\overrightarrow{r}-\overrightarrow{r_i})^2}{2\sigma_r^2}-\frac{(\overrightarrow{p}-\overrightarrow{p_i})^2)}{2\sigma_p^2}}\right]$$

$$\frac{\partial f}{\partial t}+\frac{\overrightarrow{p}}{m}\overrightarrow{\nabla_r}f-\overrightarrow{\nabla_r}U\overrightarrow{\nabla_p}f=I_{collision}(f)$$

for QMD, 1 gaussian per nucleon is used to sample the one-body distribution function $f(\overrightarrow{r},\overrightarrow{p},t)$. *K. Niita et al. Phys. Rev. C 52, 2620-2635 (1995)*

Ni + Au, 7 MeV/u, b=4 fm

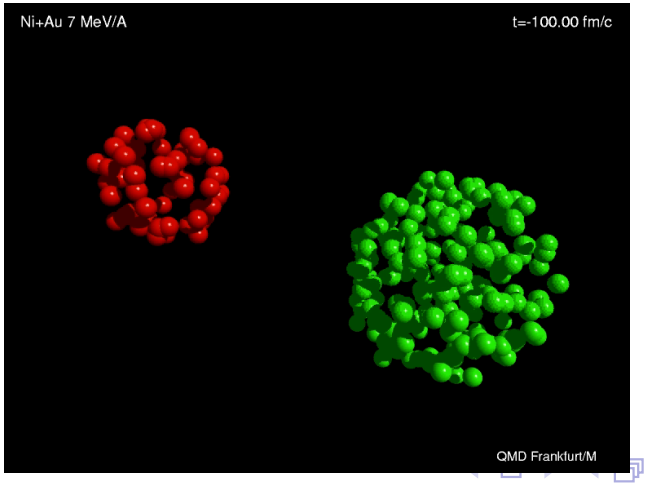

Statistical decay models

The basis

- For each decay configuration $\{Z_i, A_i\}$ a weight $\mathcal{W}(E^*, J, \{Z_i, A_i\})$ is computed.
- The decay configuration is chosen according to its statistical weight $\mathcal{P}(\{Z_i, A_i\}) = \mathcal{W}(E^*, J, \{Z_i, A_i\}) / \sum_{configurations} \mathcal{W}(E^*, J, \{Z_j, A_j\})$
- Different statistical ensembles (microcanonical, canonical, grand canonical) or formalisms may be used to compute the configurations weights.

Statistical decay models

The basis

- For each decay configuration $\{Z_i, A_i\}$ a weight $\mathcal{W}(E^*, J, \{Z_i, A_i\})$ is computed.
- The decay configuration is chosen according to its statistical weight $\mathcal{P}(\{Z_i, A_i\}) = \mathcal{W}(E^*, J, \{Z_i, A_i\}) / \sum_{configurations} \mathcal{W}(E^*, J, \{Z_j, A_j\})$
- Different statistical ensembles (microcanonical, canonical, grand canonical) or formalisms may be used to compute the configurations weights.

The "evaporation" models

- The configurations with two particles only are taken into account.
- EVAP model: only the emissions of light particles $(n, p, d, t, {}^3He, \alpha)$ are considered.
- Generalized Evaporation Model: all the configurations with two particles are considered.

Statistical decay models

The basis

- For each decay configuration $\{Z_i, A_i\}$ a weight $\mathcal{W}(E^*, J, \{Z_i, A_i\})$ is computed.
- The decay configuration is chosen according to its statistical weight $\mathcal{P}(\{Z_i, A_i\}) = \mathcal{W}(E^*, J, \{Z_i, A_i\}) / \sum_{configurations} \mathcal{W}(E^*, J, \{Z_j, A_j\})$
- Different statistical ensembles (microcanonical, canonical, grand canonical) or formalisms may be used to compute the configurations weights.

The "evaporation" models

- The configurations with two particles only are taken into account.
- EVAP model: only the emissions of light particles $(n, p, d, t, {}^3He, \alpha)$ are considered.
- Generalized Evaporation Model: all the configurations with two particles are considered.

The fragmentation models

- No limitations on the particles multiplicity.
- Fermi Break Up models: all the possible partitions are considered.
- Statitical Multifragmentation Model: a reduced sample of configurations is randomly chosen among all the possible configurations.

An example of statistical decay model: Fermi Break Up

Hypotheses

1. All the partitions are taken into account
2. Fragments are "cold"
3. Use of the micro-canonical ensemble: masses, charges and energy are strictly constant (no temperature or chemical potential)

Consequences

1. 171 physically acceptable partitions for ^{12}C (out of 1043 possible)
2. All the available energy will be as kinetic energy T_i of the fragments :

$$T = \sum_{i=1}^{N} T_i = E^* + Q \qquad Q = m(^{12}C)c^2 - \sum_{i=1}^{N} m_i c^2$$

3. The statistical weight of a configuration is given by :

$$\mathcal{W}(\{A_i, Z_i\}_{i=1..N}, E^*) = \alpha(N)(4\pi)^{N-1} \left(\frac{\Pi_{i=1}^{N} m_i}{\sum_{i=1}^{N} m_i} \right)^{\frac{3}{2}} (2T)^{\frac{3N-5}{2}}$$

Few configurations

Configuration	$Q(MeV)$	N
^{12}C	0	1
$^{4}He +^{4} He +^{4} He$	-7.27463	3
$^{8}Be +^{4} He$	-7.36641	2
$^{11}B + p$	-15.956	2
$^{11}C + n$	-18.7205	2
$^{7}Li +^{4} He + p$	-24.6205	3
$^{10}B + d$	-25.1857	2
$^{7}Be +^{4} He + n$	-26.2648	3
$^{9}Be +^{3} He$	-26.2787	2
$^{7}Li +^{5} Li$	-26.5846	2
$^{4}He +^{4} He + t + p$	-27.0887	4
$^{7}Be +^{5} He$	-27.1545	2
$^{8}Be + t + p$	-27.1804	3
$^{10}Be + p + p$	-27.1848	3
$^{9}B + t$	-27.3655	2
$^{10}B + p + n$	-27.4103	3
$^{4}He +^{4} He +^{3} He + n$	-27.8524	4
$^{8}Be +^{3} He + n$	-27.9442	3
$^{6}Li +^{6} Li$	-28.1707	2
$^{5}He +^{4} He +^{3} He$	-28.7421	3
$^{5}Li +^{4} He + t$	-29.0527	3
$^{6}Li +^{4} He + d$	-29.646	3
$^{4}He +^{4} He + d + d$	-31.1213	4
...	...	...

$$\mathcal{W} = \alpha(N)(4\pi)^{N-1}\left(\frac{\Pi_{i=1}^{N} m_i}{\sum_{i=1}^{N} m_i}\right)^{\frac{3}{2}}(2\mathbf{T})^{\frac{\mathbf{3N-5}}{\mathbf{2}}}$$

$$T = \sum_{i=1}^{N} T_i = E^* + Q$$

$$Q = m(^{12}C)c^2 - \sum_{i=1}^{N} m_i c^2$$

$$T > 0 \implies E^* > -Q$$

Few configurations

Configuration	$Q(MeV)$	N
^{12}C	0	1
$^{4}He +^{4} He +^{4} He$	-7.27463	3
$^{8}Be +^{4} He$	-7.36641	2
$^{11}B + p$	-15.956	2
$^{11}C + n$	-18.7205	2
$^{7}Li +^{4} He + p$	-24.6205	3
$^{10}B + d$	-25.1857	2
$^{7}Be +^{4} He + n$	-26.2648	3
$^{9}Be +^{3} He$	-26.2787	2
$^{7}Li +^{5} Li$	-26.5846	2
$^{4}He +^{4} He + t + p$	-27.0887	4
$^{7}Be +^{5} He$	-27.1545	2
$^{8}Be + t + p$	-27.1804	3
$^{10}Be + p + p$	-27.1848	3
$^{9}B + t$	-27.3655	2
$^{10}B + p + n$	-27.4103	3
$^{4}He +^{4} He +^{3} He + n$	-27.8524	4
$^{8}Be +^{3} He + n$	-27.9442	3
$^{6}Li +^{6} Li$	-28.1707	2
$^{5}He +^{4} He +^{3} He$	-28.7421	3
$^{5}Li +^{4} He + t$	-29.0527	3
$^{6}Li +^{4} He + d$	-29.646	3
$^{4}He +^{4} He + d + d$	-31.1213	4
...	...	...

$$\mathcal{W} = \alpha(N)(4\pi)^{N-1}\left(\frac{\Pi_{i=1}^{N} m_i}{\sum_{i=1}^{N} m_i}\right)^{\frac{3}{2}}(2\mathbf{T})^{\frac{\mathbf{3N-5}}{\mathbf{2}}}$$

$$T = \sum_{i=1}^{N} T_i = E^* + Q$$

$$Q = m(^{12}C)c^2 - \sum_{i=1}^{N} m_i c^2$$

$$T > 0 \implies E^* > -Q$$

Few configurations

Configuration	$Q(MeV)$	N
^{12}C	0	1
$^{4}He +^{4} He +^{4} He$	-7.27463	3
$^{8}Be +^{4} He$	-7.36641	2
$^{11}B + p$	-15.956	2
$^{11}C + n$	-18.7205	2
$^{7}Li +^{4} He + p$	-24.6205	3
$^{10}B + d$	-25.1857	2
$^{7}Be +^{4} He + n$	-26.2648	3
$^{9}Be +^{3} He$	-26.2787	2
$^{7}Li +^{5} Li$	-26.5846	2
$^{4}He +^{4} He + t + p$	-27.0887	4
$^{7}Be +^{5} He$	-27.1545	2
$^{8}Be + t + p$	-27.1804	3
$^{10}Be + p + p$	-27.1848	3
$^{9}B + t$	-27.3655	2
$^{10}B + p + n$	-27.4103	3
$^{4}He +^{4} He +^{3} He + n$	-27.8524	4
$^{8}Be +^{3} He + n$	-27.9442	3
$^{6}Li +^{6} Li$	-28.1707	2
$^{5}He +^{4} He +^{3} He$	-28.7421	3
$^{5}Li +^{4} He + t$	-29.0527	3
$^{6}Li +^{4} He + d$	-29.646	3
$^{4}He +^{4} He + d + d$	-31.1213	4
...	...	...

$$\mathcal{W} = \alpha(N)(4\pi)^{N-1}\left(\frac{\Pi_{i=1}^{N} m_i}{\sum_{i=1}^{N} m_i}\right)^{\frac{3}{2}}(2\mathbf{T})^{\frac{\mathbf{3N-5}}{\mathbf{2}}}$$

$$T = \sum_{i=1}^{N} T_i = E^* + Q$$

$$Q = m(^{12}C)c^2 - \sum_{i=1}^{N} m_i c^2$$

$$T > 0 \implies E^* > -Q$$

Statistical weights for Fermi Break Up

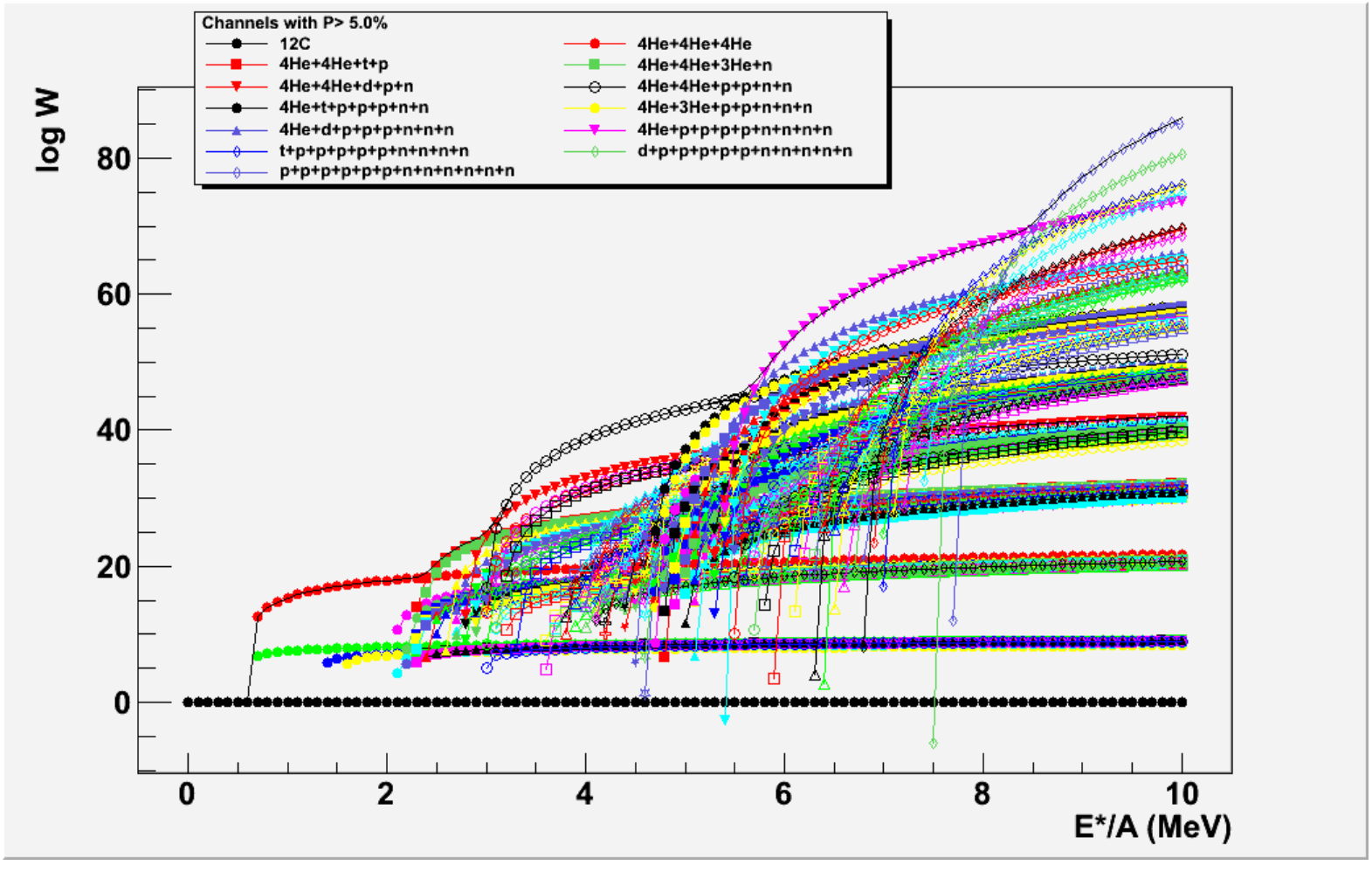

Statistical weights for Fermi Break Up

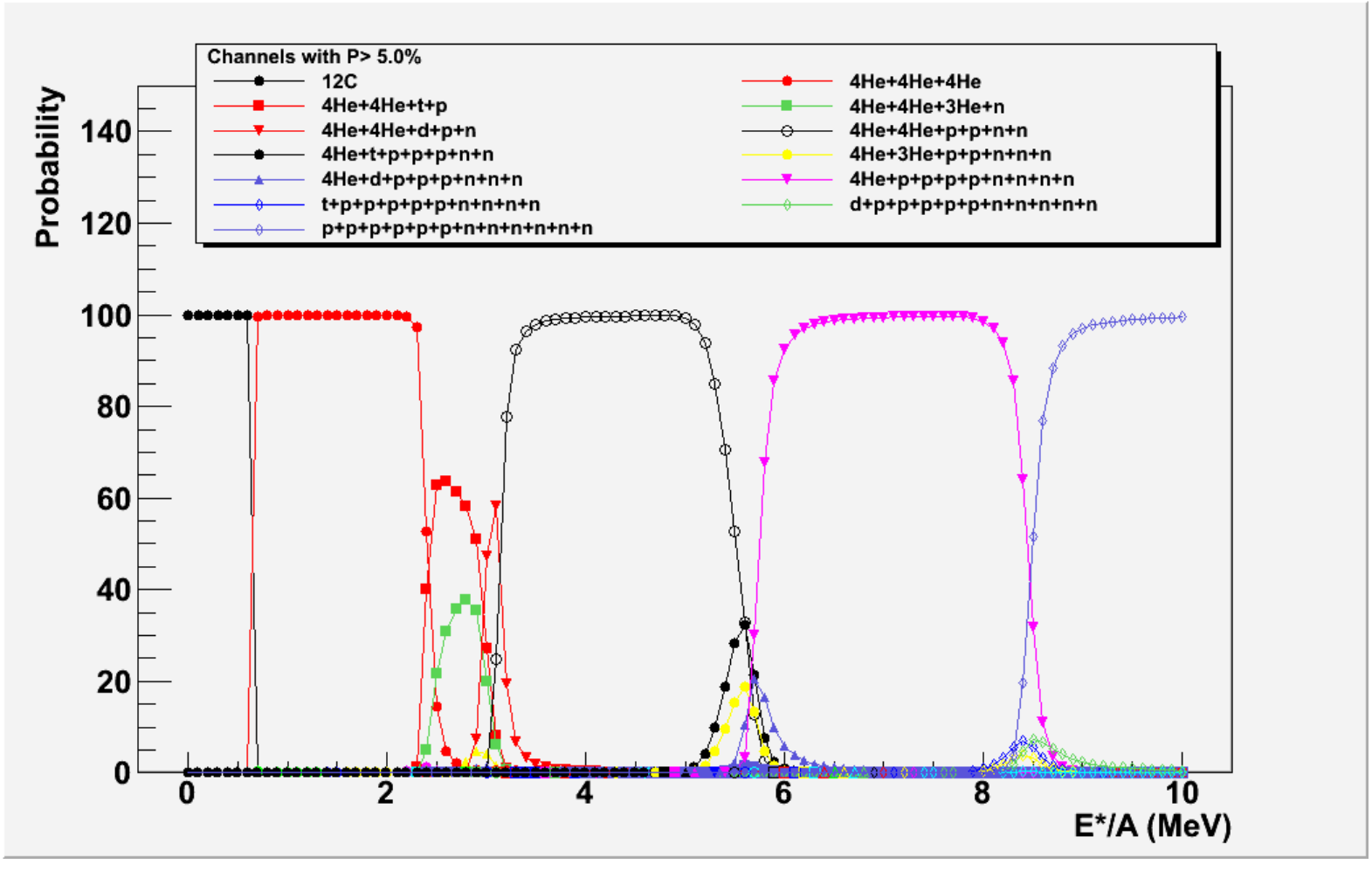

Influence of the model for protons

GEANT4 simulations

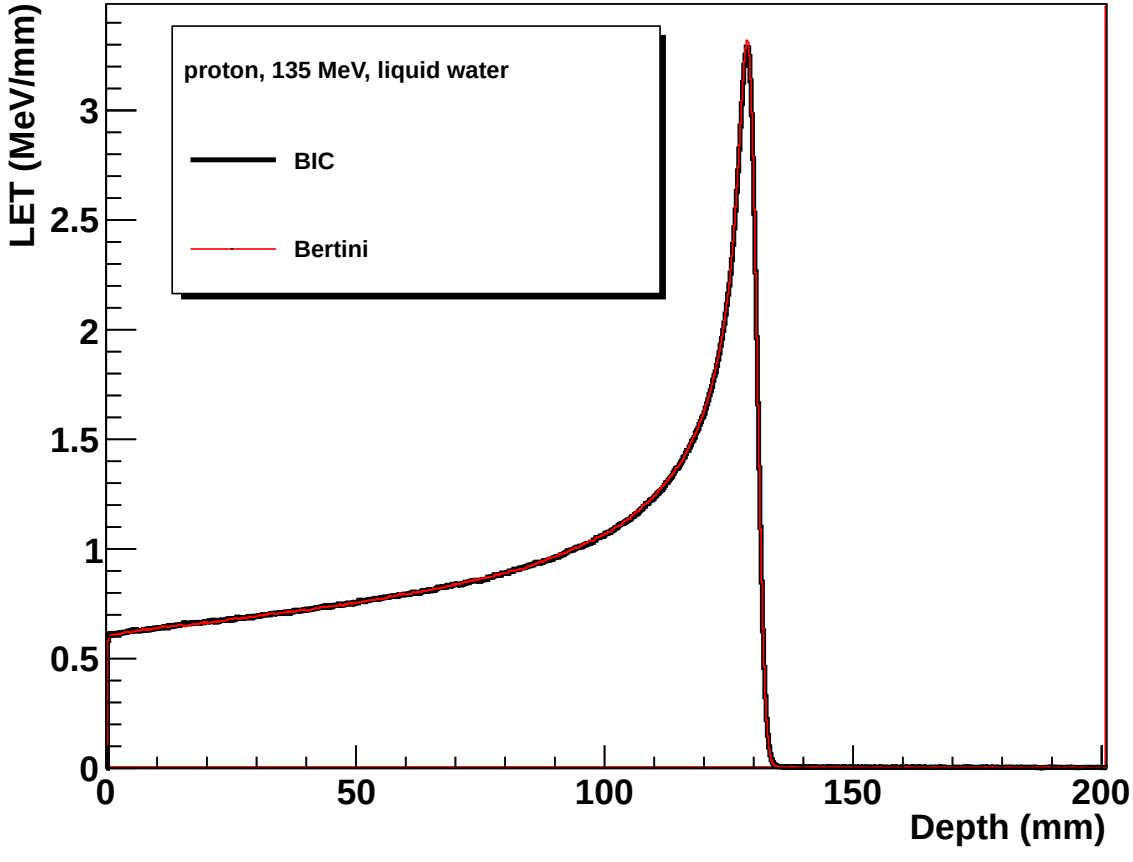

Influence of the model for ^{12}C

GEANT4 simulations

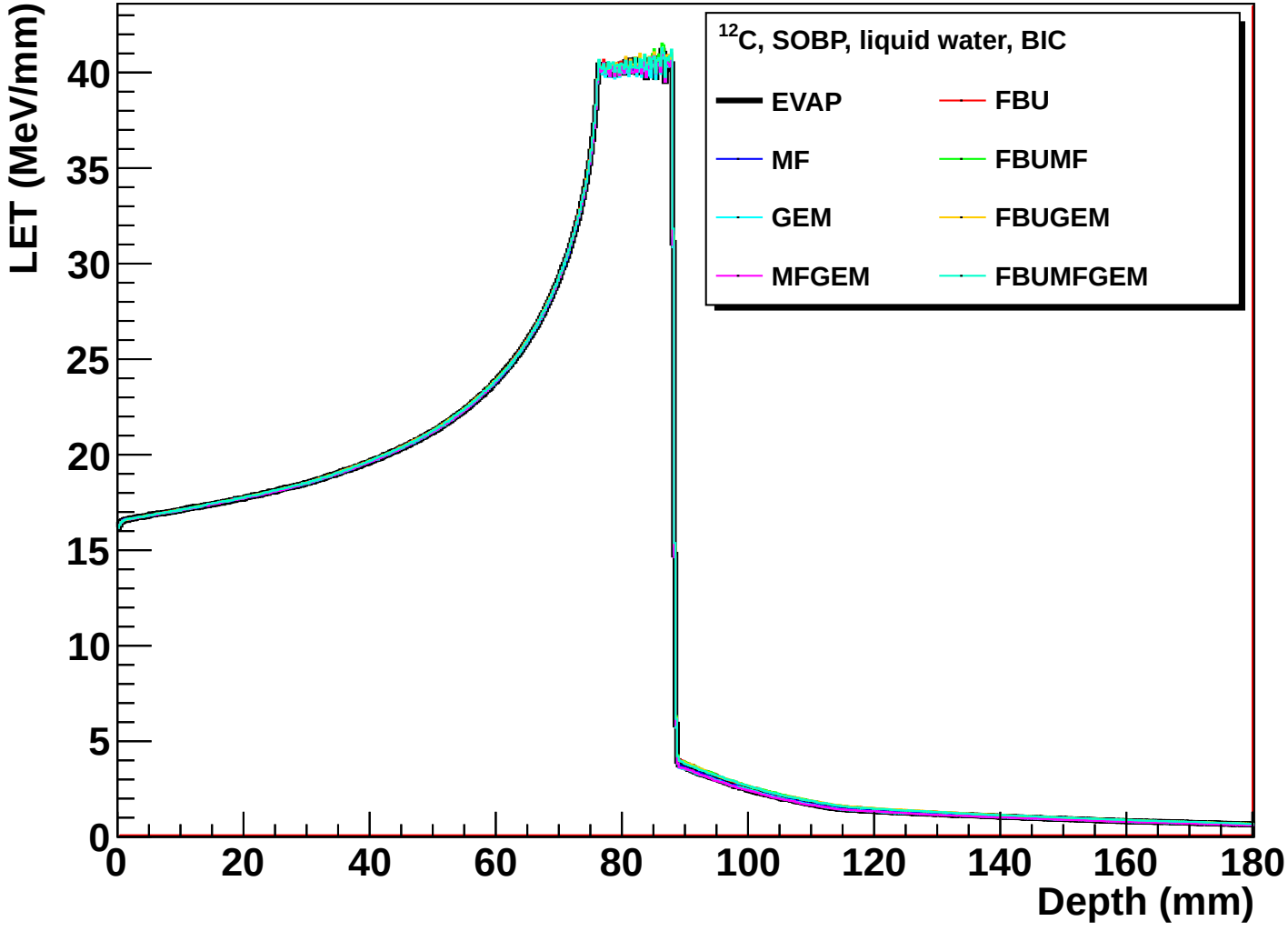

Influence of the model for ^{12}C

GEANT4 simulations

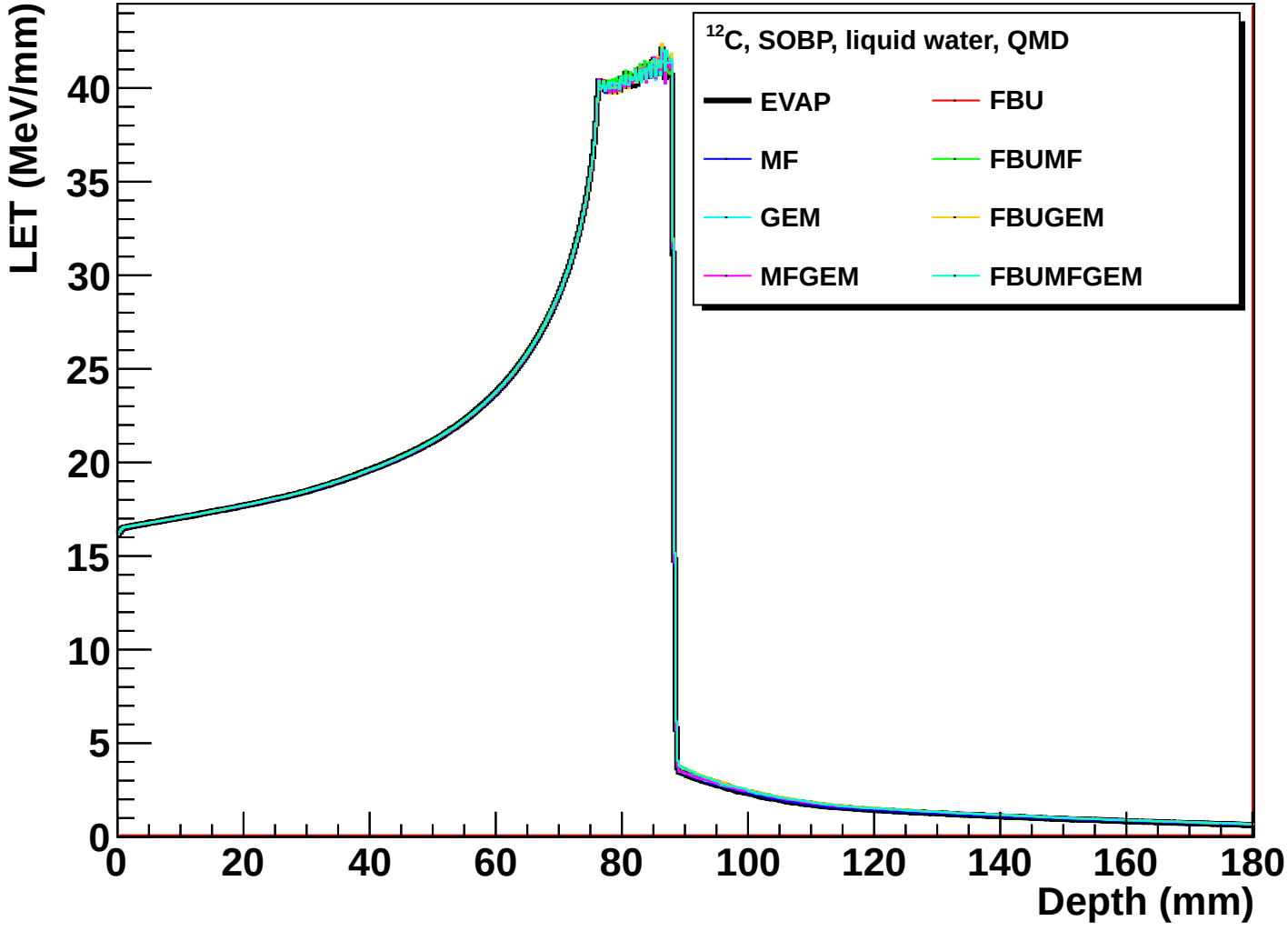

Comparison of Bragg Curves: Relative Gap

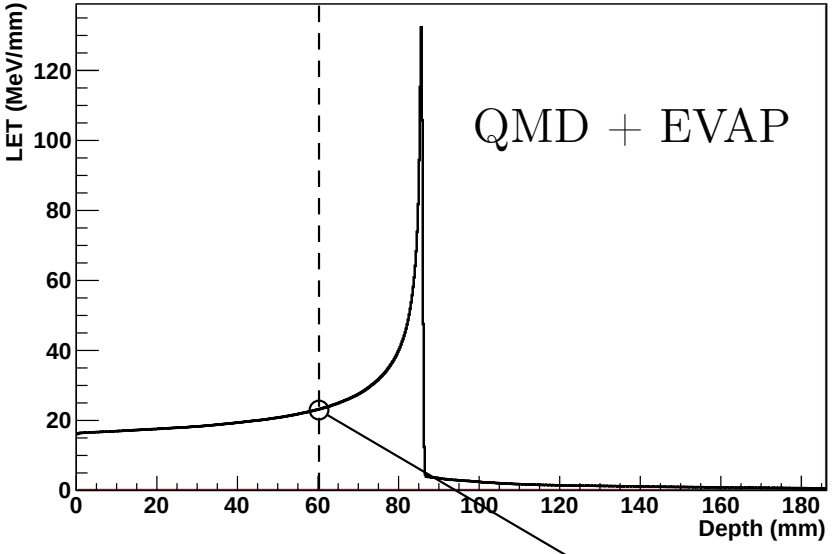

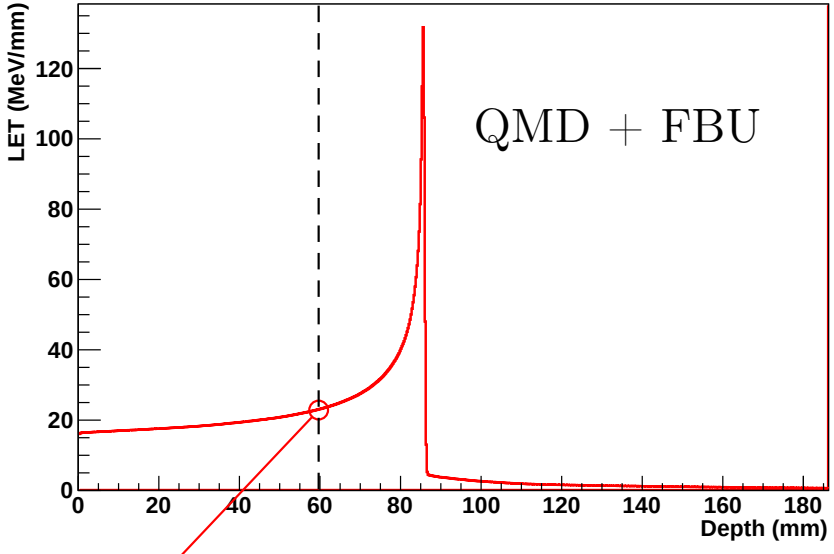

$$R(x) = \frac{Curve_1(x) - Curve_2(x)}{Curve_1(x)} \times 100$$

Influence of the decay model for ^{12}C

GEANT4 simulations

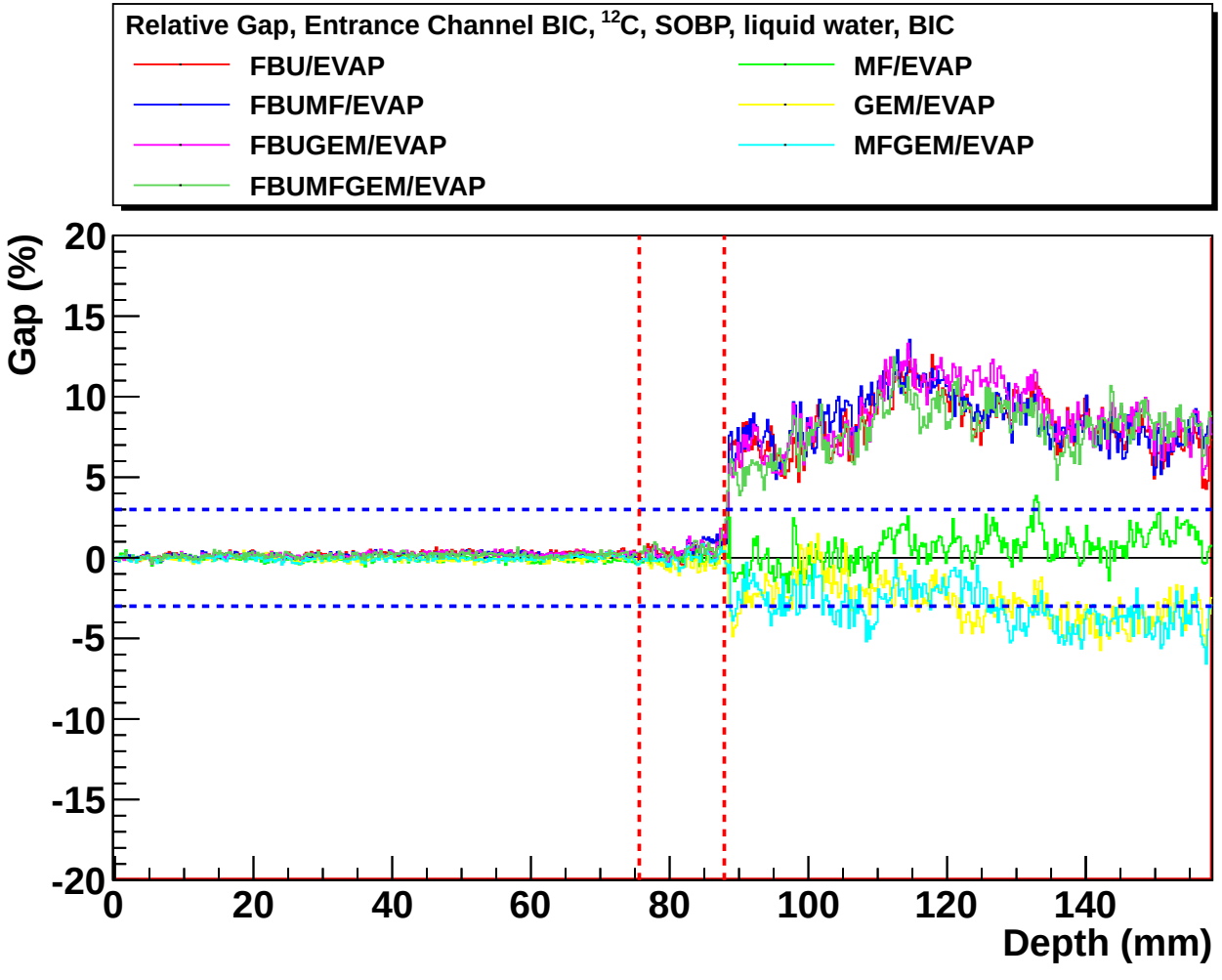

Influence of the decay model for ^{12}C

GEANT4 simulations

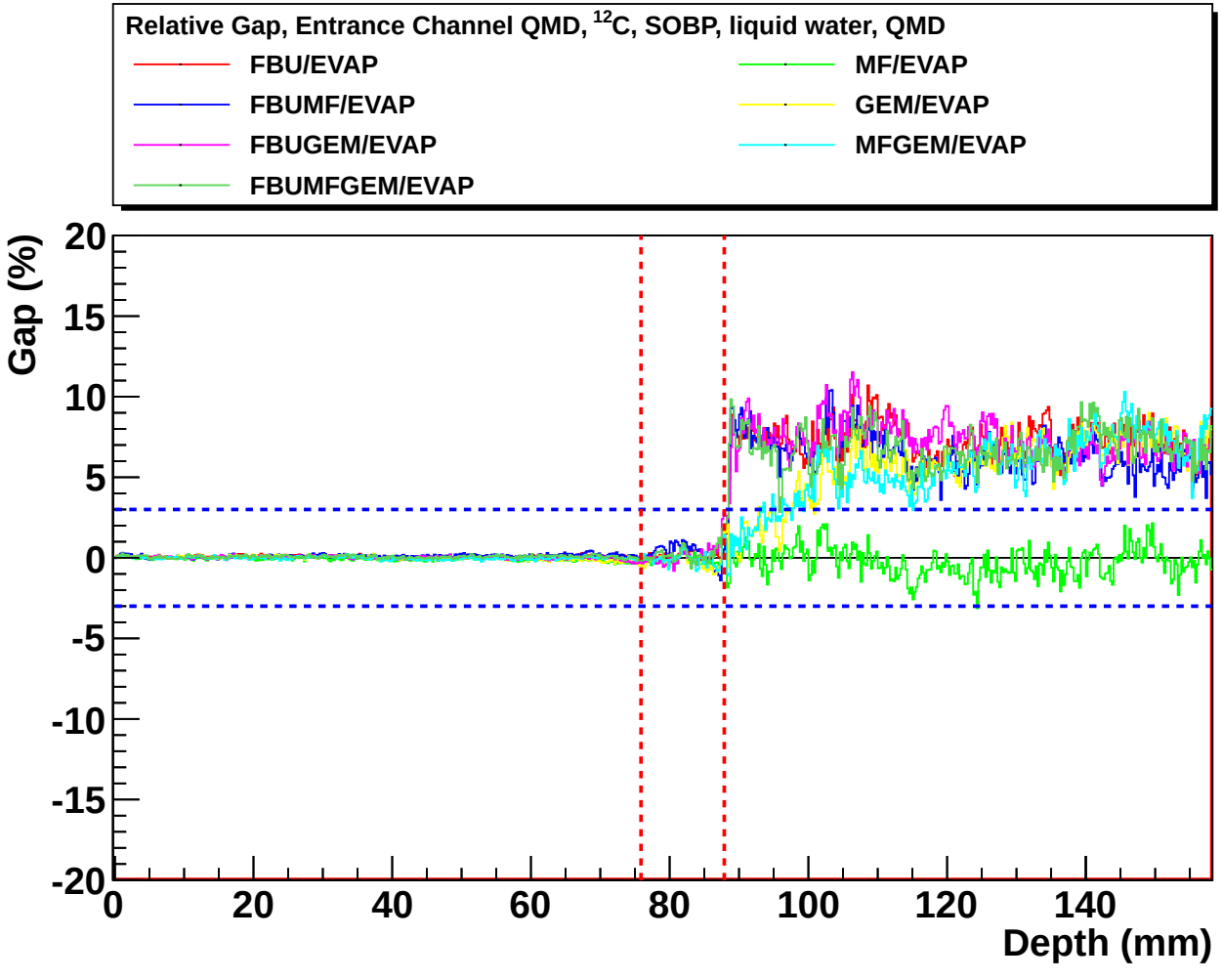

Influence of the entrance channel model for ^{12}C

GEANT4 simulations

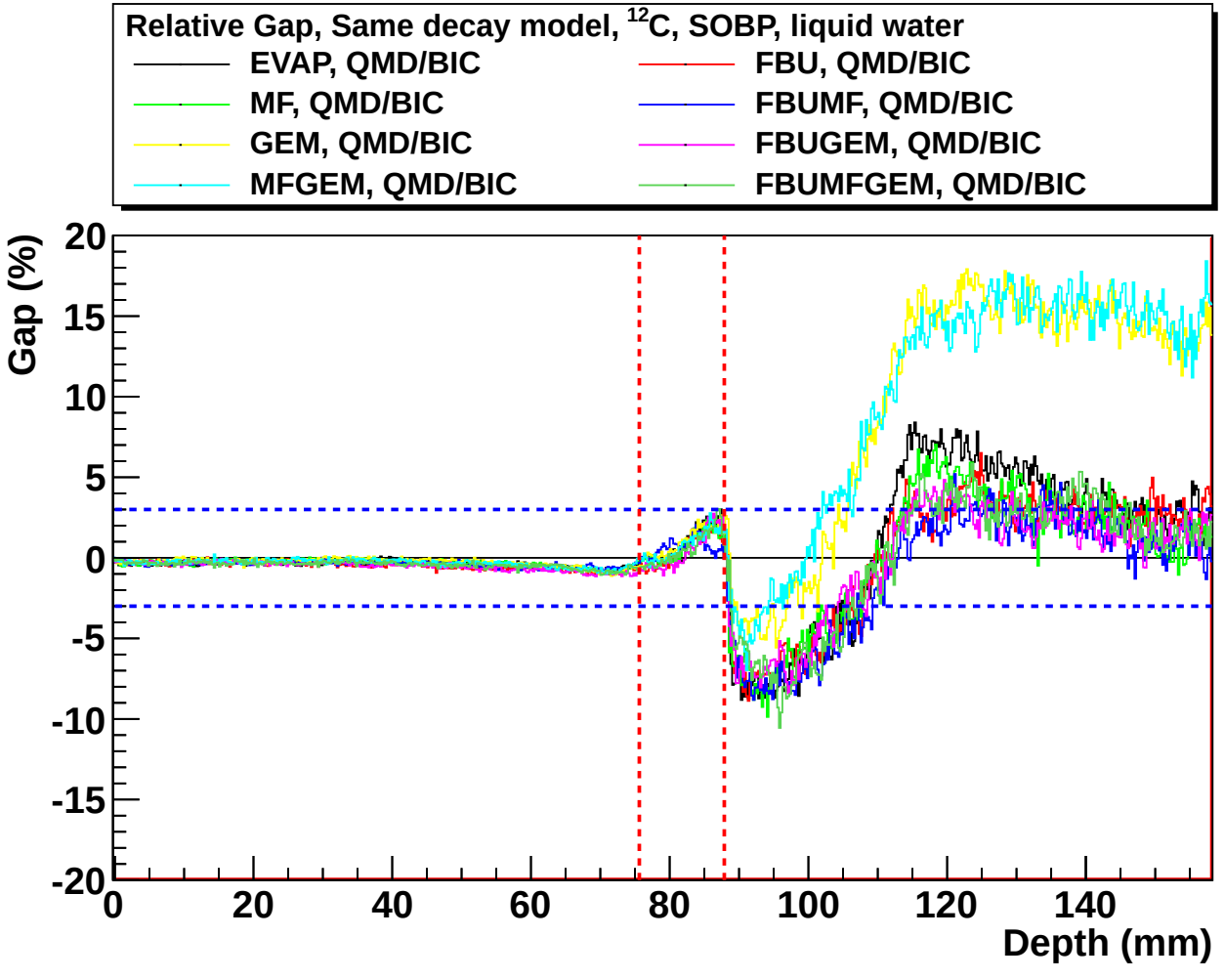

Influence of the model on fragments production

GEANT4 simulations

protons

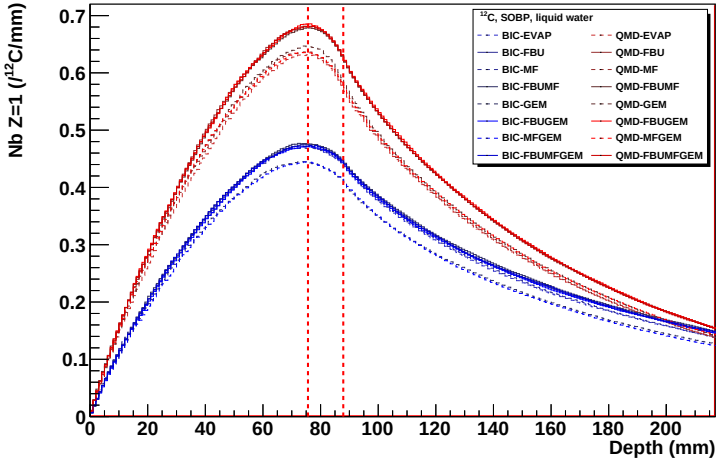

α

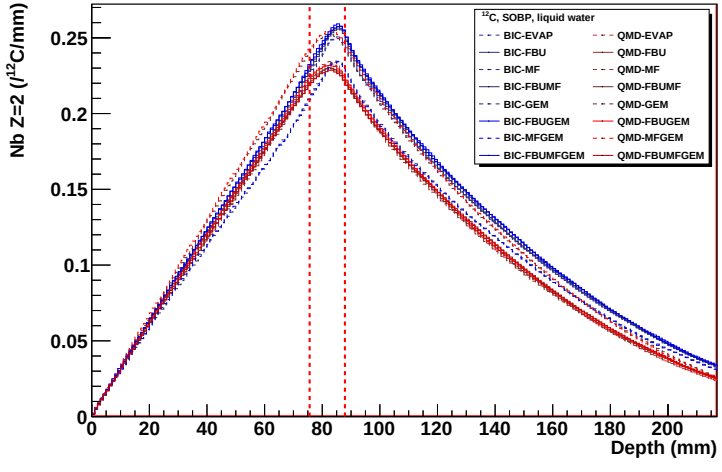

^{10}B

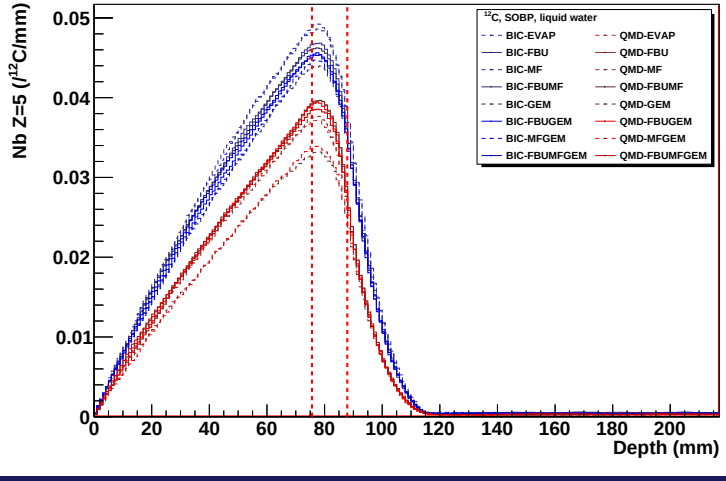

neutrons

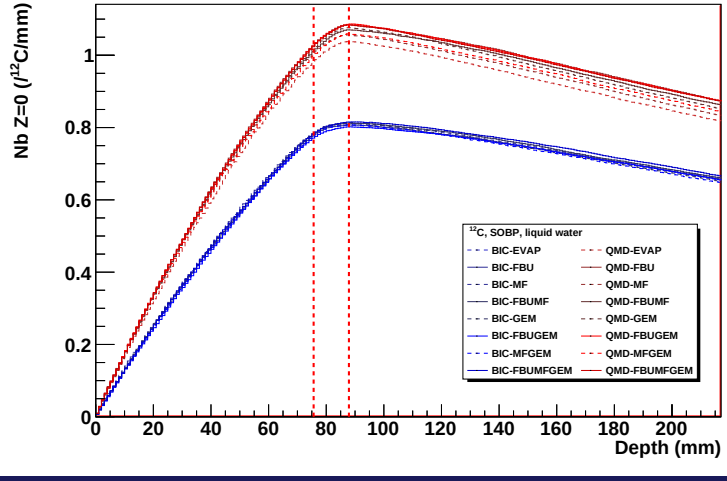

Influence of the collision model for ^{12}C: Summary

Decay model effect

- before the Bragg Peak: the relative gap is smaller than $\lesssim 0.5\%$
- after the Bragg Peak: the relative gap can reach $\approx 15\%$ but the doses are small

Entrance channel model effect

- before the Bragg Peak: the relative gap is smaller than $\lesssim 0.5\%$
- close to the Bragg Peak: the relative gap can reach $\approx 3\%$
- after the Bragg Peak: the relative gap can reach $\approx 20\%$ but the doses are small

As a consequence...

- the influence of the collision model on the dose is small ($\lesssim 3\%$)
- greater influence of the entrance channel model
- models have a big influence on secondary fragments multiplicities
- big influence of the collision model if one wants tu use the secondary particles to monitor the dose!

1 Simulations for hadrontherapy

2 The role of nucleus-nucleus collisions

3 Nucleus-nucleus collision models

4 Benchmarking models to data

5 Nuclear Physics methods for hadrontherapy

Fragmentation experiments on thick targets

E600 experiment at Ganil (IPN Lyon, IPHC Stasbourg, LPC Caen)

^{12}C at 95 MeV/u on thick PMMA targets

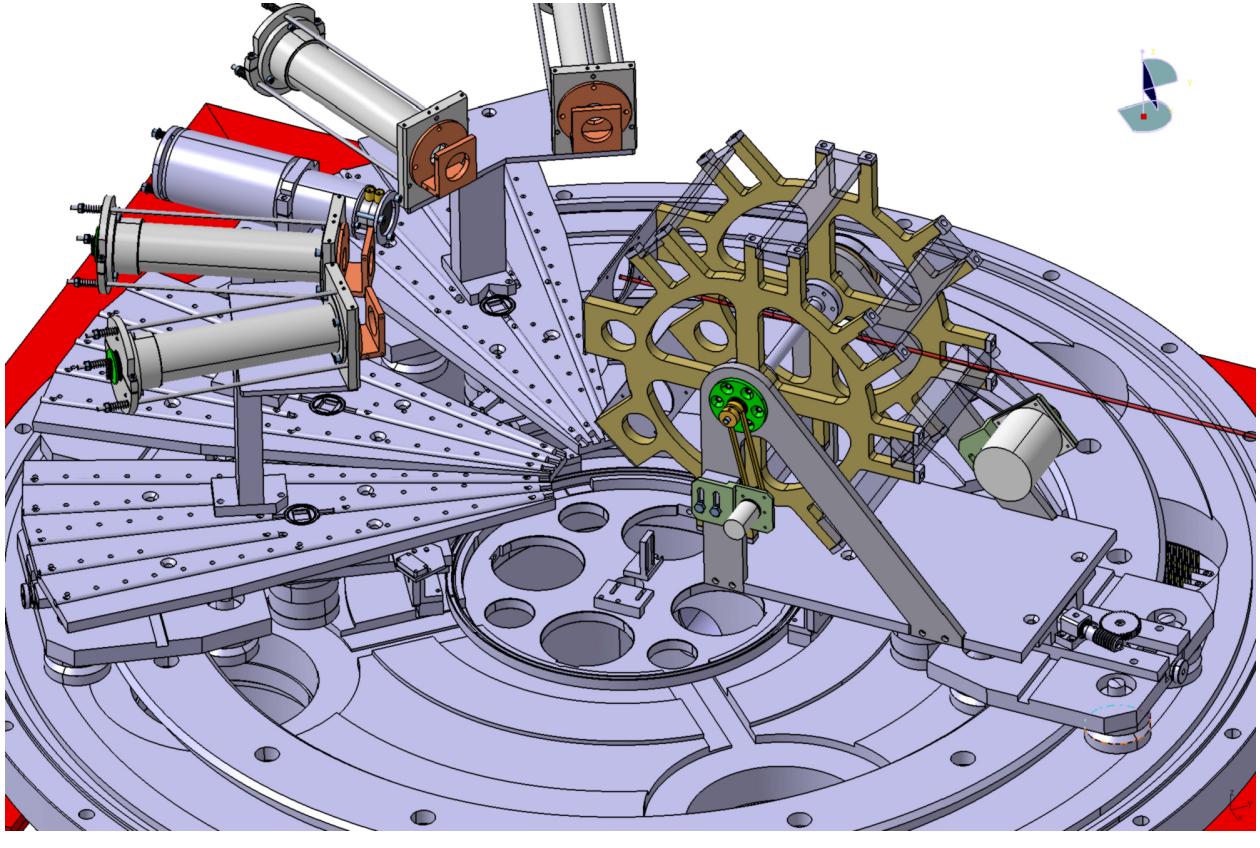

Fragmentation experiments on thick targets (results)

^{12}C at 95 MeV/u (GANIL)

PMMA 25 mm, $\vartheta = 0°$

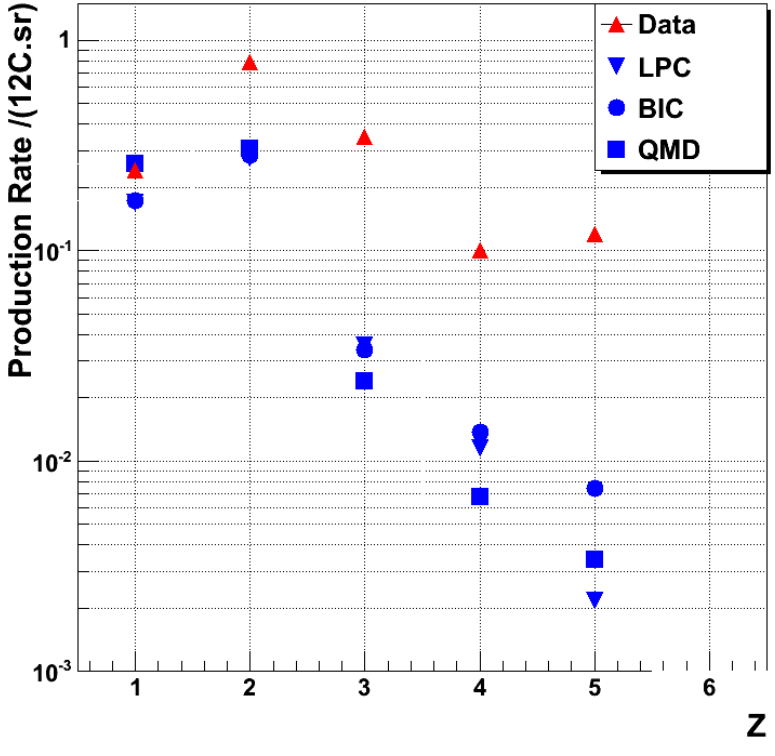

PMMA 5 mm, $\vartheta = 7°$

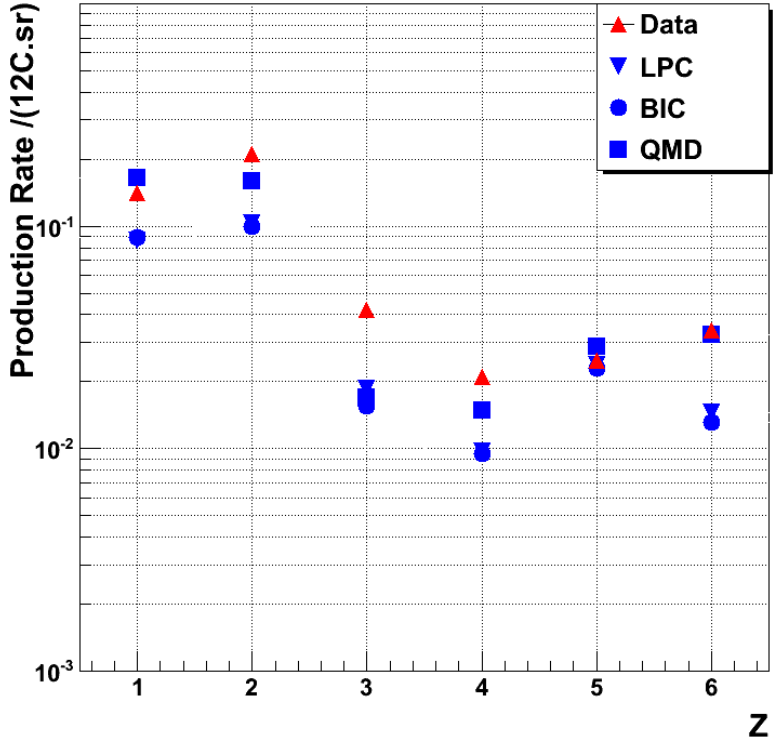

B. Braunn *et al.*, Nuc. Instrum. Methods B 269 (2011) 2676-2684

B. Braunn PhD thesis (2011)

Fragmentation experiments on thin targets at GANIL

$$\frac{d\sigma}{d\Omega}({}^{Z}_{A}X) = \frac{N({}^{Z}_{A}X)\times A_{target}}{N({}^{12}C)\times\Omega\times\rho\times th\times \mathrm{N}_{\mathcal{A}}}$$

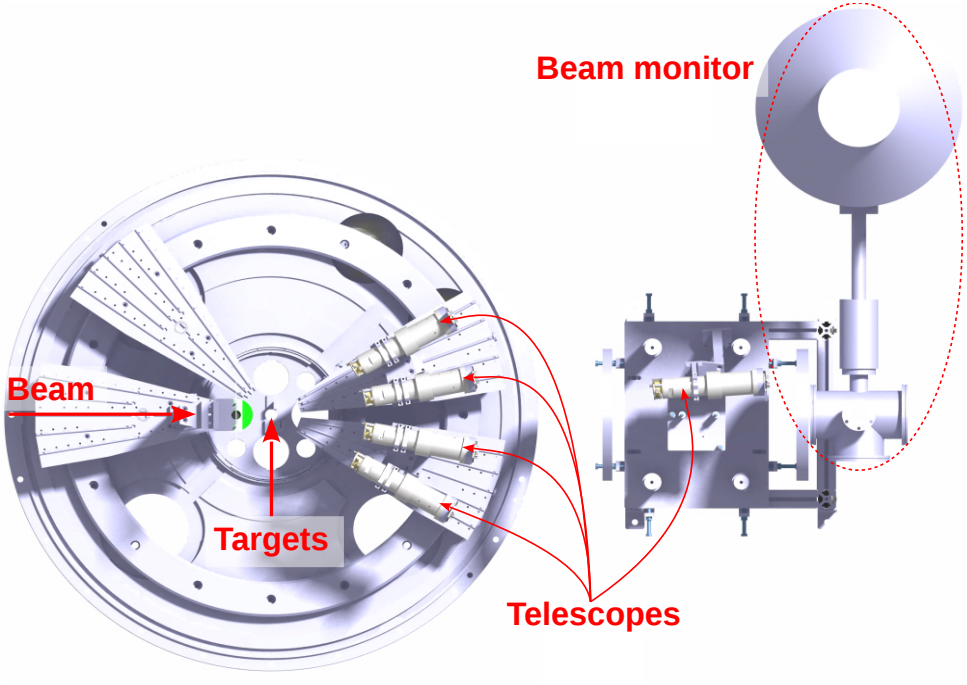

may 2011 & september 2013 & march 2015

- Collaboration LPC Caen, IPHC Strasbourg, GANIL, CEA/SPhN Saclay, IPN Lyon
- Projectile: 95 MeV/u ${}^{12}C$, 50 MeV/u ${}^{12}C$ (FrHad, 2015)
- Thin targets: C, CH_2, Al, Al_2O_3, ^{nat}Ti and PMMA ($C_5H_8O_2$)
- Angular range: from 4° to 43 ° (E600, 2011), 0° (FrHad, 2013)

$\Rightarrow \frac{\partial^2\sigma}{\partial\Omega\partial E}$ fragmentation measurements of ${}^{12}C$ on C, H, O and Ca ($A_{Ti} \sim A_{Ca}$)

$\approx$ 95% of a human body composition

Fragmentation experiments results

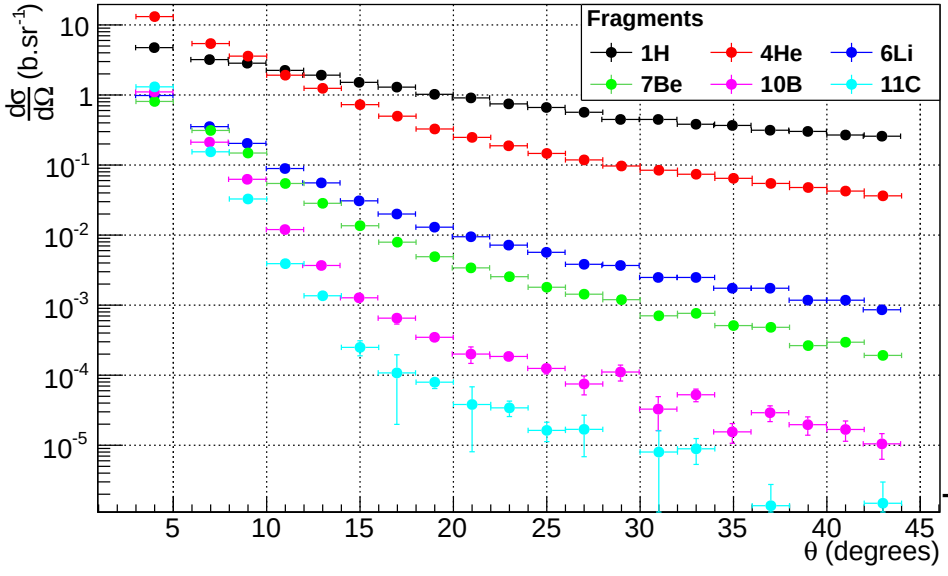

C Target

Data available on: `http://hadrontherapy-data.in2p3.fr`

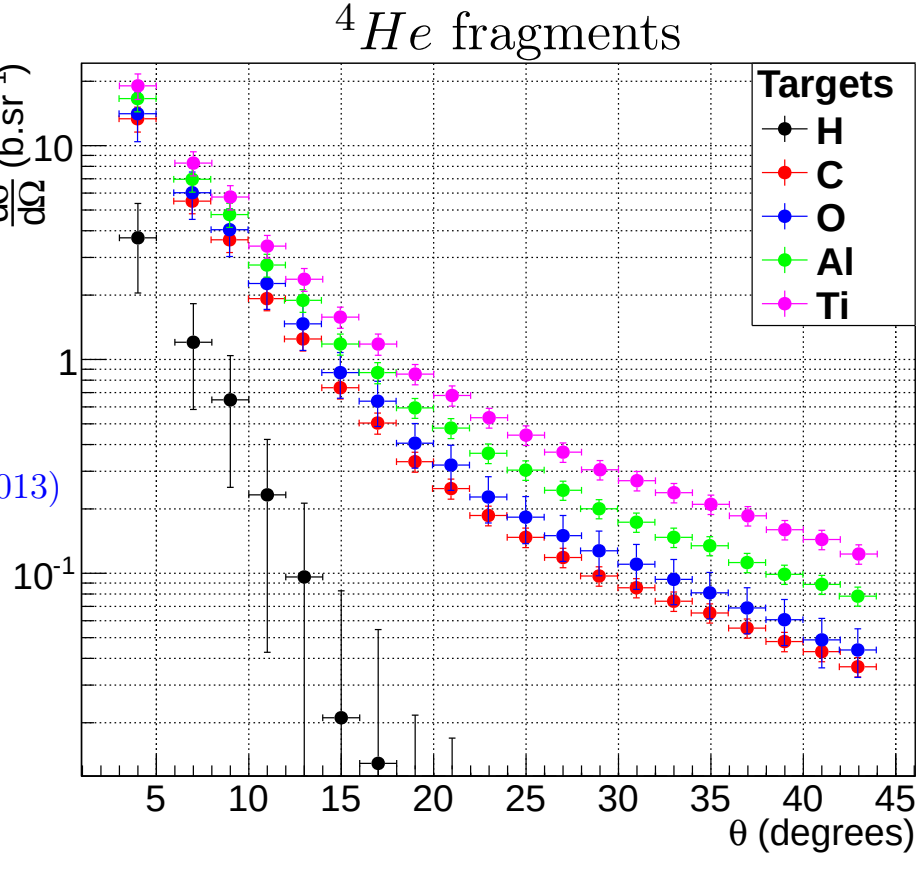

J. Dudouet *et al.*, Nucl. Instrum. Methods A 715, 98 (2013)

J. Dudouet *et al.*, Phys. Rev. C 88, 024606 (2013)

J. Dudouet *et al.*, Phys. Rev. C 89, 054616 (2014)

J. Dudouet *et al.*, Phys. Rev. C 89, 064615 (2014)

J. Dudouet PhD Thesis (2014)

Experimental energy distributions

α distribution for Carbon target

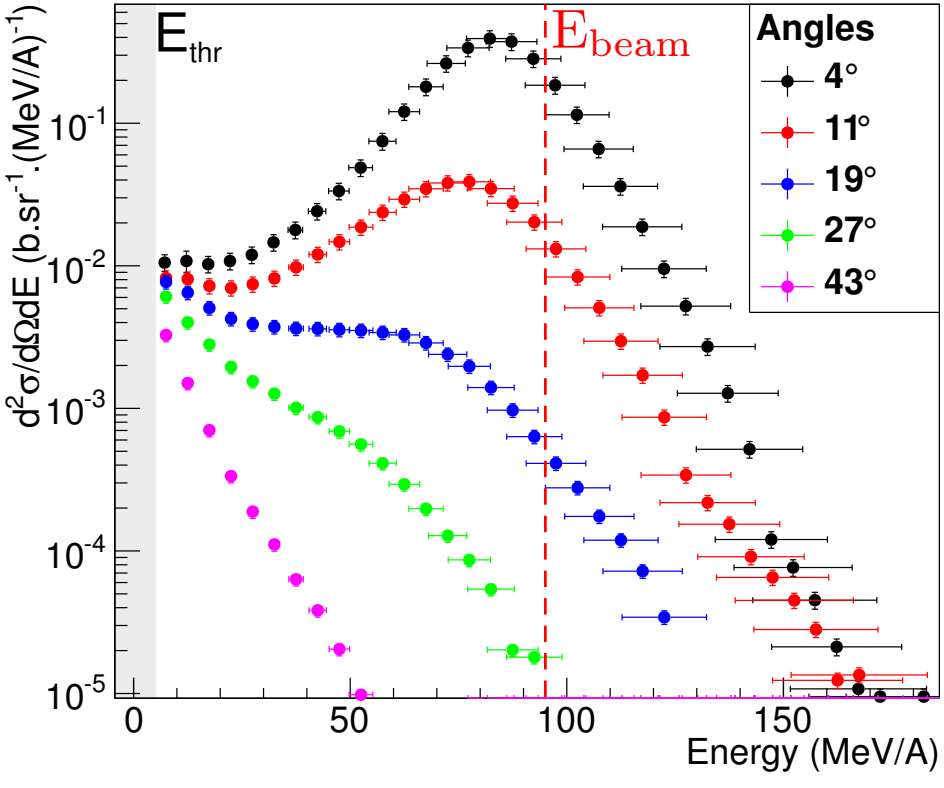

α distribution for all targets

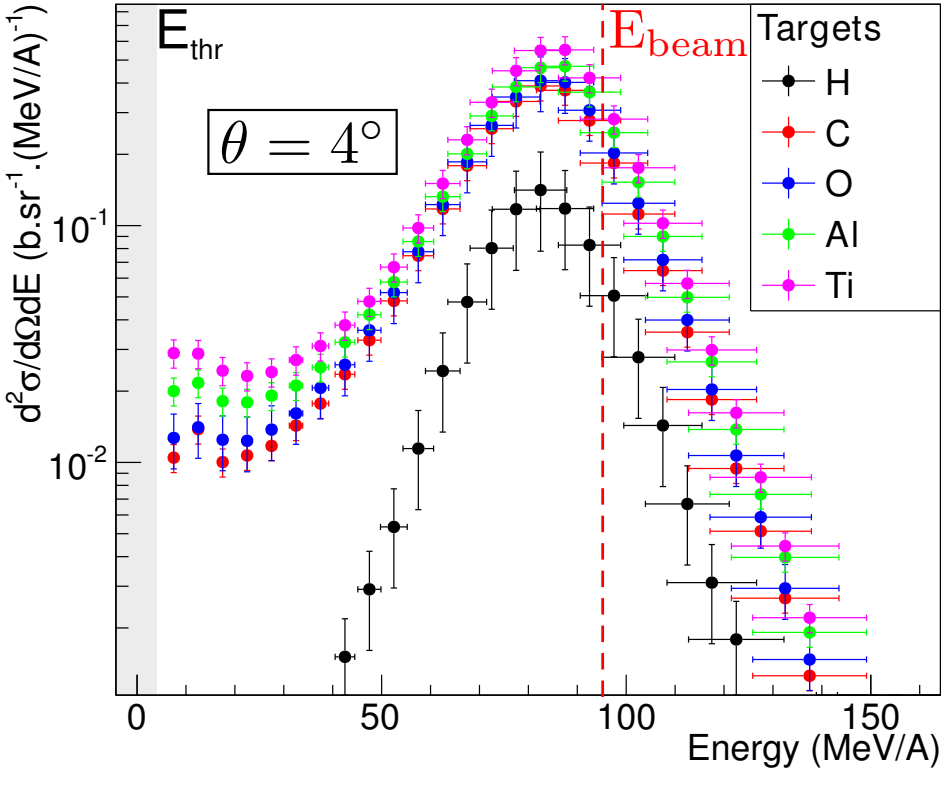

Material reconstruction with elemental data

Angular distributions

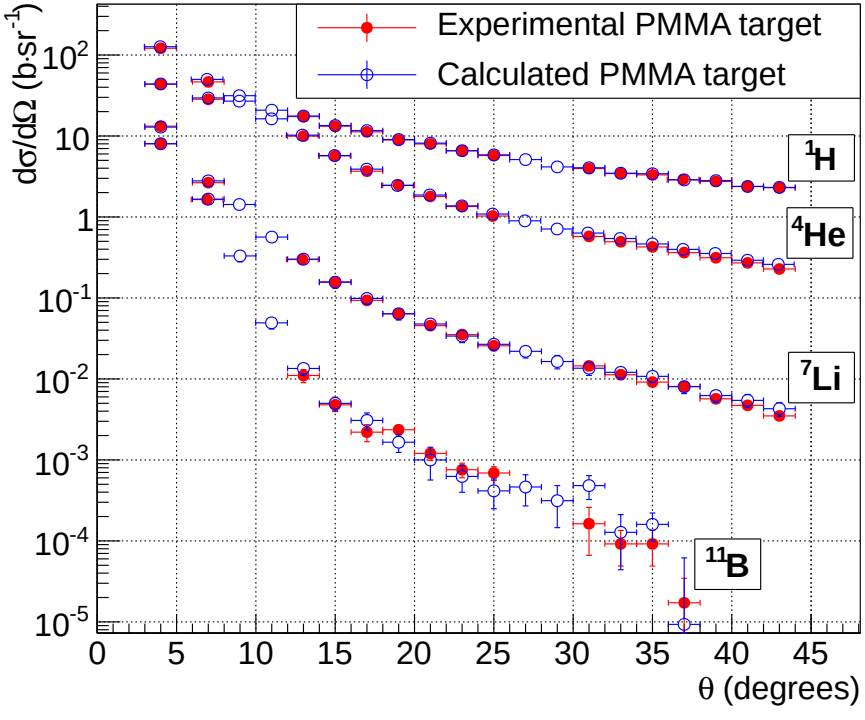

α Energy distributions

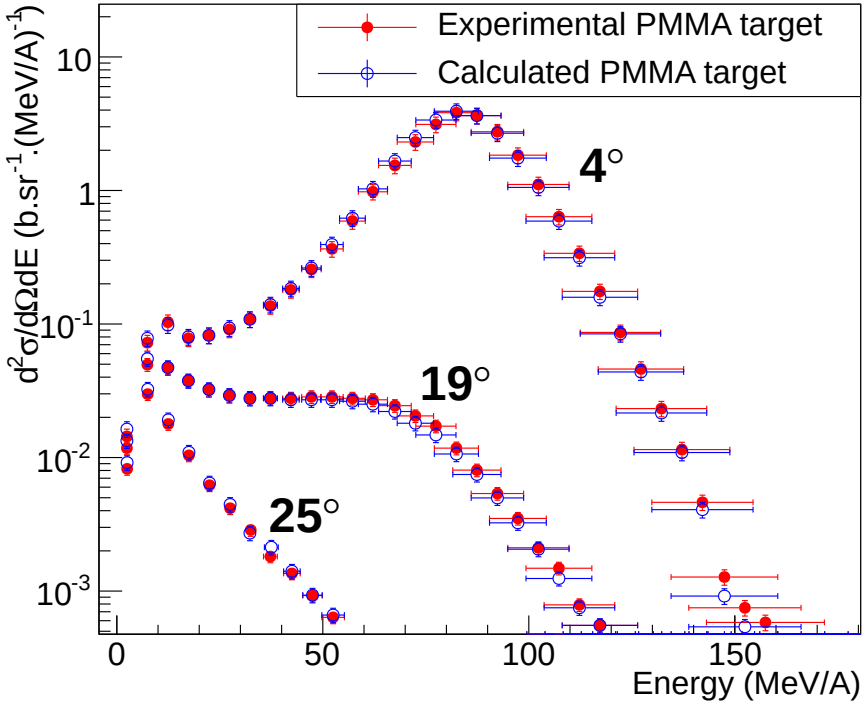

$$\text{PMMA} \Rightarrow C_5H_8O_2 \qquad M_{mol} = 100\,g/mol \qquad \rho = 1.19\,g/cm^3$$

Data available on: `http://hadrontherapy-data.in2p3.fr`

Material reconstruction with elemental data

Angular distributions

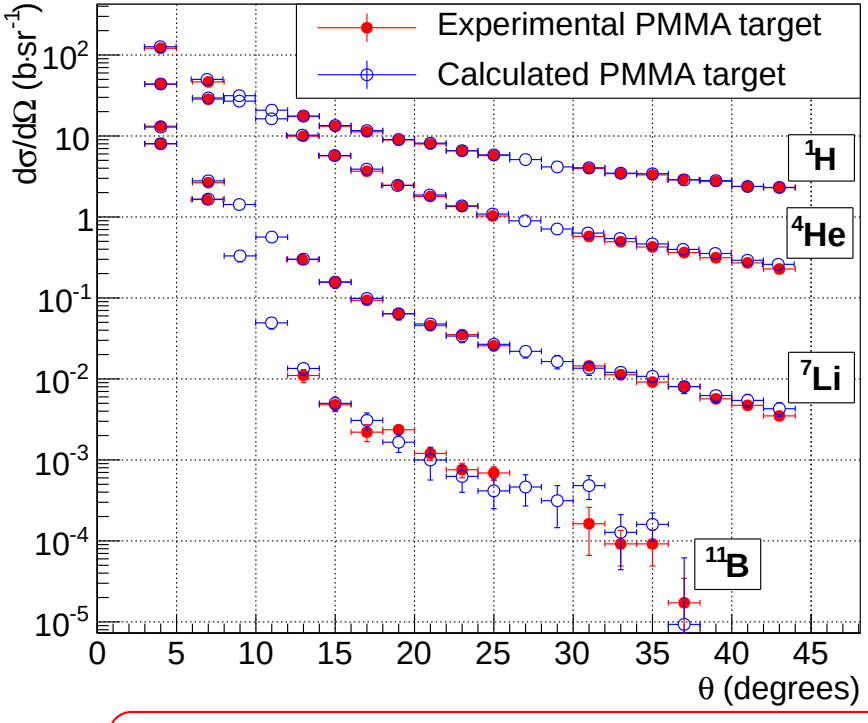

α Energy distributions

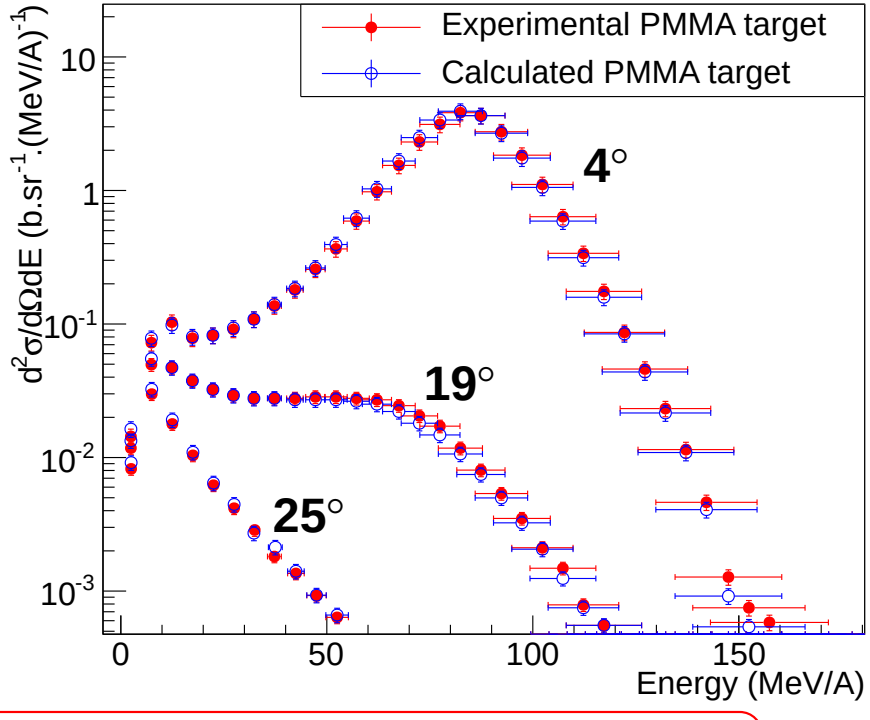

Very good reconstruction of the experimental PMMA target cross sections by combining the H, C and O targets cross sections ⇒ all tissues can be described!

Data available on: `http://hadrontherapy-data.in2p3.fr`

GEANT4 models benchmark: Angular distributions

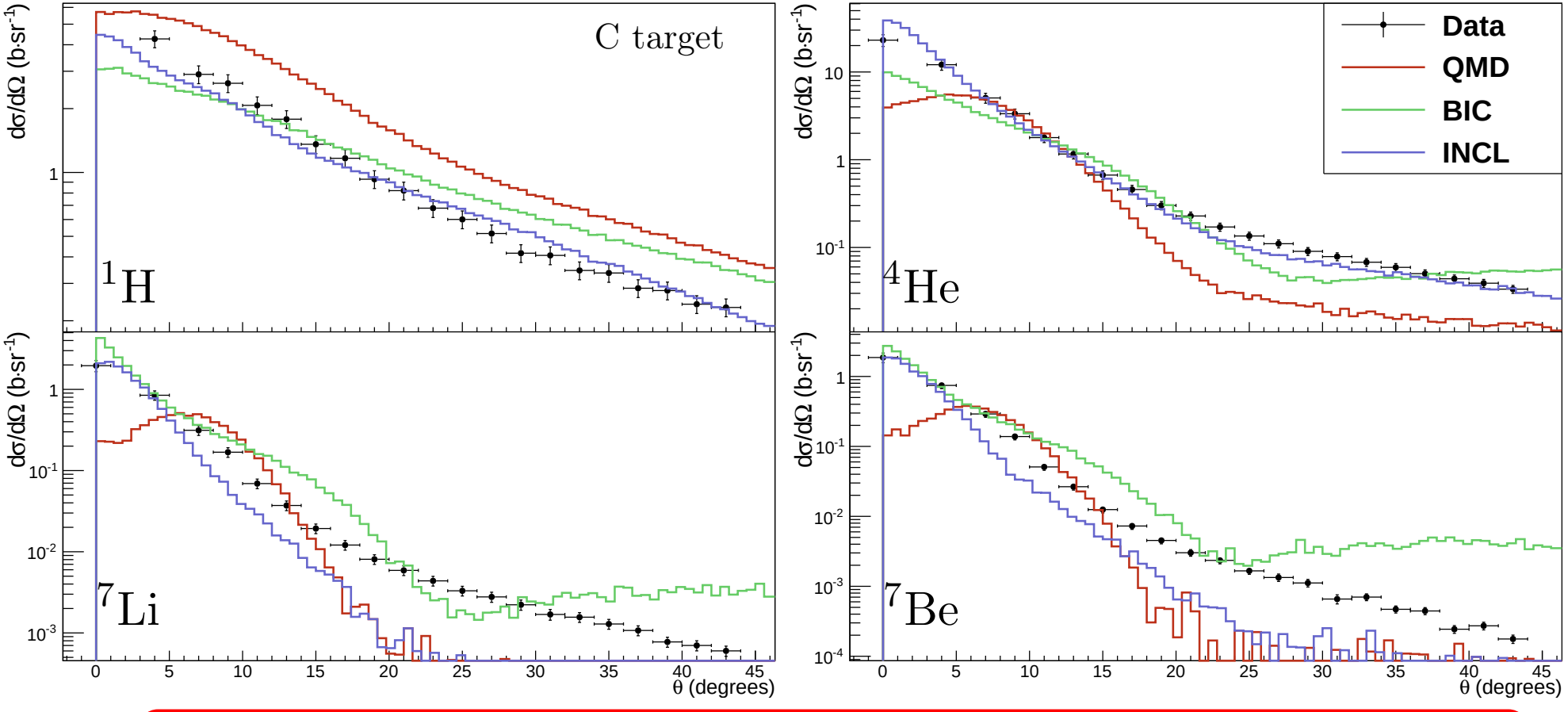

GEANT4 models benchmark: Angular distributions

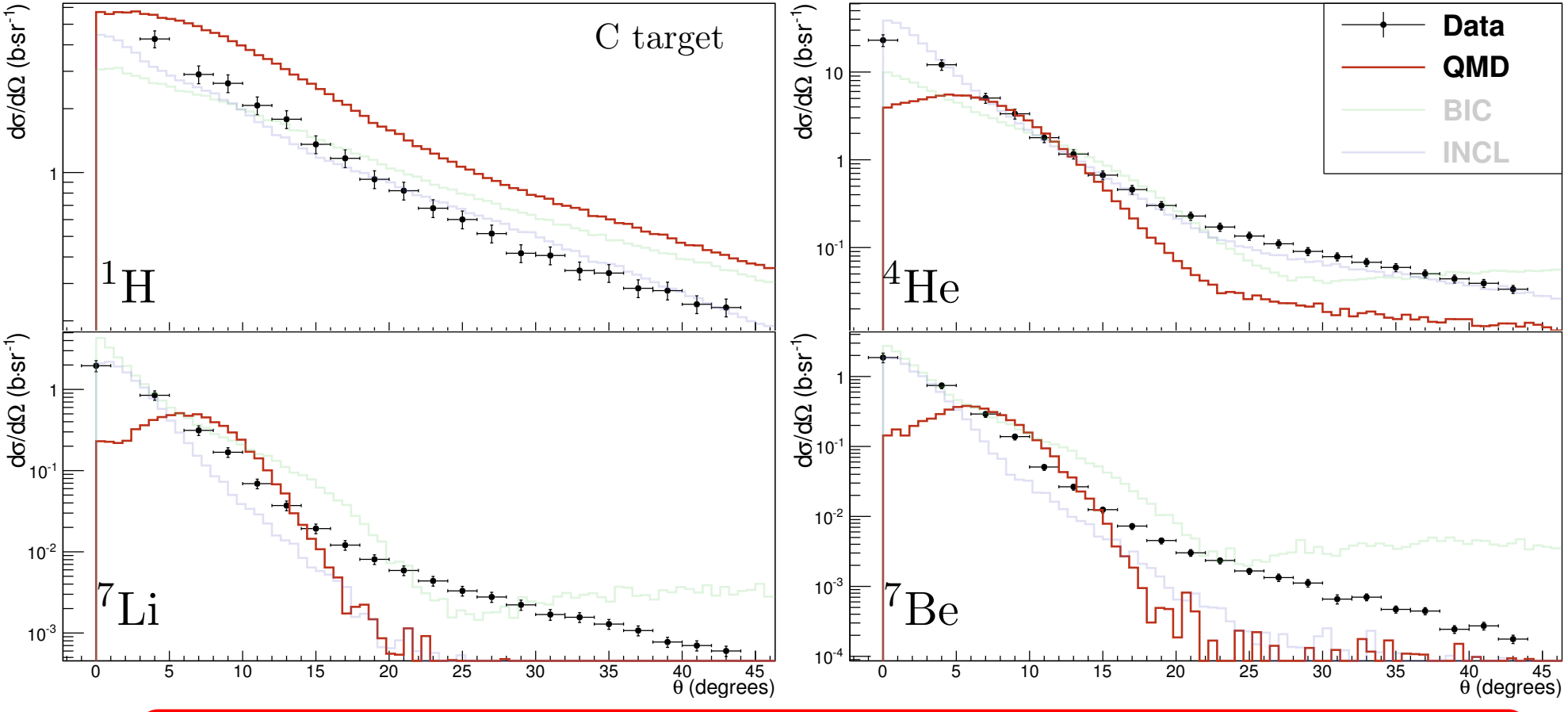

- QMD fails to reproduce the angular distributions.

GEANT4 models benchmark: Angular distributions

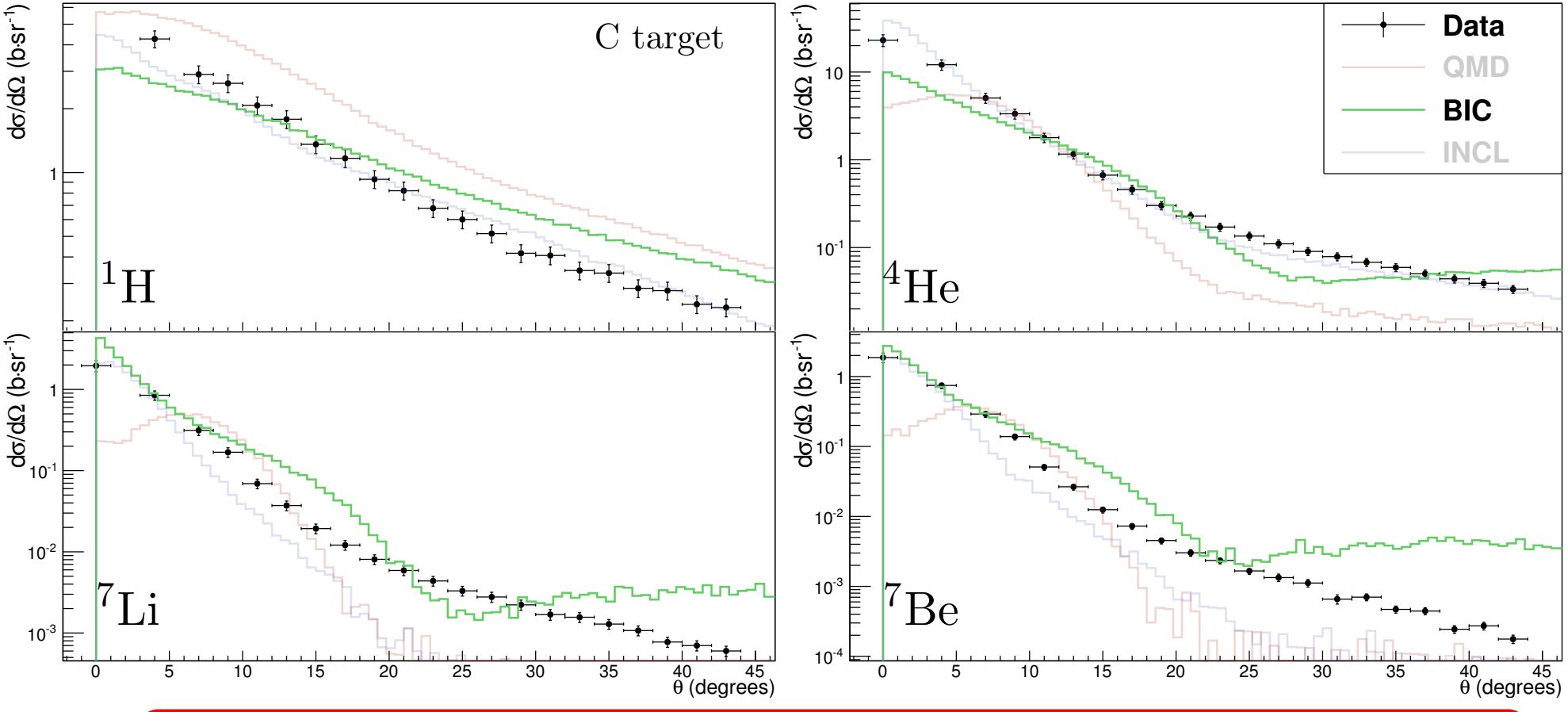

- QMD fails to reproduce the angular distributions.
- BIC is slightly better at forward angles but does not reproduce large angles.

GEANT4 models benchmark: Angular distributions

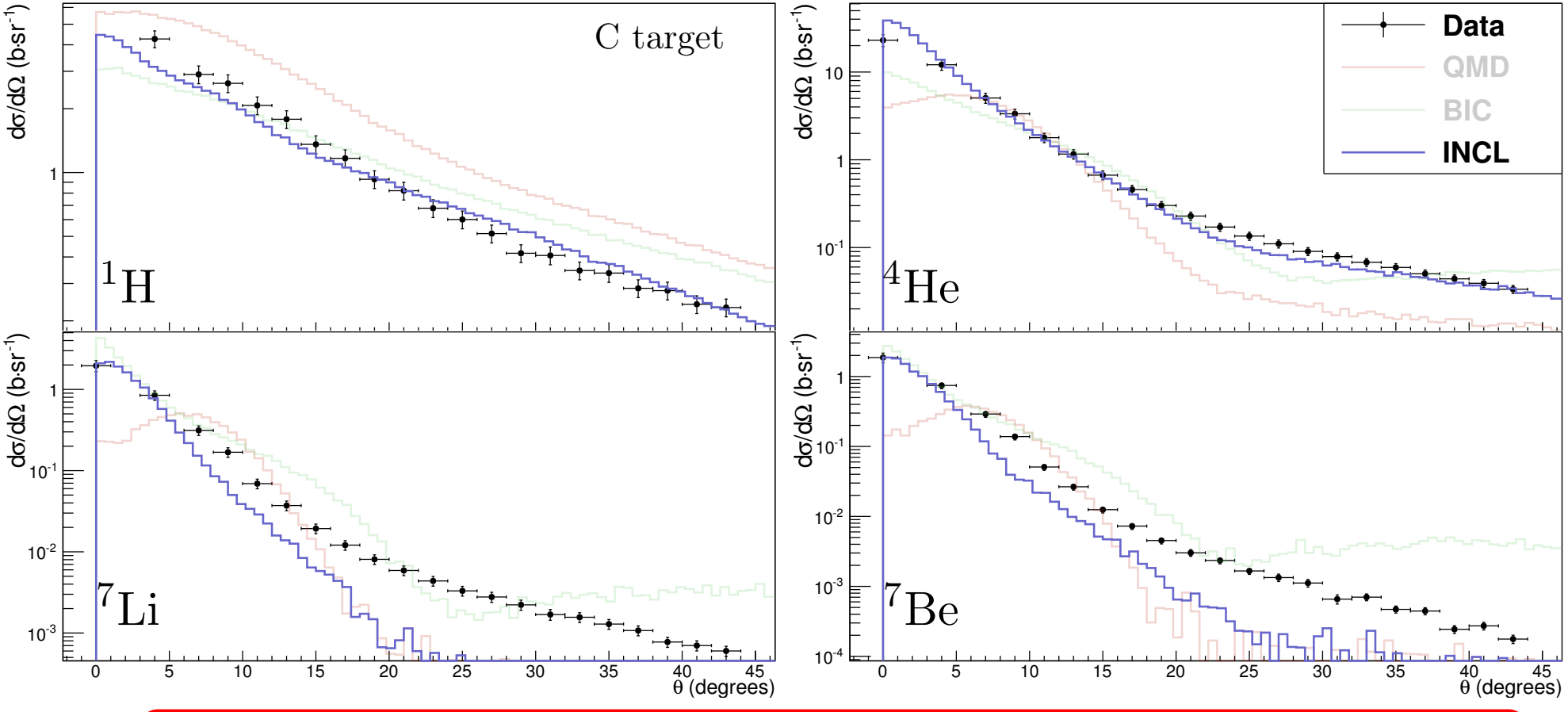

- QMD fails to reproduce the angular distributions.
- BIC is slightly better at forward angles but does not reproduce large angles.
- INCL gives better results for Z$\leq$2, but only at forward angles for Z>2.

GEANT4 models benchmark: Energy distributions

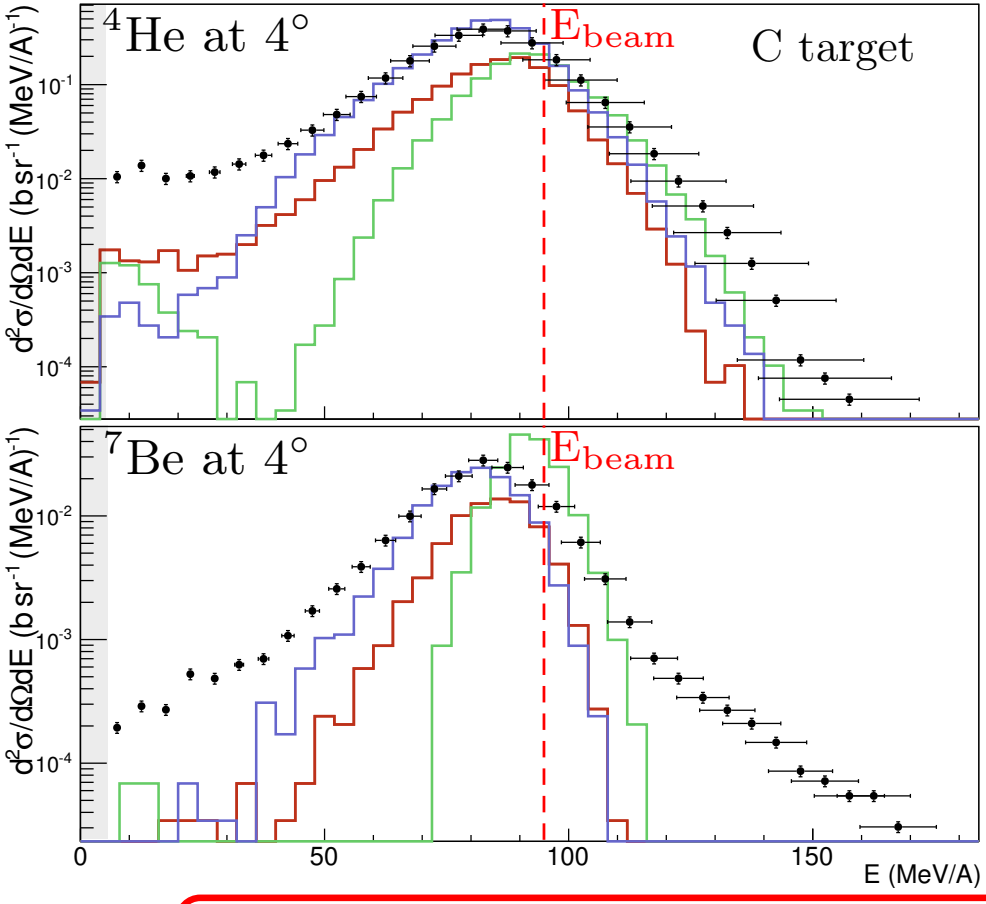

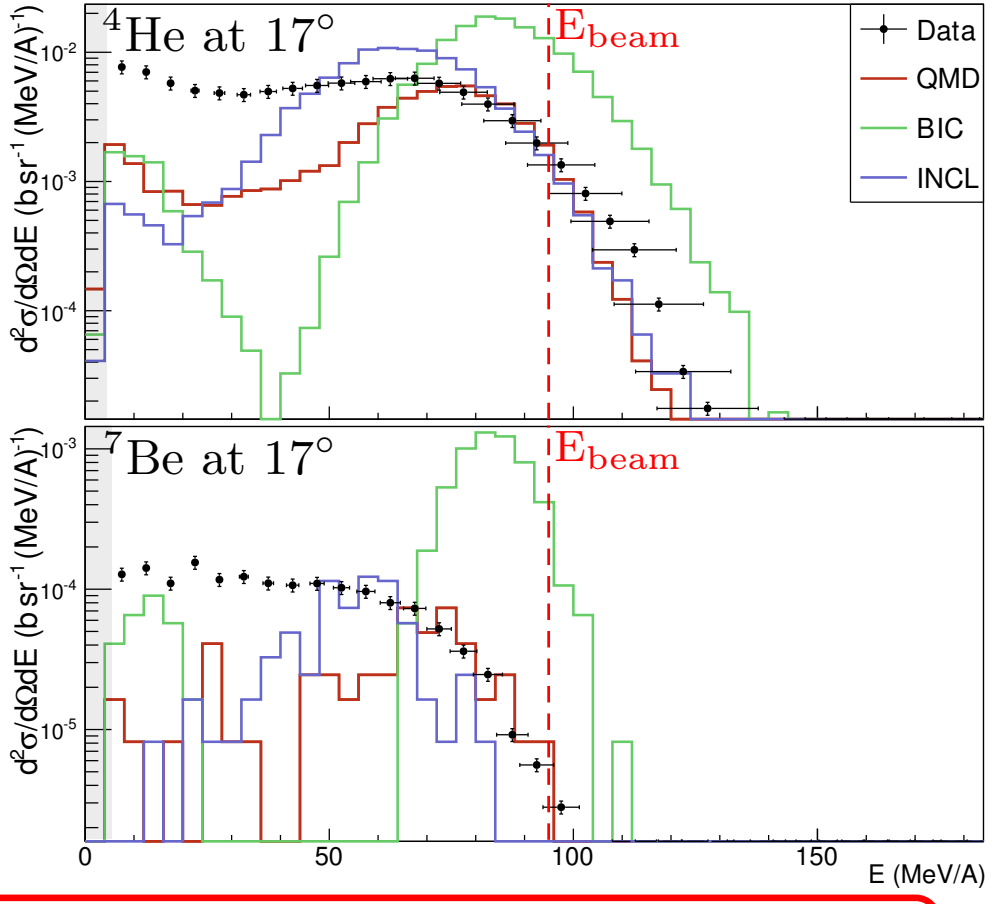

GEANT4 models benchmark: Energy distributions

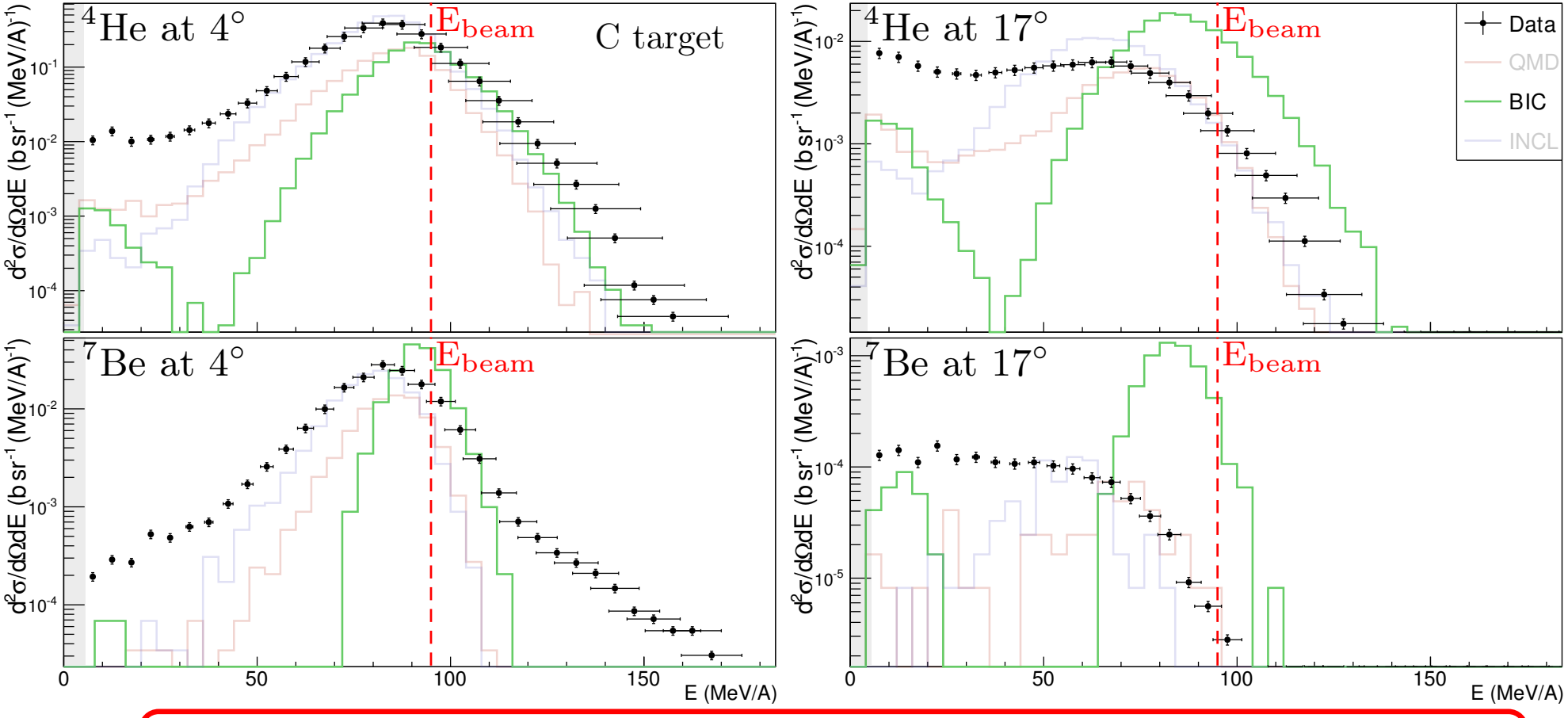

- BIC : Width too small, E mean too high, no mid-rapidity emission

GEANT4 models benchmark: Energy distributions

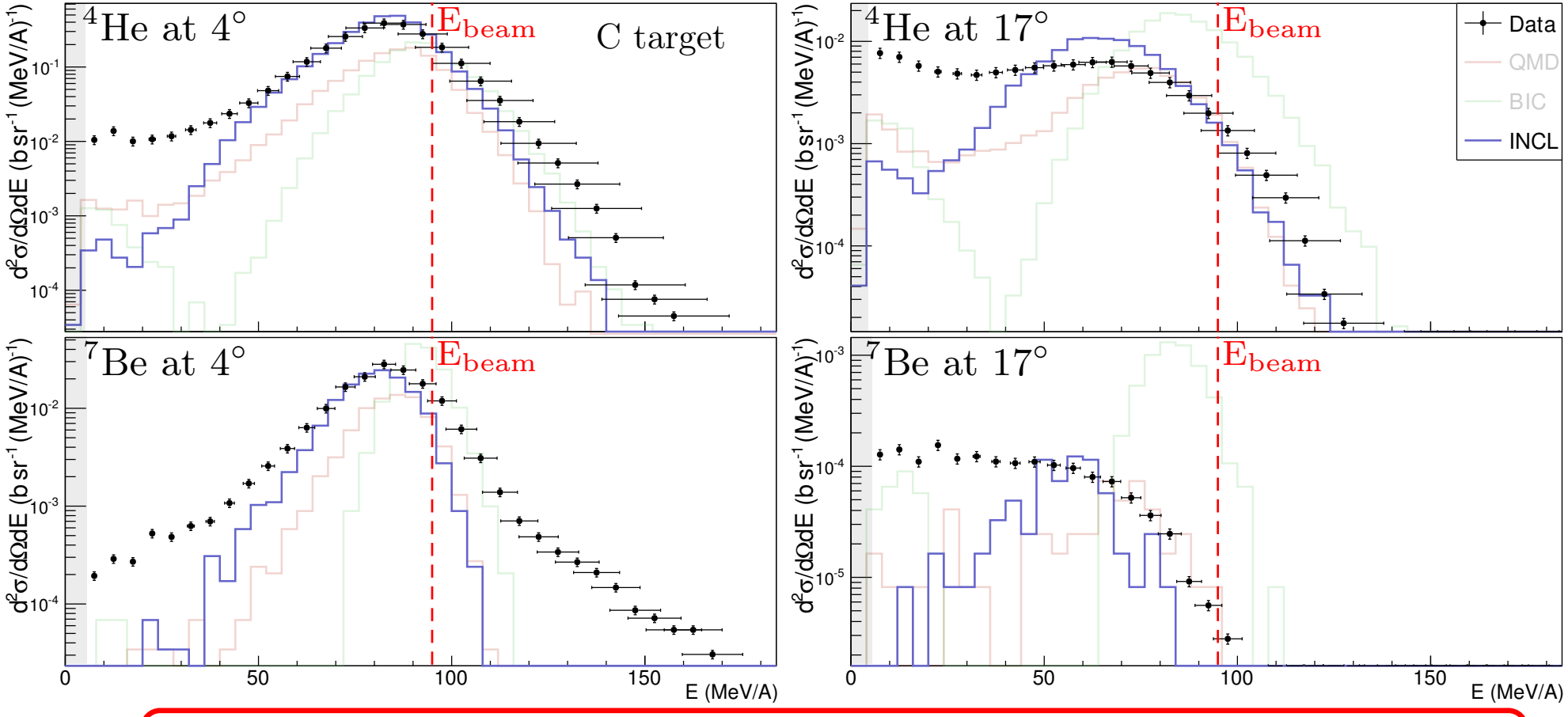

- BIC : Width too small, E mean too high, no mid-rapidity emission
- INCL: QP well reproduced, mid-rapidity shape not reproduced

GEANT4 models benchmark: Energy distributions

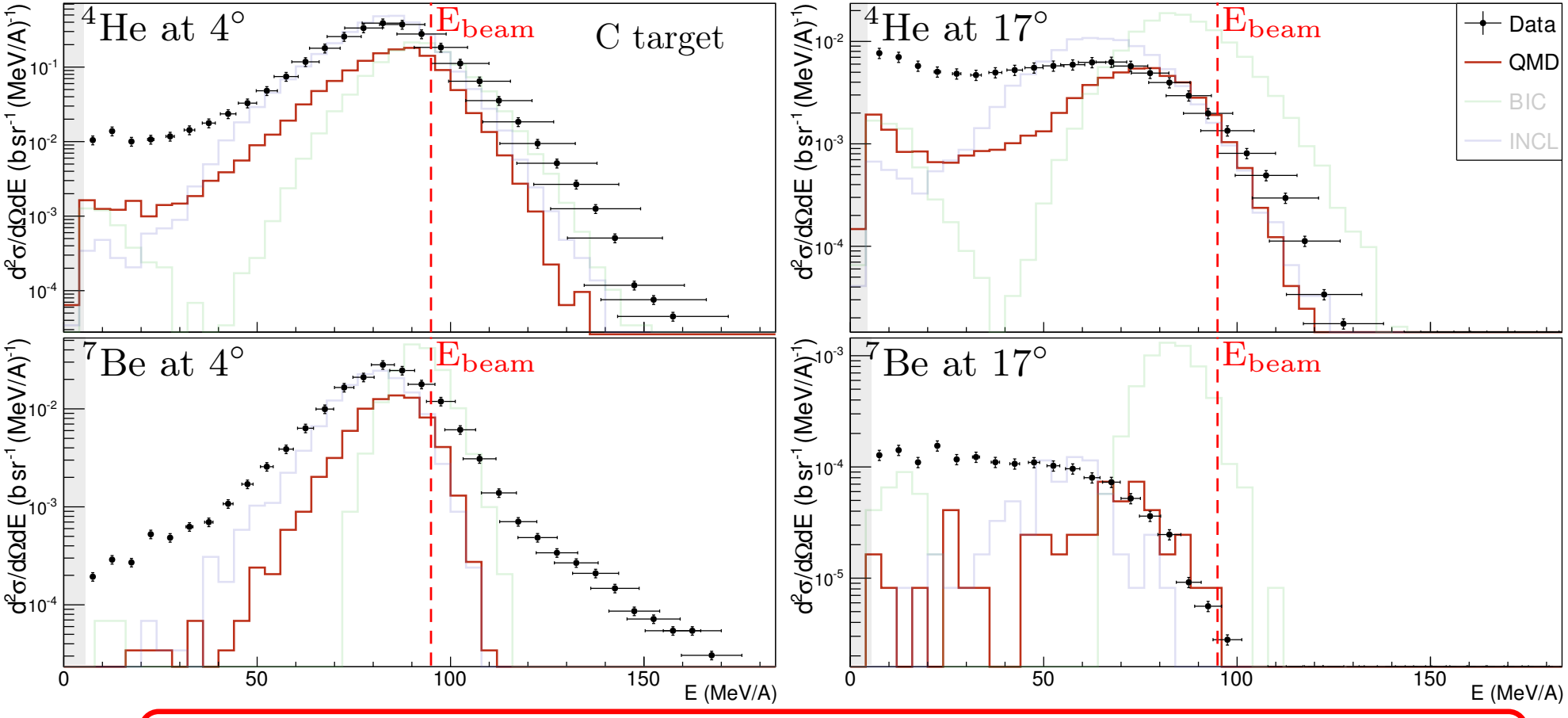

- BIC : Width too small, E mean too high, no mid-rapidity emission
- INCL: QP well reproduced, mid-rapidity shape not reproduced
- QMD: Best global shape but mid-rapidity still underestimated

Conclusions

- None of the nucleus-nucleus collision models in GEANT4 is able to reproduce all angular distributions and all energy distributions.
- **QMD** : fails in reproducing angular distributions but reproduces fairly the energy distribution characteristics (but far for beeing perfect!)
- **BIC** : good reproduction of angular distributions at small angles but fails to reproduce data at high angles; fails to reproduce energy distributions
- **INCL** : angular distributions well reproduced for light fragments; mid-rapidity contribution missing for energy distributions.

Need for new models to better predict the secondary particles production !

1 Simulations for hadrontherapy

2 The role of nucleus-nucleus collisions

3 Nucleus-nucleus collision models

4 Benchmarking models to data

5 Nuclear Physics methods for hadrontherapy

Treatment constraints for a clinical dose control

For a typical treatment

- The irradiation lasts 2 minutes at most
- The dose delivered per fraction is 2 Gy
- the total duration of an irradiation fraction is 20 minutes (positioning + irradiation)

To be efficient a control has to:

- use a process which produces enough statistics within the 2 Gy constraint
- have detectors with the best possible efficiency
- have a fast electronics and computer processing
- leave enough room for the patient, the positionning control devices, the irradiation table, ...

Dose control by using β^+ emitters

PMMA Target

protons at 140 MeV

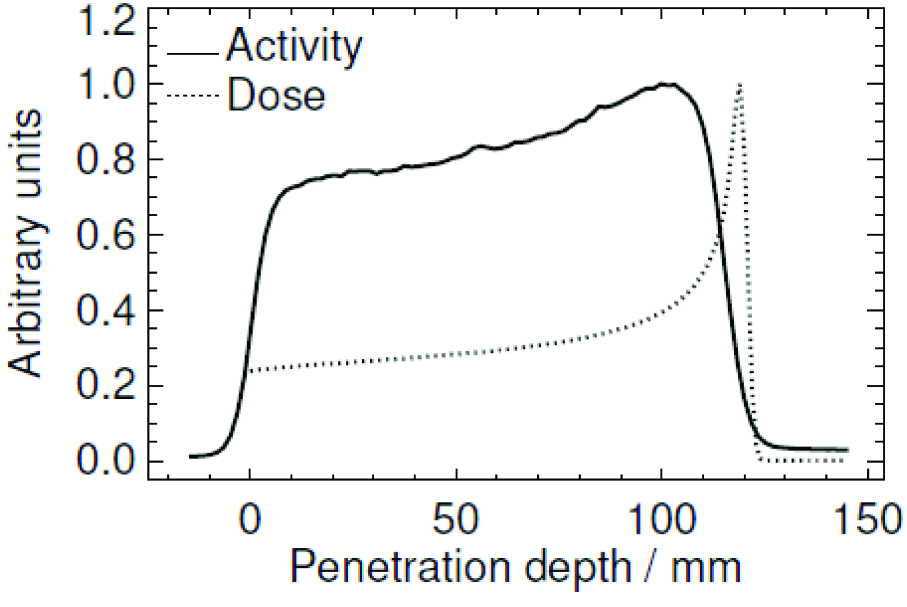

^{12}C at 259.5 MeV/u

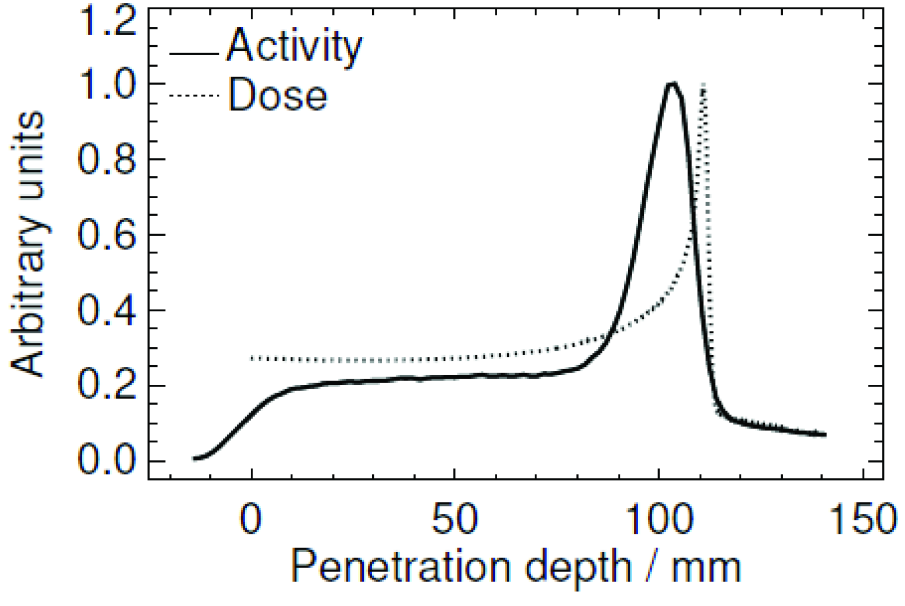

The main β^+ emitters are $^{11}C(T_{1/2} = 20.3\,mn)$, $^{10}C(T_{1/2} = 19.3\,s)$ and $^{15}O(T_{1/2} = 121.8\,s)$.

K. Parodi Ph.D. thesis (2004) Technische Universität Dresden, Fakultät Mathematik und Naturwissenschaften

Dose control by using β^+ emitters (continued)

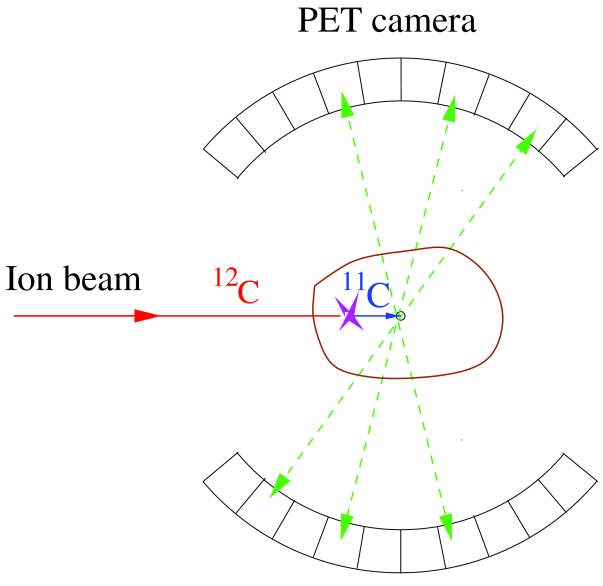

The PET camera at GSI

K. Parodi et al, Nucl. Instrum. Methods Phys. Res. A 591 (2008) 282–286.

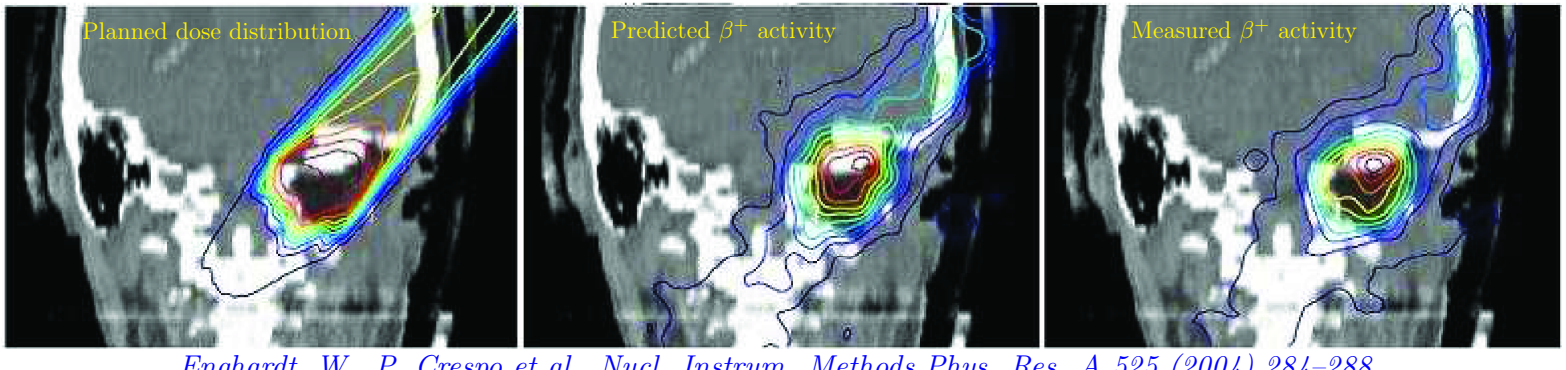

Enghardt, W., P. Crespo et al., Nucl. Instrum. Methods Phys. Res. A 525 (2004) 284–288.

Dose control by using prompt γ emissions

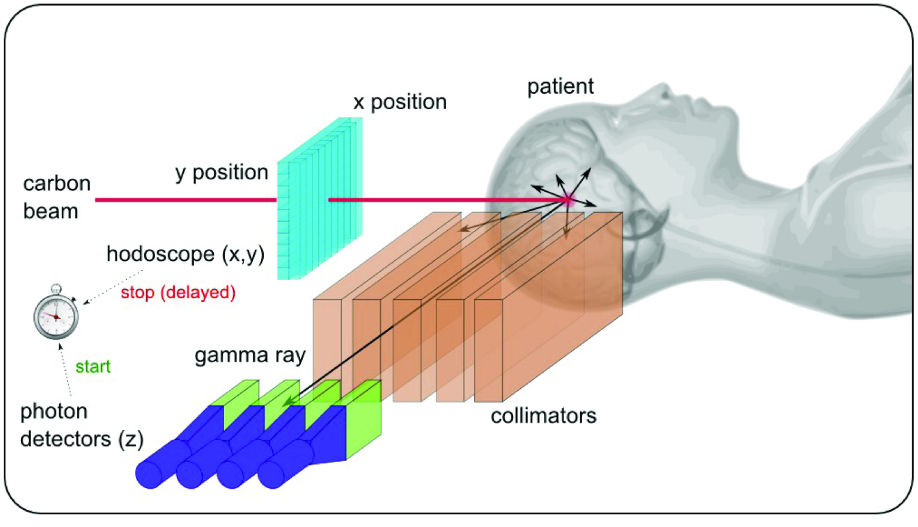

Collimated γ camera

F. Le Fouhler PhD thesis, 2010, Université Claude Bernard Lyon 1

Compton γ camera

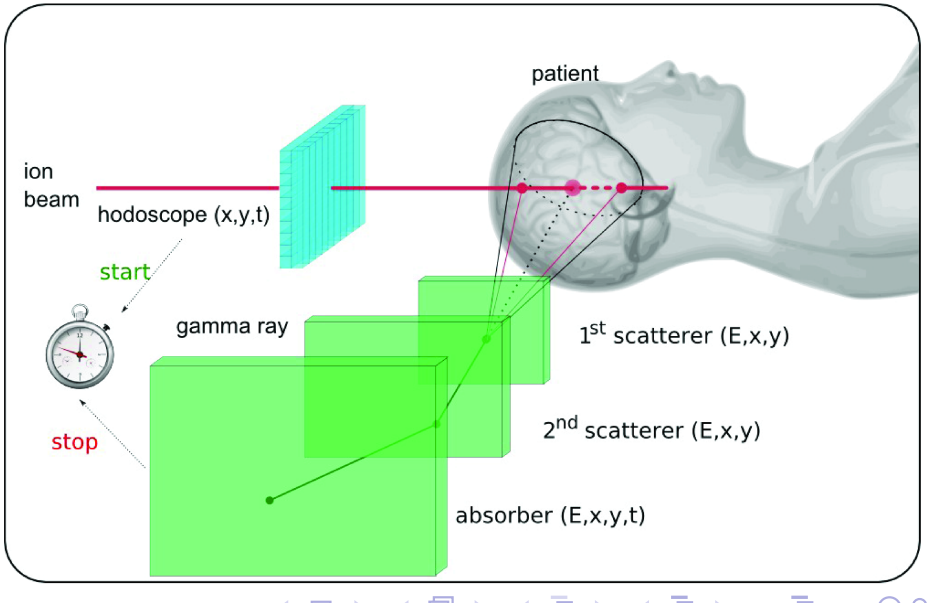

Dose control by using prompt γ emissions (continued)

PMMA thick target

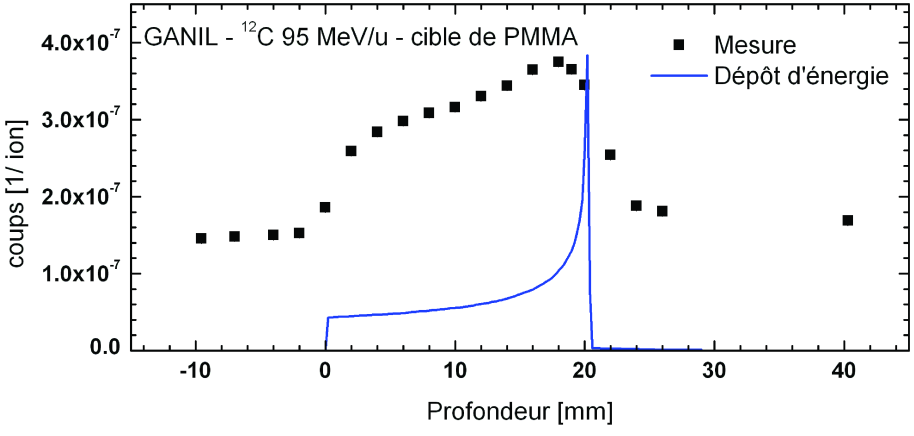

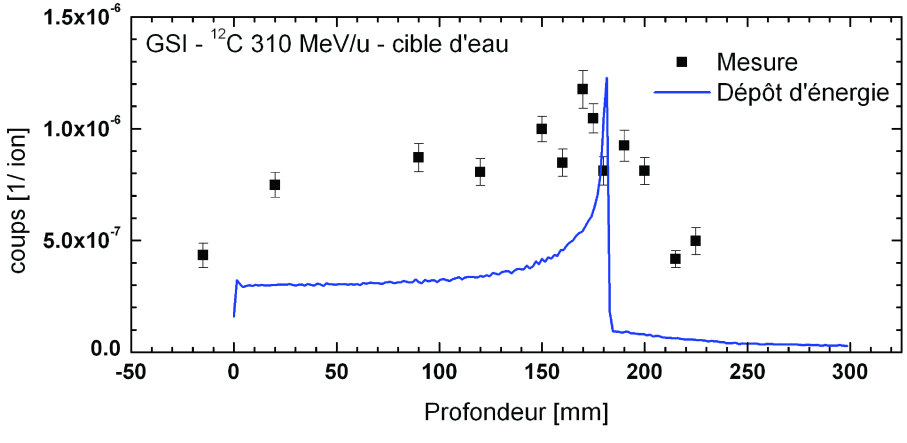

F. Le Fouhler PhD thesis, 2010, Université Claude Bernard Lyon 1

Dose control by using prompt γ emissions (continued)

PMMA thick target

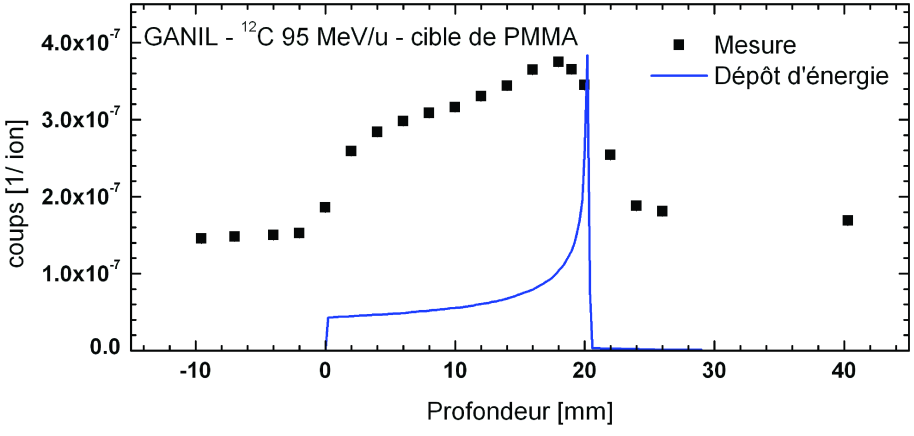

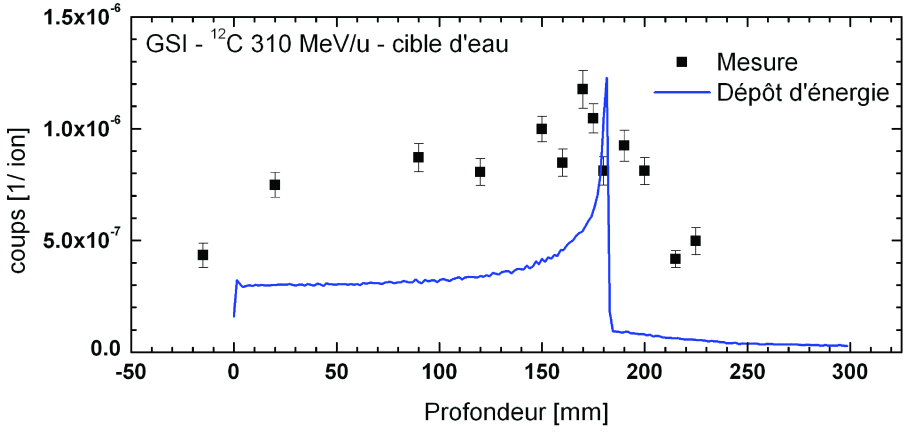

GEANT4 simulations, QMD+FBU

^{12}C at 95 MeV/u

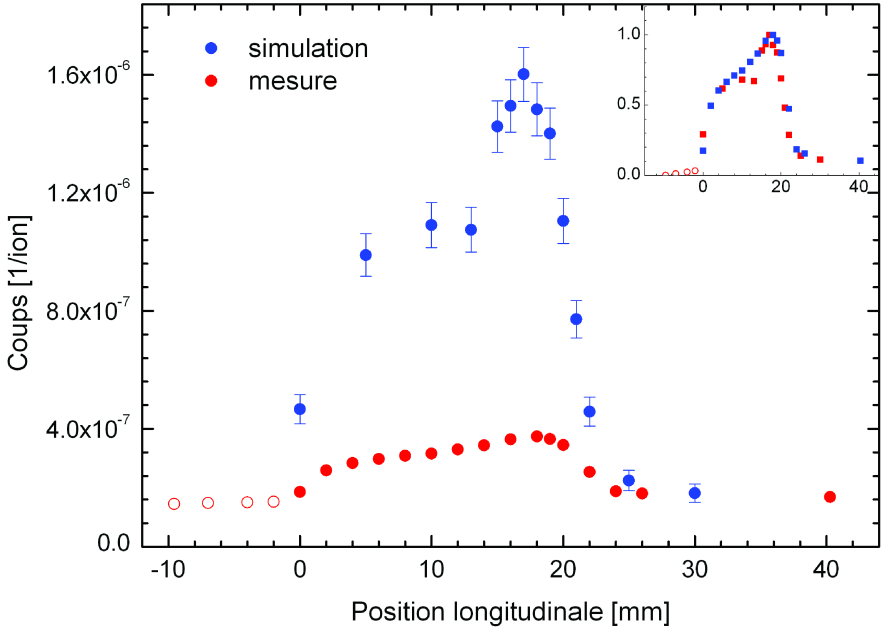

F. Le Fouhler PhD thesis, 2010, Université Claude Bernard Lyon 1

Dose control by using prompt γ emissions (continued)

PMMA thick target

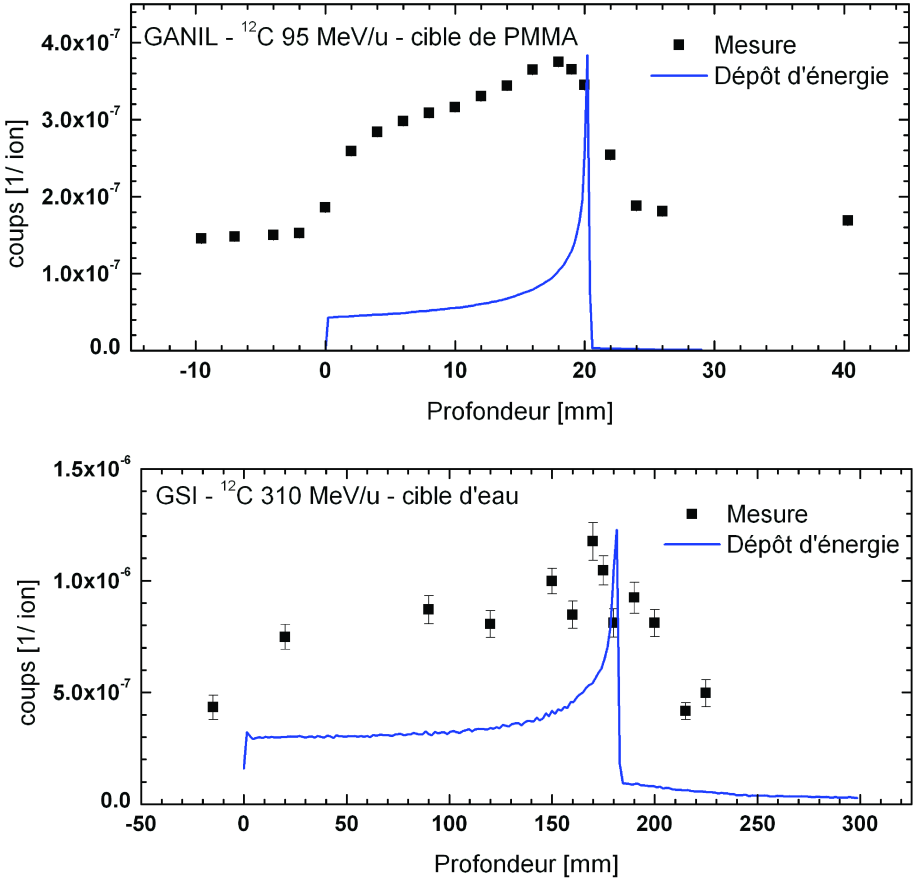

GEANT4 simulations, QMD+FBU

^{12}C at 310 MeV/u

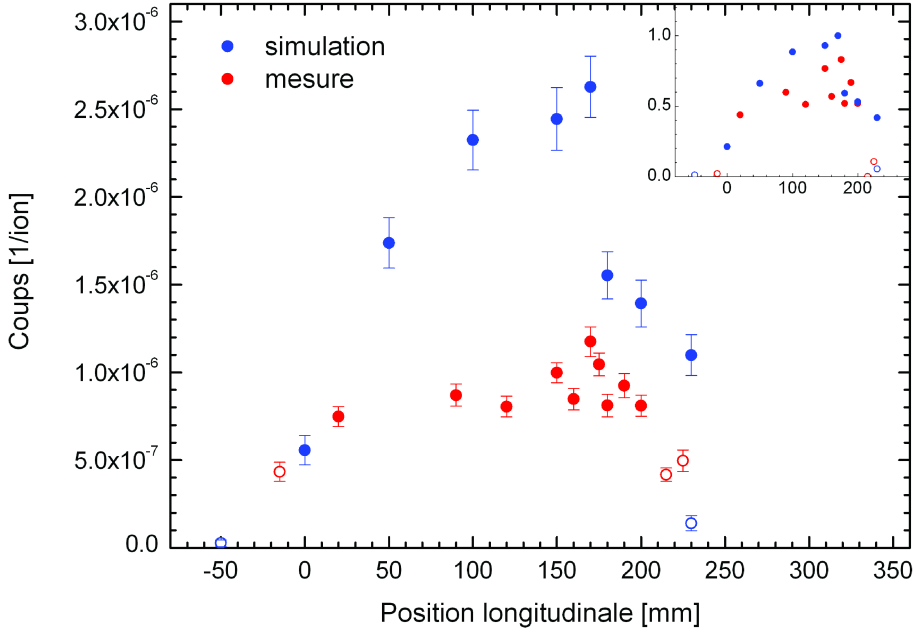

F. Le Fouhler PhD thesis, 2010, Université Claude Bernard Lyon 1

Dose control by using secondary charged particles

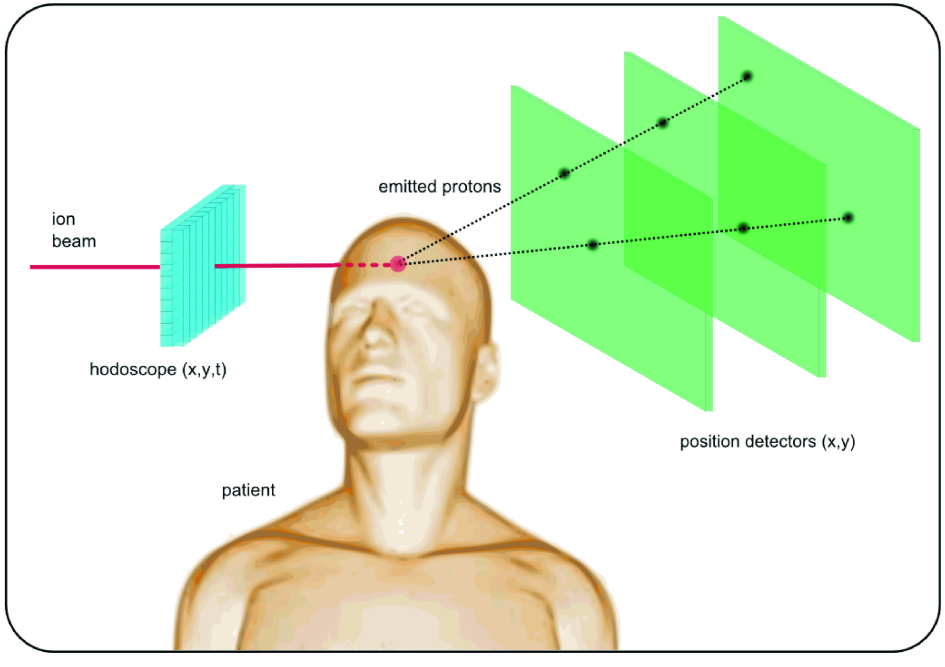

P. Henriquet PhD thesis, 2010,
Université Claude Bernard Lyon 1

Vertex distributions

GEANT4 Simulations

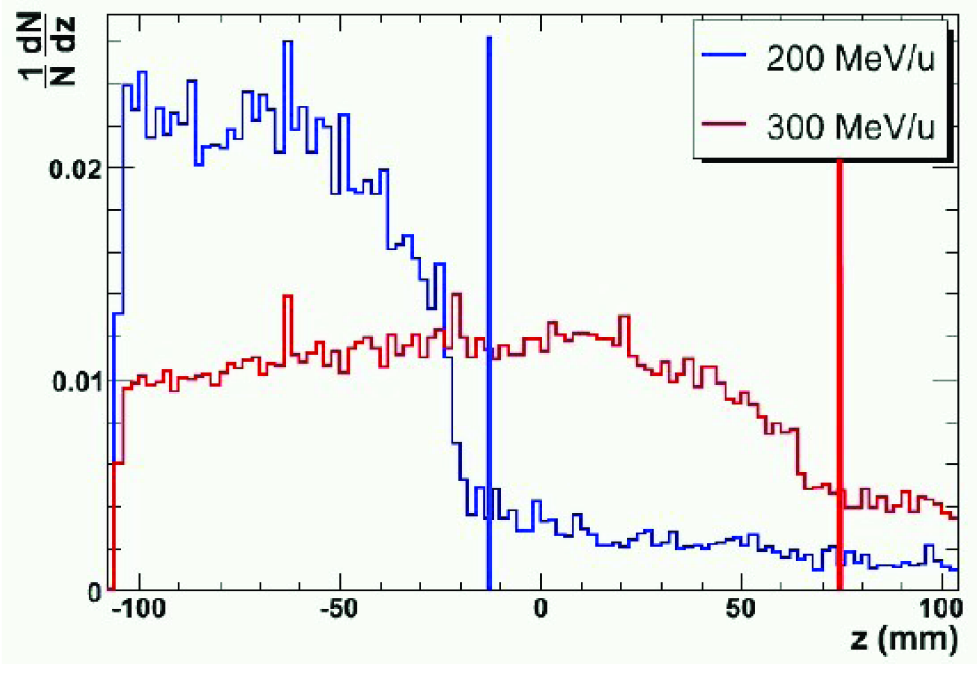

Clinical imaging

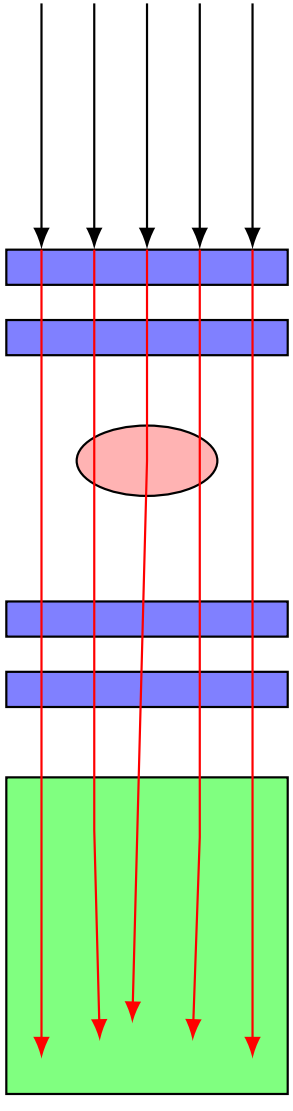

proton beam

position sensitive detector

range or energy detector

Clinical imaging

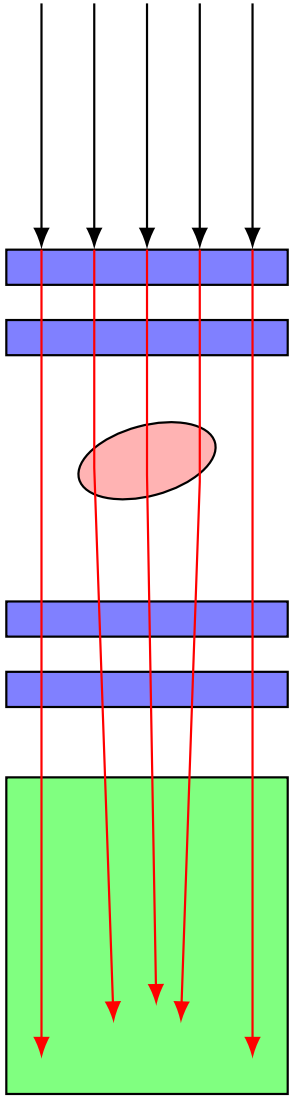

proton beam

position sensitive detector

range or energy detector

Clinical imaging

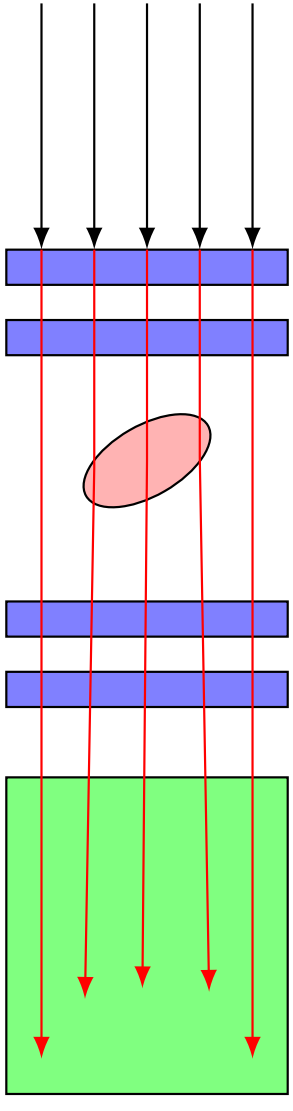

proton beam

position sensitive detector

range or energy detector

Clinical imaging

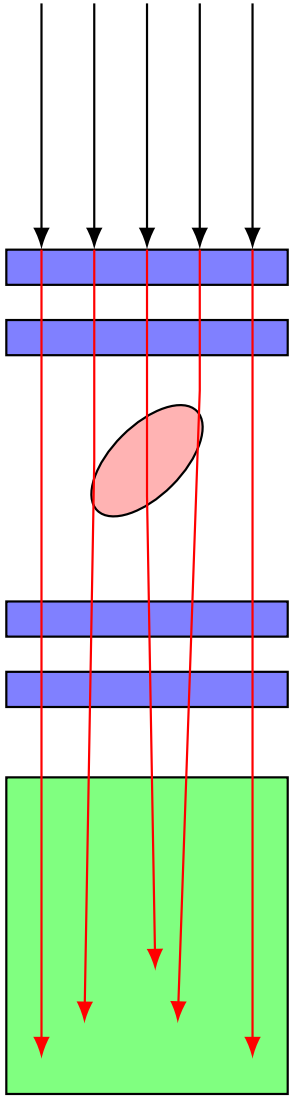

proton beam

position sensitive detector

range or energy detector

Clinical imaging

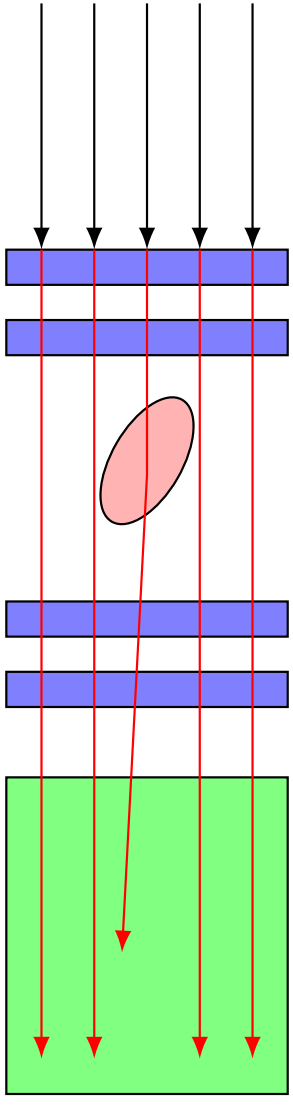

proton beam

position sensitive detector

range or energy detector

Clinical imaging

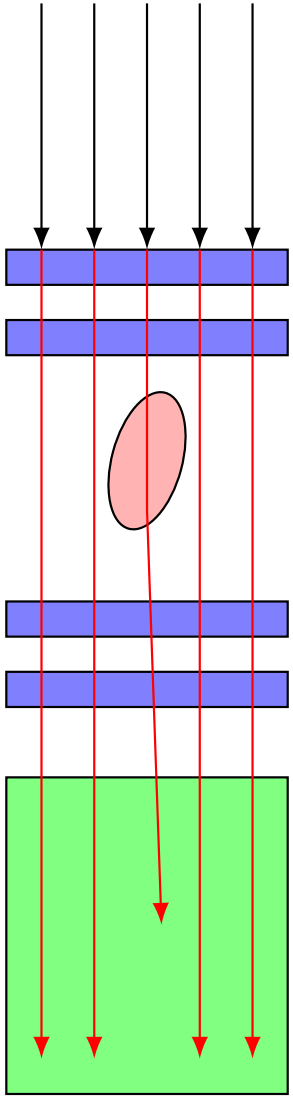

proton beam

position sensitive detector

range or energy detector

Clinical imaging

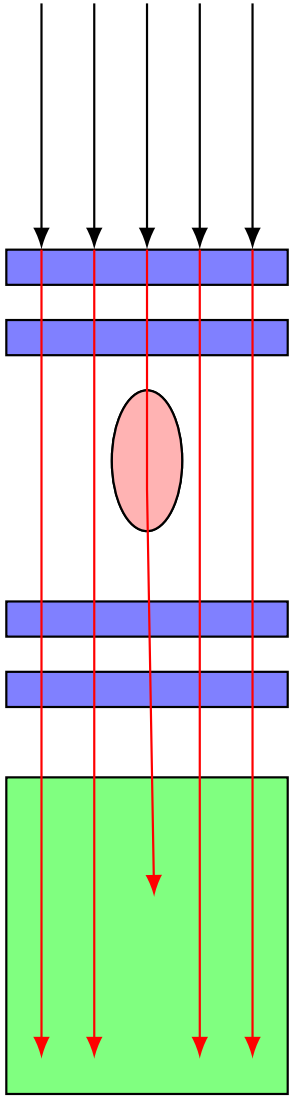

proton beam

position sensitive detector

range or energy detector

Clinical imaging

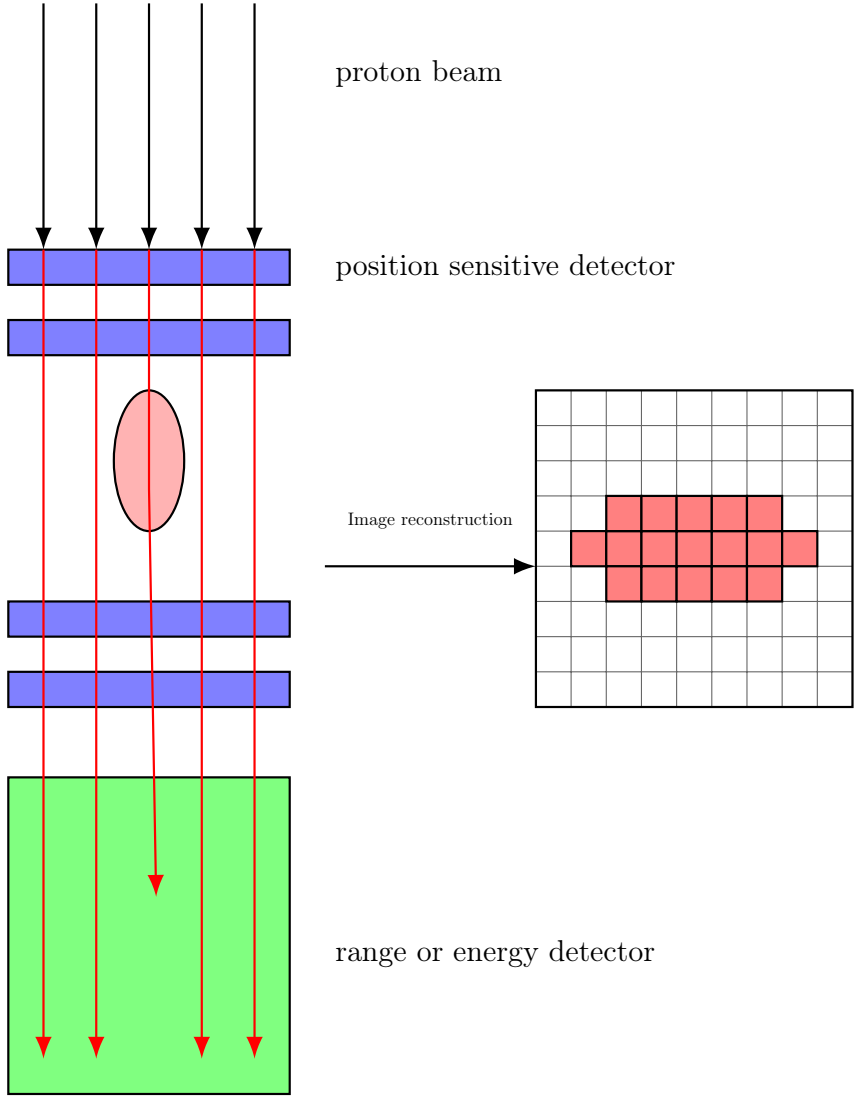

Clinical imaging

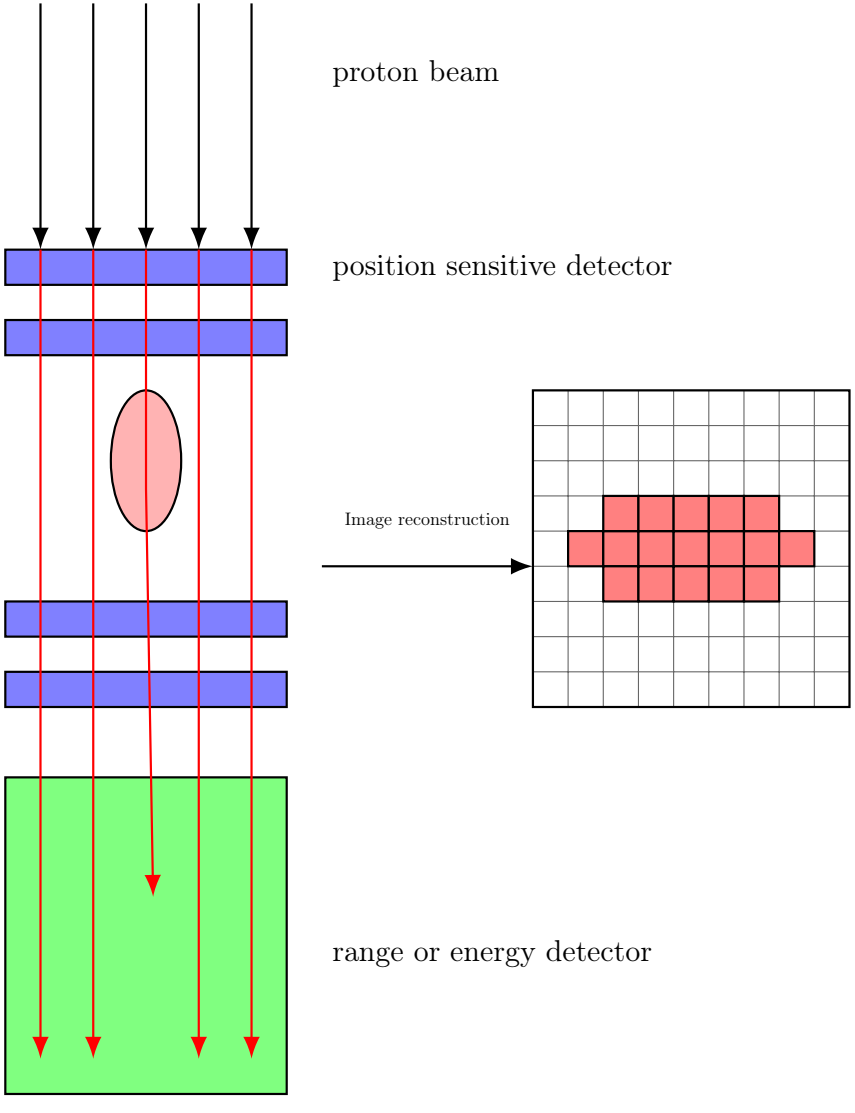

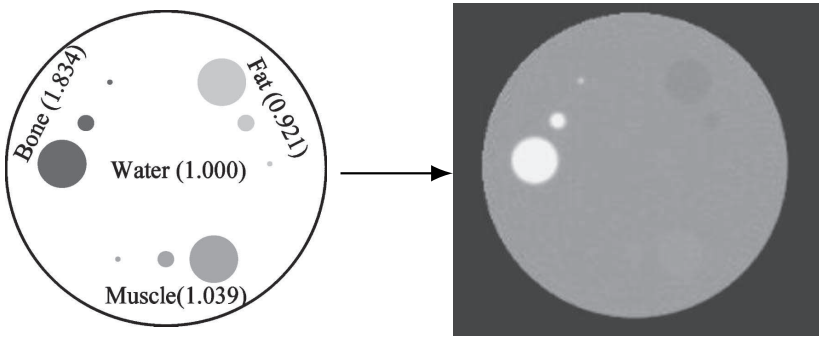

Schulte et al., Med. Phys. **32** *(2005) 1035.*

Clinical imaging

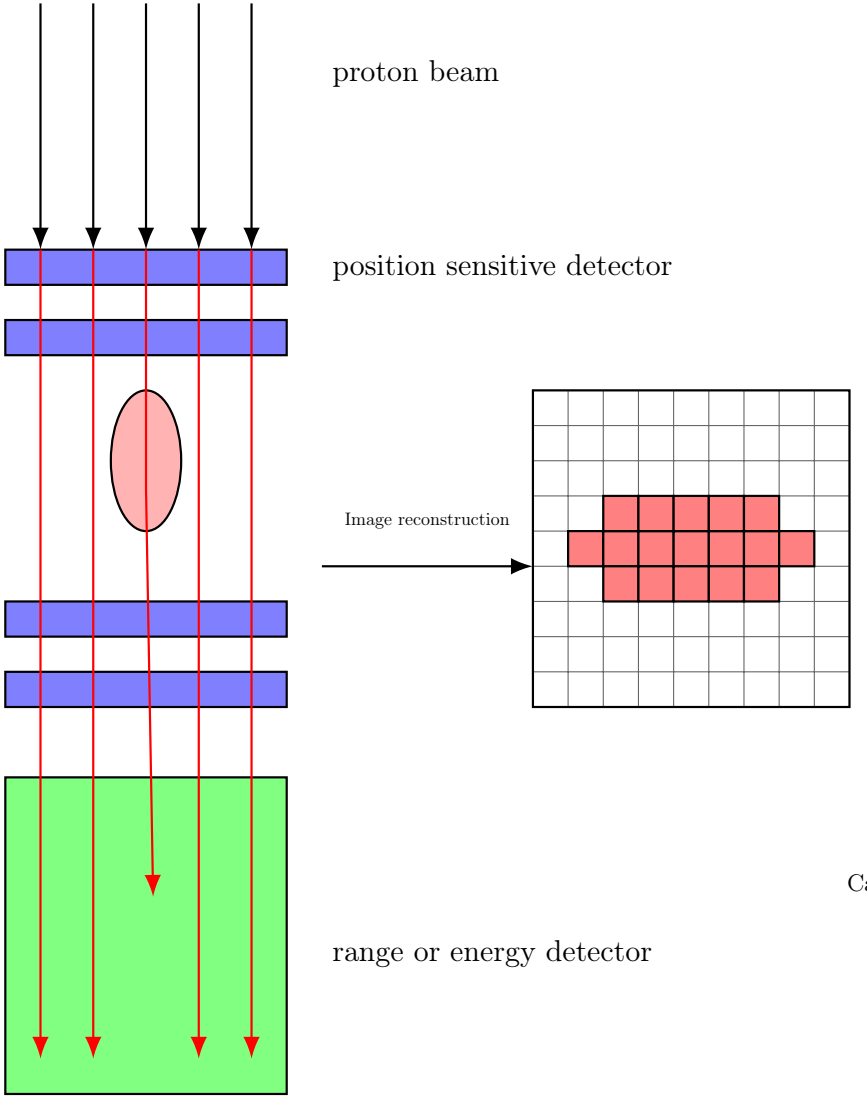

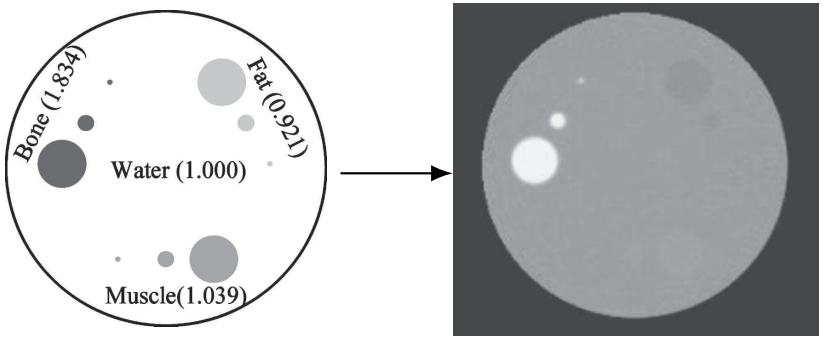

Schulte et al., Med. Phys. **32** *(2005) 1035.*

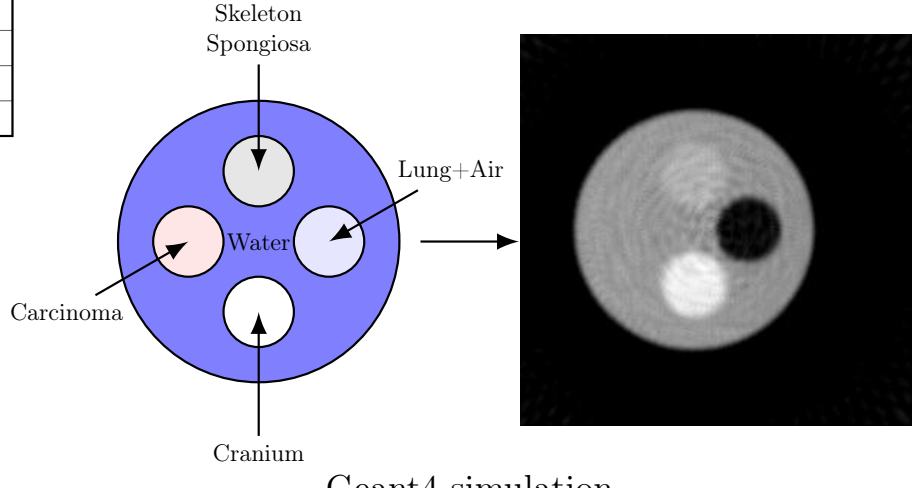

Geant4 simulation

Clinical imaging

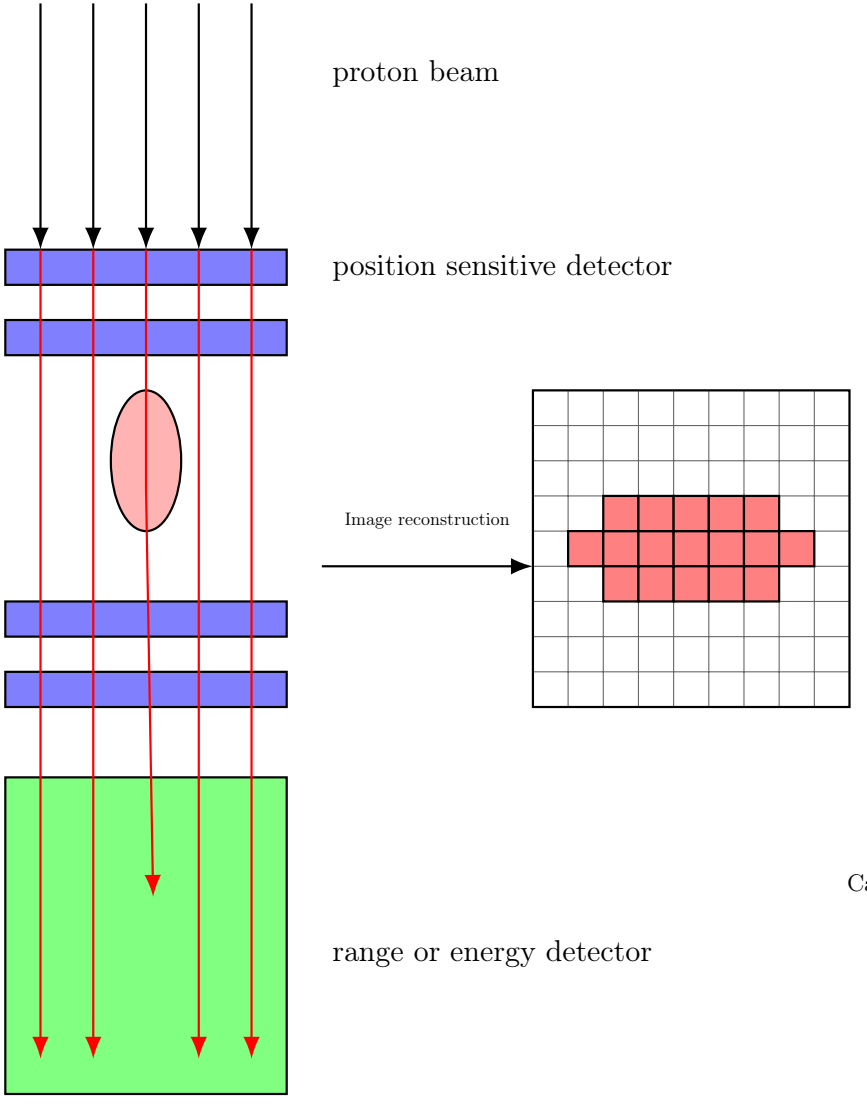

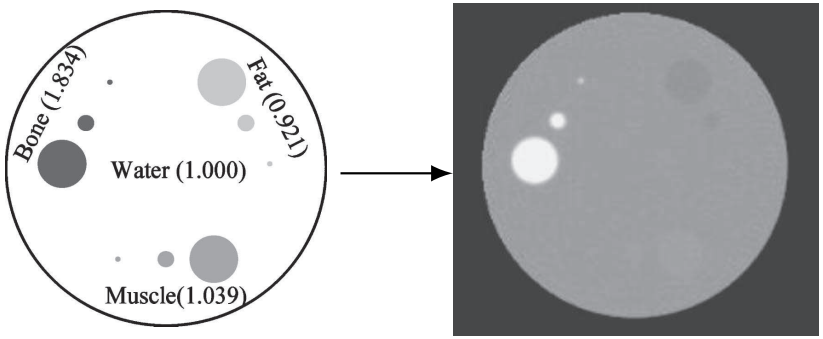

Schulte et al., Med. Phys. **32** *(2005) 1035.*

Higher accuracy, less dose!

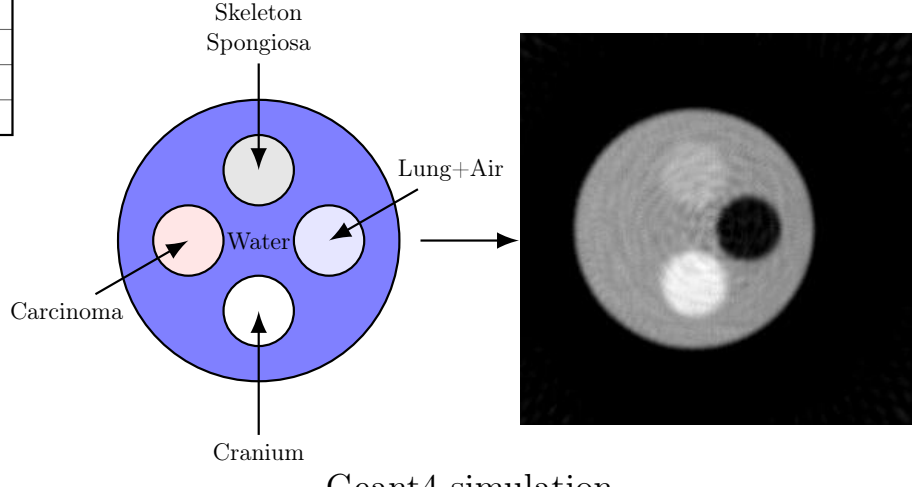

Geant4 simulation

Final remarks

Simulations

- Used to compute the dose maps in Treatment Planning Systems
- "Analytical" calculations : fast but moderately accurate
- "Monte-Carlo" calculations : accurate but slow

Final remarks

Simulations

- Used to compute the dose maps in Treatment Planning Systems
- "Analytical" calculations : fast but moderately accurate
- "Monte-Carlo" calculations : accurate but slow

The nucleus-nucleus collisions

- do not modify the range
- modify significantly the dose map
  - projectiles consumption $\longrightarrow \sigma_{reaction}$
  - lead to an energy deposition beyond the Bragg Peak ("fragmentation tail")
- may provide new tools to perform in-line dose controls $\longrightarrow$ nucleus-nucleus collision models

Final remarks

Simulations

- Used to compute the dose maps in Treatment Planning Systems
- "Analytical" calculations : fast but moderately accurate
- "Monte-Carlo" calculations : accurate but slow

The nucleus-nucleus collisions

- do not modify the range
- modify significantly the dose map
  - projectiles consumption $\longrightarrow \sigma_{reaction}$
  - lead to an energy deposition beyond the Bragg Peak ("fragmentation tail")
- may provide new tools to perform in-line dose controls $\longrightarrow$ nucleus-nucleus collision models

Nucleus-nucleus collision models

- small influence on the physical dose map
- strong influence on the secondary fragments multiplicities
  - potential strong influence on the biological effects estimation beyond the Bragg-Peak (toxicity)
  - strong influence on the design of monitoring devices based on the detection of secondary fragments escaping from the patient's body
- need for new models to reproduce experimental data